

Fault slip rates,
distributed deformation rates,
and long-term seismicity
estimated with kinematic F-E program

NeoKinema

Peter Bird
UCLA



2012.06.20, CIG's CDM workshop,
Golden CO

F-E models of deformation of the lithosphere:

Time-scale	Method	Rheology	Domain	Example(s)
Short-term (interseismic and/or coseismic)	Dynamic (forward)	Elastic, Viscoelastic, Elastoviscoplastic, ...	2-D + t or 3-D + t	PyLith, LithoMop, Gale, SNAC, ConMan, CitCom, ...
Long-term- average ($10^4 \sim 10^6$ years; no earthquake stress-drops)	Dynamic (forward)	Friction + Dislocation-creep (not elastic).	“2.5-D” (3-D density + strength; 2-D velocity field); no time.	Shells
Long-term- average ($10^4 \sim 10^6$ years; no earthquake stress-drops)	Kinematic (inverse)	Soft isotropic microplates (straining minimized + aligned with stress); elastic halfspace used in converting timescale of GPS.	2-D (map-view on a sphere); two kinds of time (steady interseismic vs. long-term-average)	NeoKinema

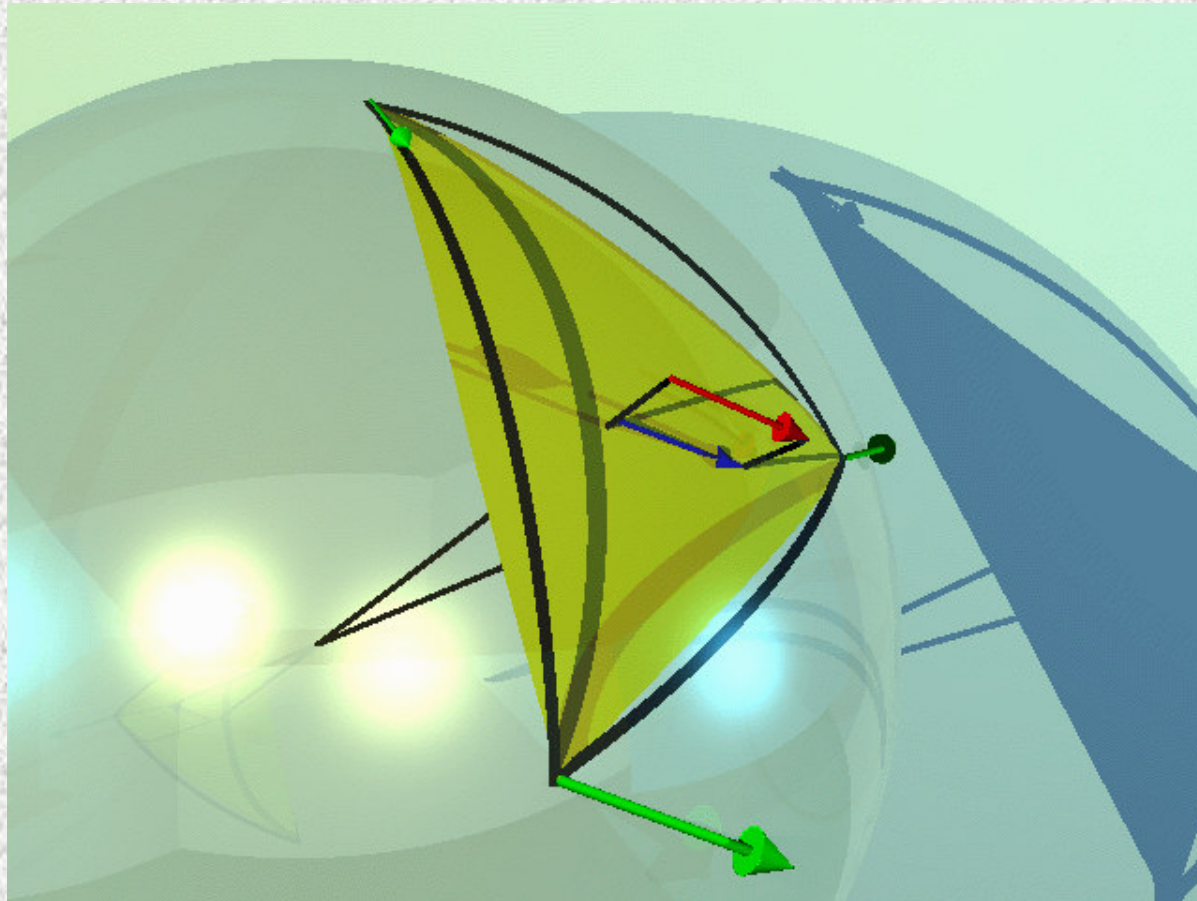
Assumptions of *NeoKinema*:

- ❖ Distributed permanent deformation (*that which occurs off the mapped fault traces, and is not elastic*) should be minimized.
- ❖ Principle axes of distributed deformation strain-rates should be ~parallel to principal stress axes (*either from data, or interpolated, with uncertainties*).
- ❖ Interseismic GPS velocities can be corrected to long-term velocities with a self-consistent *Savage & Burford* [1973] model (using current model long-term offset rates, and seismicity-based locking depths from *Nazareth & Hauksson* [2004]).

Methods

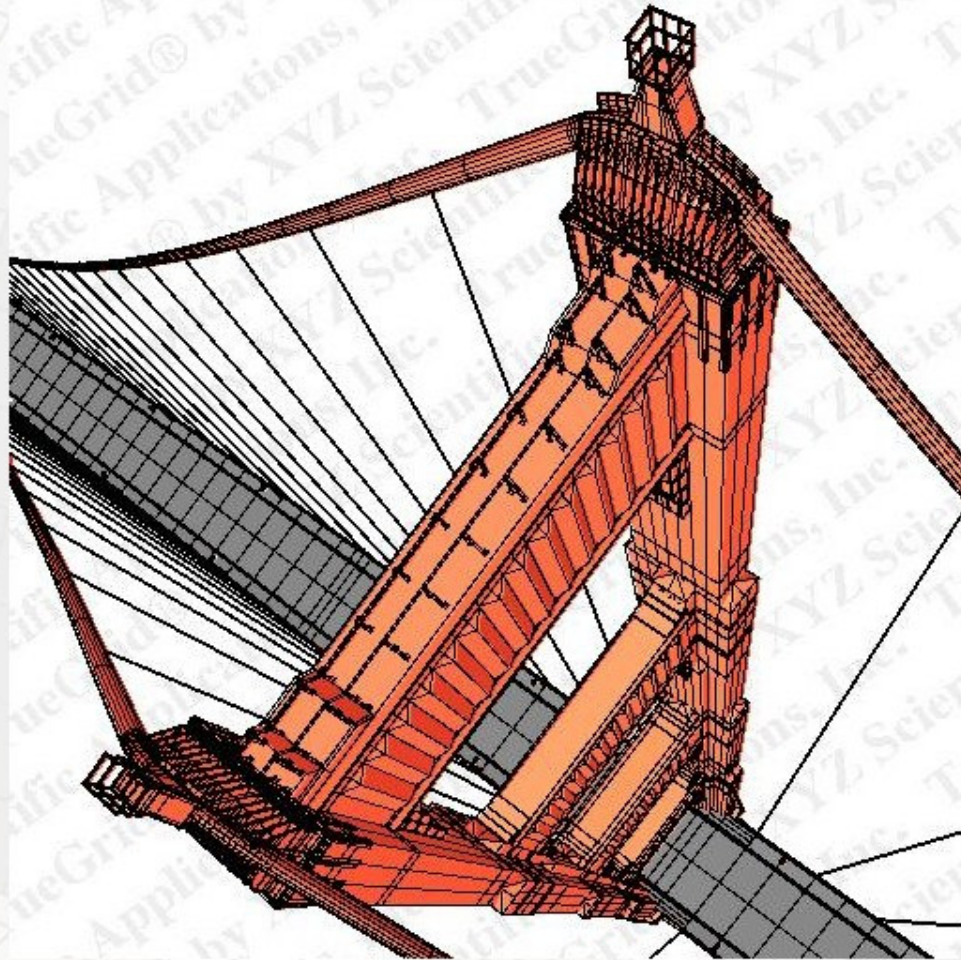
- Solve for long-term velocities of nodes on the Earth's solid spherical surface (only).
- Solution method is weighted-least-squares, using data uncertainties (and 2 adjustable modelling parameters) as inverse weights.
- Nonlinearities are handled by iterating the solution ~20 times, to convergence.
- If multiple faults lie between adjacent nodes, their long-term offset rates are determined in a local weighted-least-squares solution where node velocities are fixed.

**spherical-triangle element
(used in both Shells & NeoKinema)**

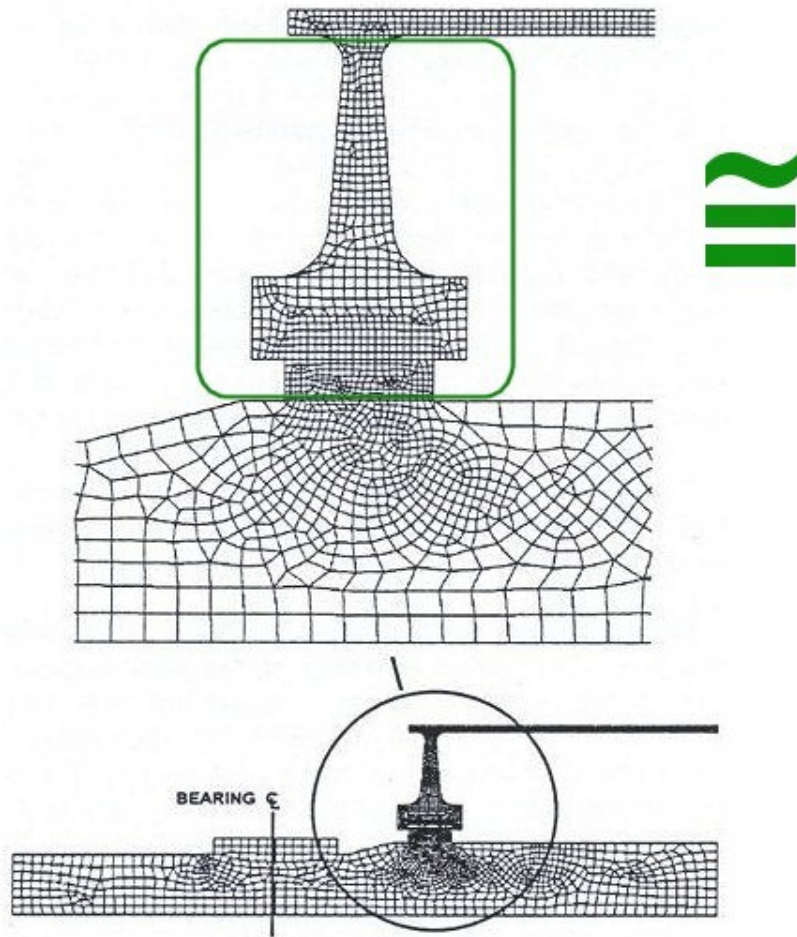


[Kong & Bird, 1995, JGR]

Lofty View of Golden Gate Bridge



This is an aerial view of the Golden Gate Bridge mesh created with **TrueGrid®**.

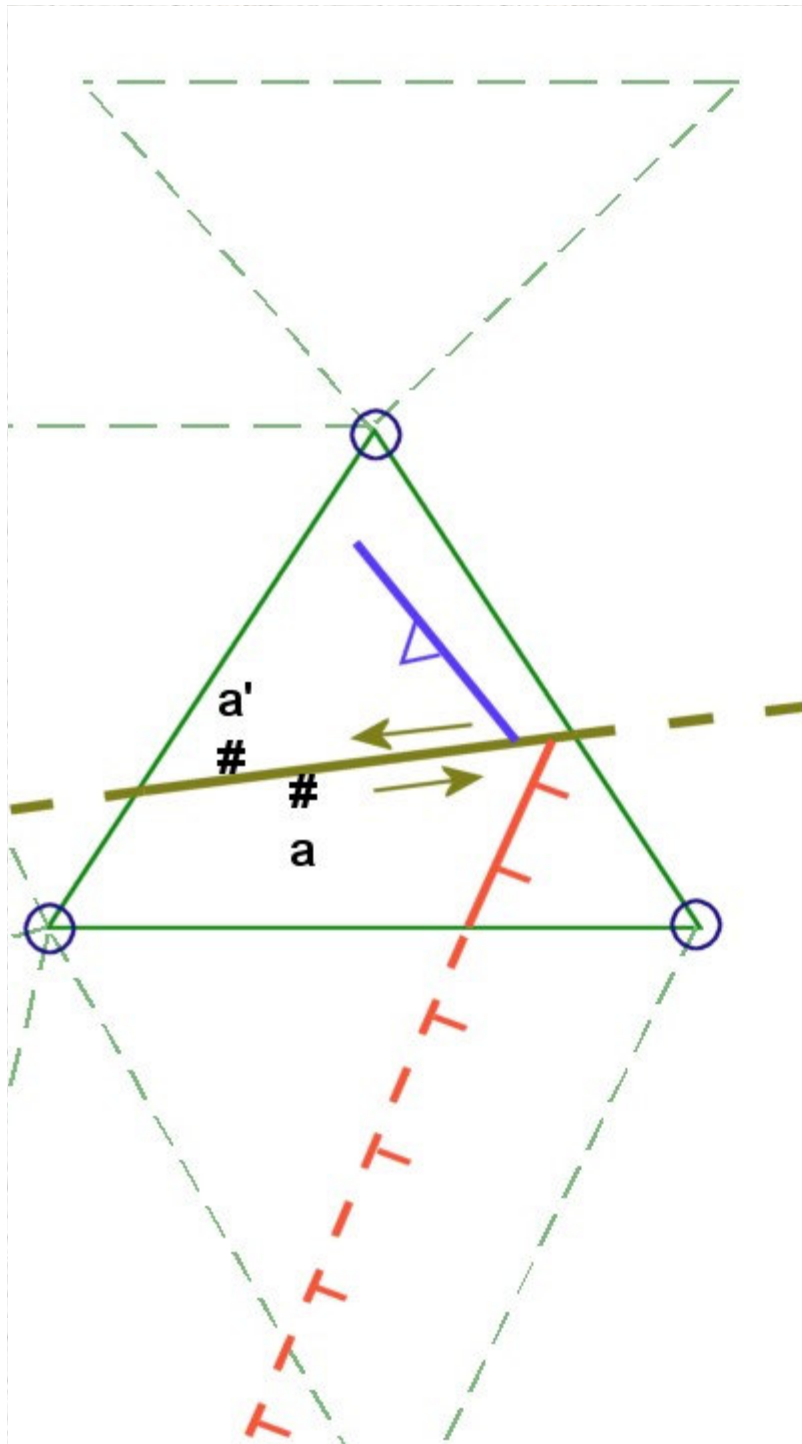


Represent the substructure by a [3x3] matrix of force/displacement ratios
 $[d f_i / d u_j]$

(or [6 x 6] if moments are transmitted as well).

SOLUTION STEPS:

- 1) Solve the large problem using the simplified substructure.
- 2) Determine displacement (/rotation) boundary conditions on substructure.
- 3) Solve small problem within the substructure.



In NeoKinema, each faulted element is a substructure:

- Known offset rates contribute to target strain-rate [3-vector];
- Uncertainty in offset rate contributes to covariance of strain-rate [3x3 matrix];
- Compliance of continuum adds an isotropic part to the covariance;
- This is all that the global solution "needs to know";
- Once velocities of nodes are known, element strain-rate is partitioned into fault slip-rate and continuum strain-rate in a local solution.



“Zooming out” (that is, in the limit of very small elements):

The objective function of NeoKinema is a nondimensional function of both dimensional model predictions (p) and corresponding dimensional data values (r), normalized by dimensional covariance matrix (\tilde{C}) or by individual datum standard deviations (σ):

$$\Pi \equiv -(\bar{p} - \bar{r})^T [\tilde{C}_{\text{GPS}}^{-1}] (\bar{p} - \bar{r}) - \frac{1}{L_0} \sum_{m=1}^M \int_{\text{length}} \frac{(p_m - r_m)^2}{\sigma_m^2} d\ell - \frac{1}{A_0} \sum_{n=1}^3 \iint_{\text{area}} \frac{(p_n - r_n)^2}{\sigma_n^2} da$$

where the first term is a quadratic form involving the great vector of all geodetic velocity components and its covariance matrix \tilde{C}_{GPS} , the second term concerns the M long-term fault offset-rates r_m with their uncertainties σ_m , and the third term concerns the constraints on sizes and orientations of distributed anelastic deformation-rate tensors (in 2-D, with 3 independent components) in between the mapped faults.

Note that weight of geodetic data is fixed, but weight of fault-trace based slip-rate data is controlled by $1/L_0$, while weight of continuum constraints (rigidity and isotropy) is controlled by $1/A_0$.



The objective function of NeoKinema is a nondimensional functional of both dimensional model predictions (p) and corresponding dimensional data values (r), normalized by dimensional covariance matrix (\tilde{C}) or by individual datum standard deviations (σ):

$$\Pi \equiv -(\bar{p} - \bar{r})^T [\tilde{C}_{\text{GPS}}^{-1}] (\bar{p} - \bar{r}) - \frac{1}{L_0} \sum_{m=1}^M \int_{\text{length}} \frac{(P_m - r_m)^2}{\sigma_m^2} d\ell - \frac{1}{A_0} \sum_{n=1}^3 \iint_{\text{area}} \frac{(P_n - r_n)^2}{\sigma_n^2} da$$

where the first term is a quadratic form involving the great vector of all geodetic velocity

component
offset-rates
and orienta
component

form fault
s on sizes
pendent

One of the 3 continuum terms in this sum is:

$$-\frac{1}{A_0} \iint_{\text{area}} \frac{(\dot{\epsilon} - 0)^2}{\mu^2} da \equiv -\frac{1}{A_0} \iint_{\text{area}} \frac{\dot{\epsilon}_{\text{NS}}^2 + \dot{\epsilon}_{\text{NS}} \dot{\epsilon}_{\text{EW}} + \dot{\epsilon}_{\text{EW}}^2 + \dot{\epsilon}_{\text{NE}}^2}{\mu^2} da$$

Note that v
is controlle
controlled

ta

which has the effect of minimizing distributed deformation in unfaulted finite elements.

The tolerance allowed (μ) is another important input parameter.

Trivial applications of *NeoKinema* which illustrate its algorithm

by Peter Bird
UCLA

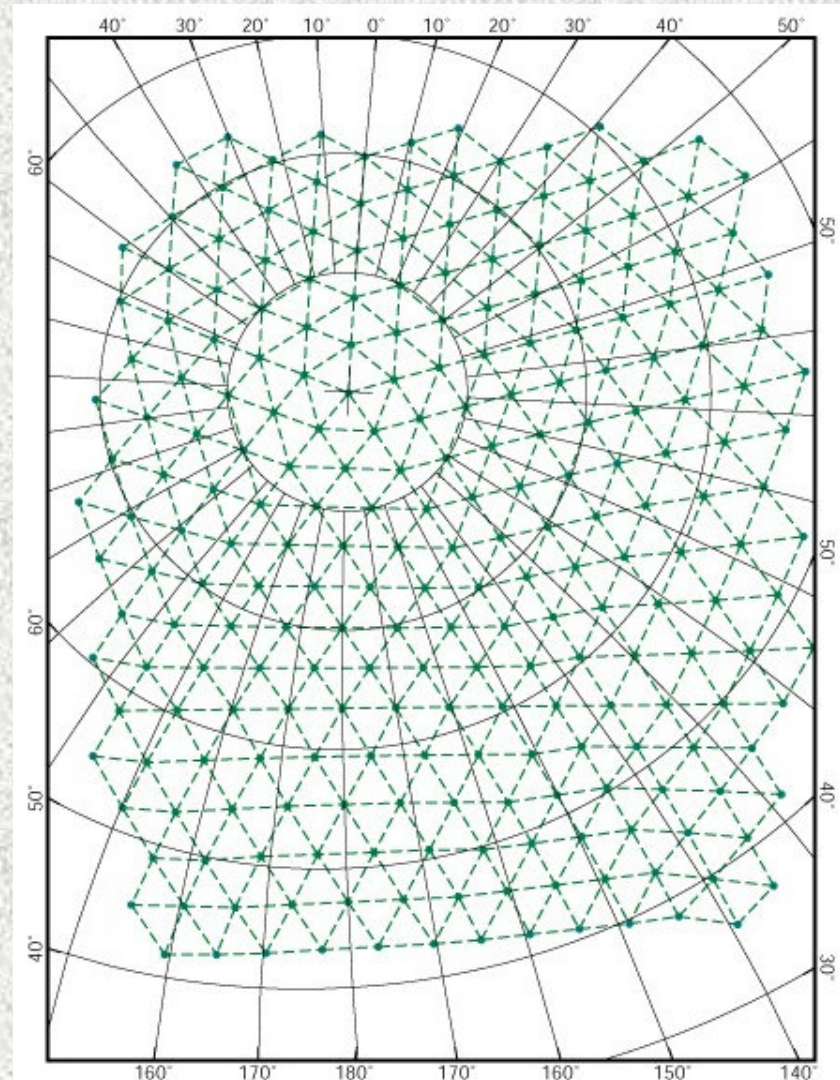


2002/2009

Support from NSF & USGS are gratefully acknowledged.

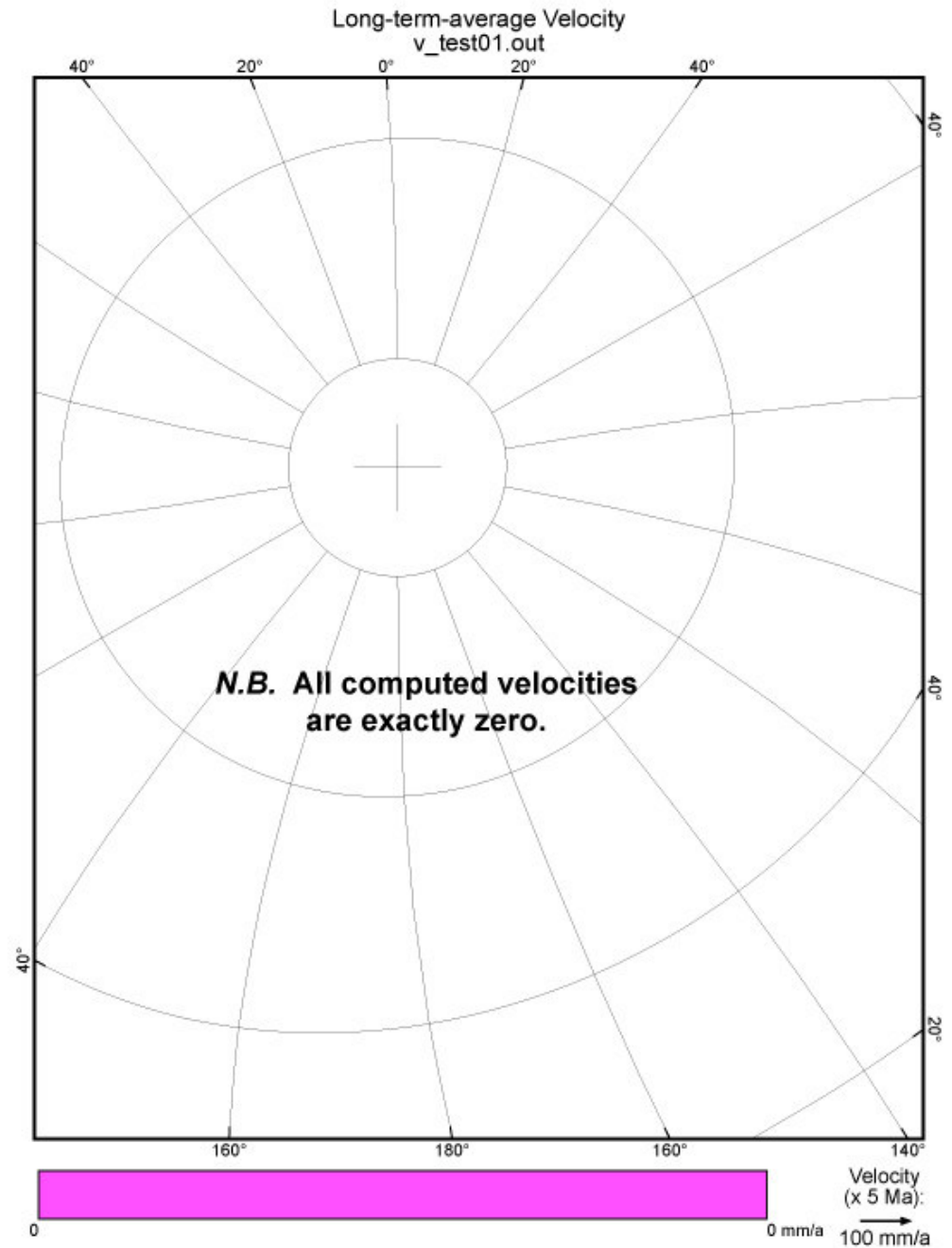


Many grids used for testing overlap the pole and the international date line. Thus, they demonstrate nicely that there are no singularities, and that the spherical algebra was done correctly.



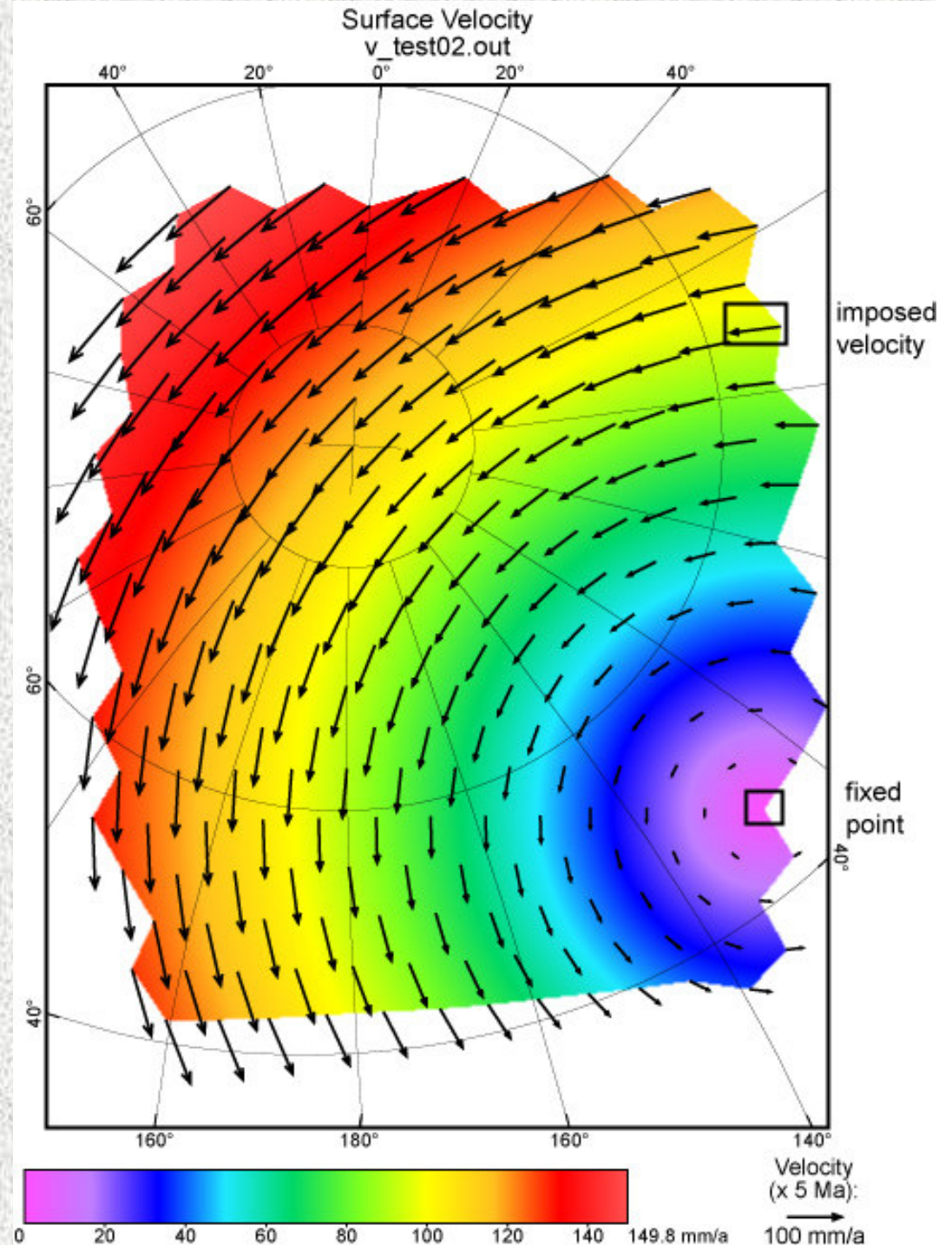
TEST01:

No input data,
zero velocity at
two nodes →
static solution.



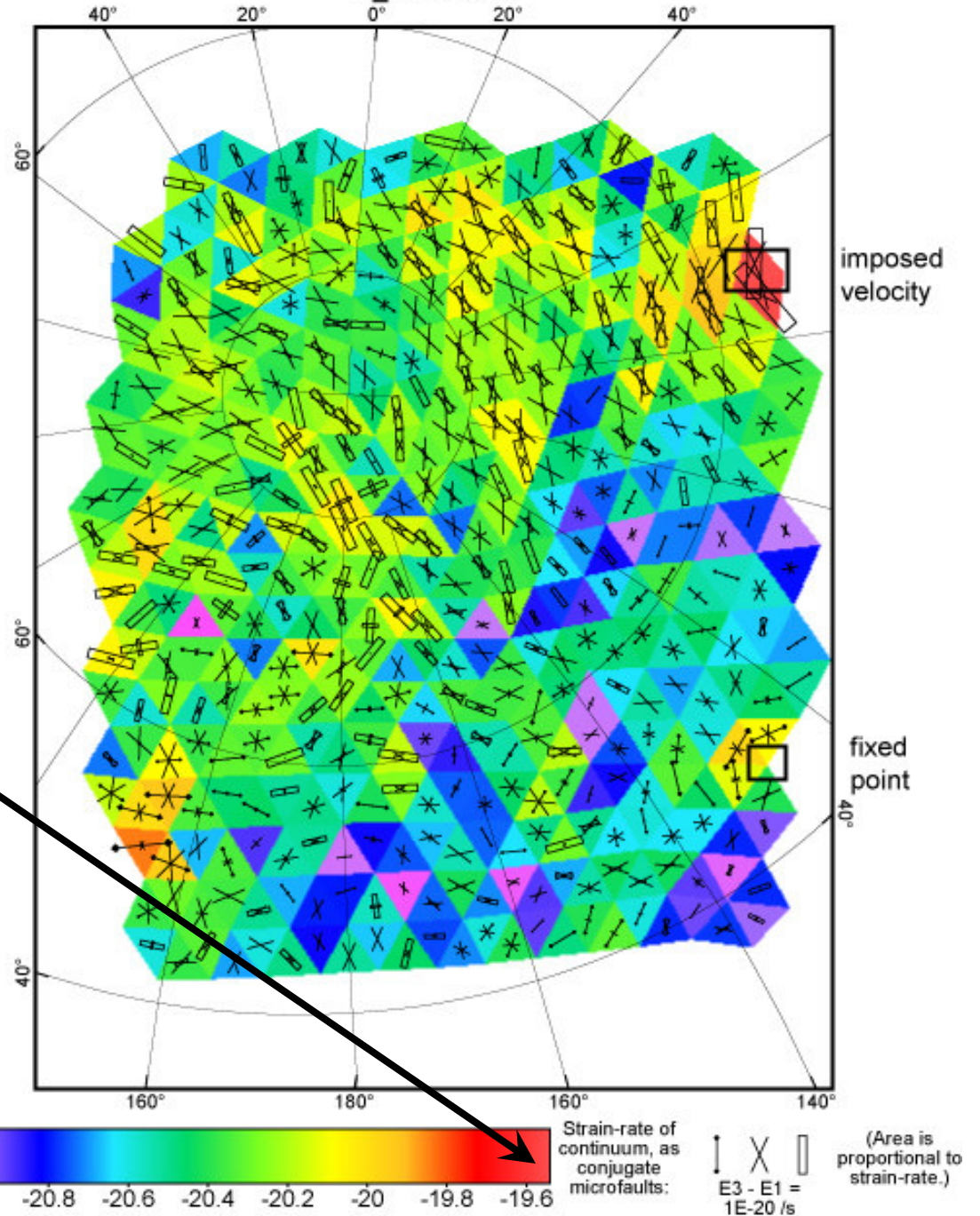
TEST02:

No input data,
one fixed node,
and one
boundary node
that rotates
around it.



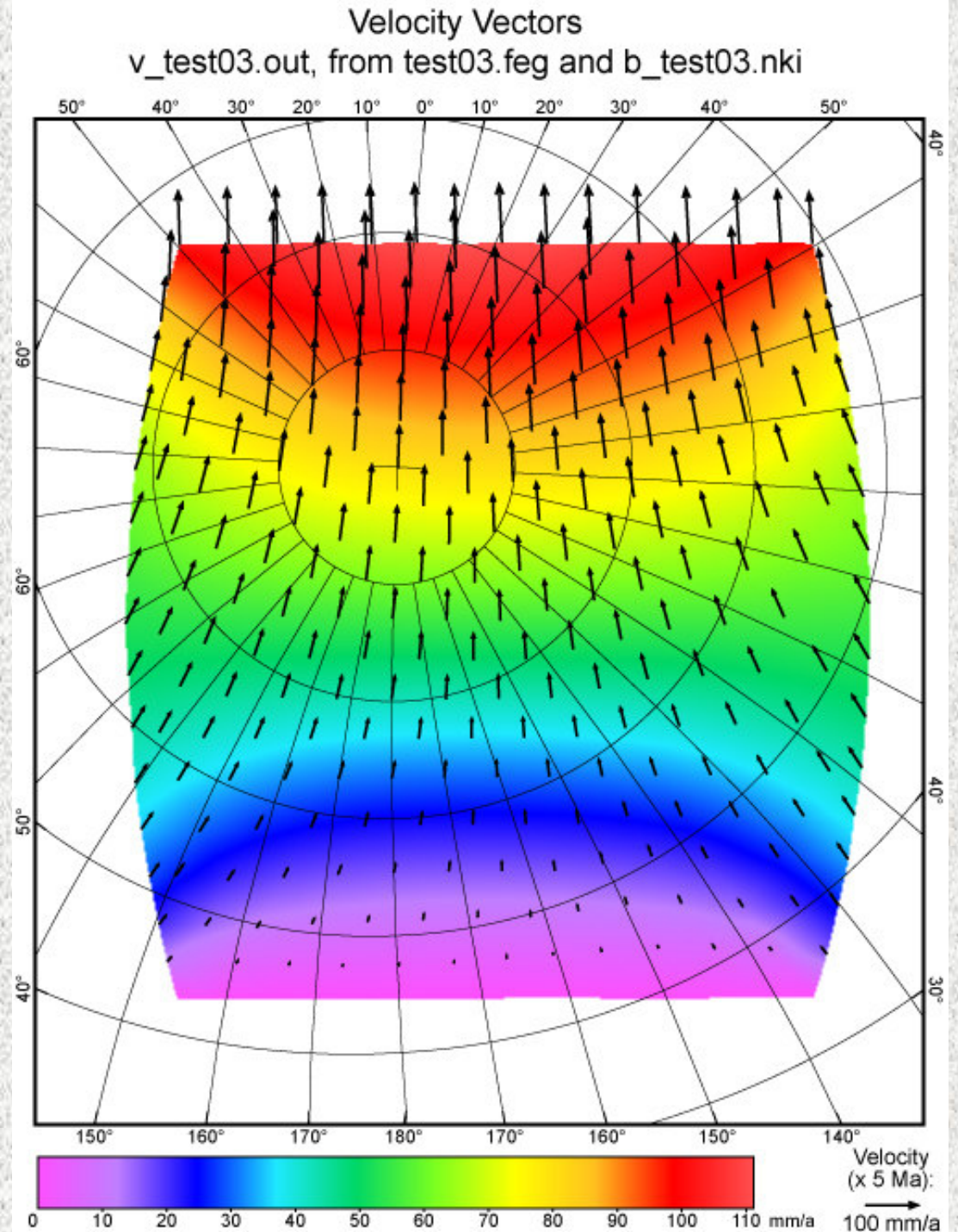
Note: Maximum strain-rate of 2×10^{-20} /s = 0.3% in 4 Ga.

Common Log of [Largest (Absolute Value) Principal Strain-Rate * 1 s]
v_test02.out

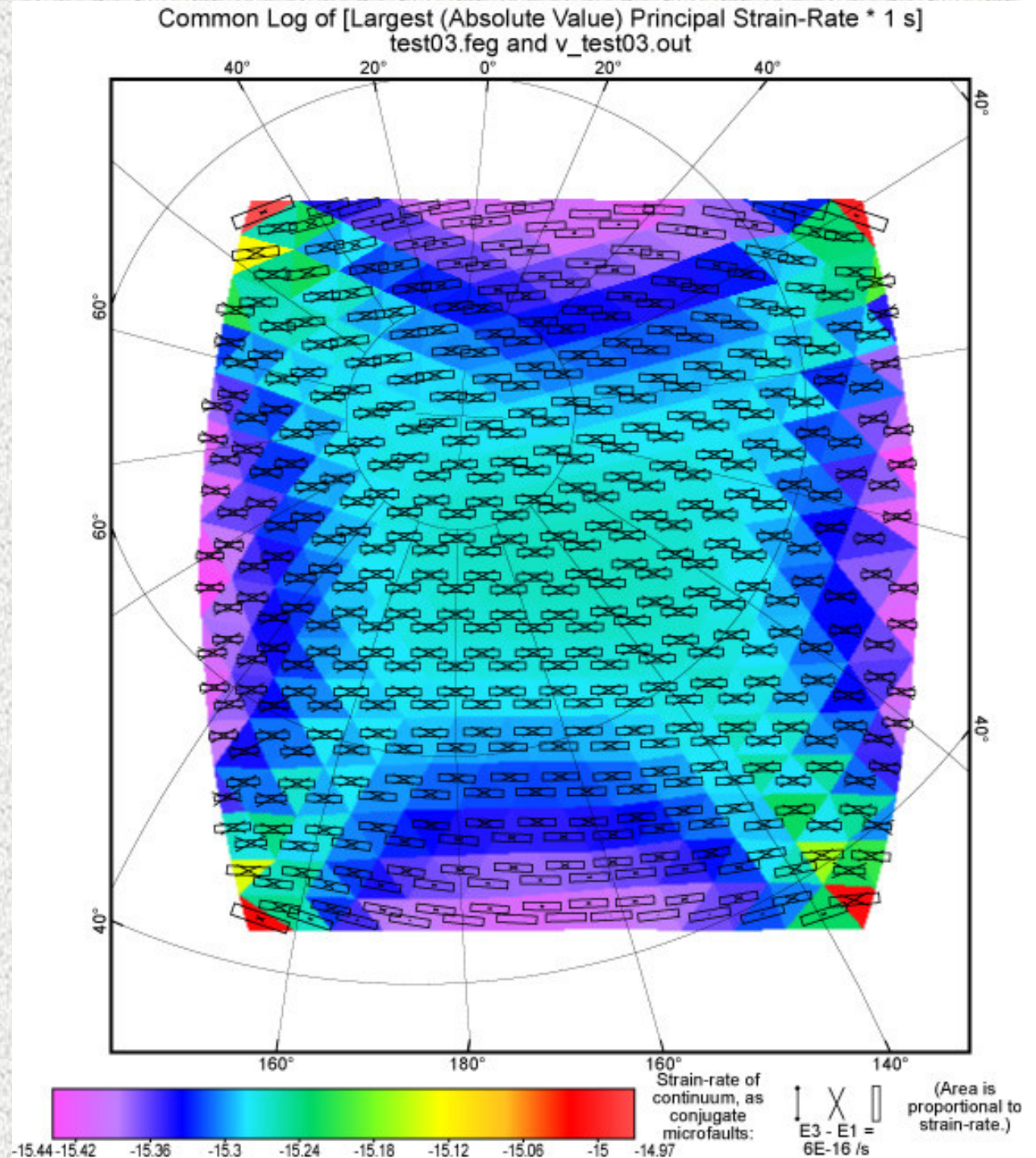


TEST03:

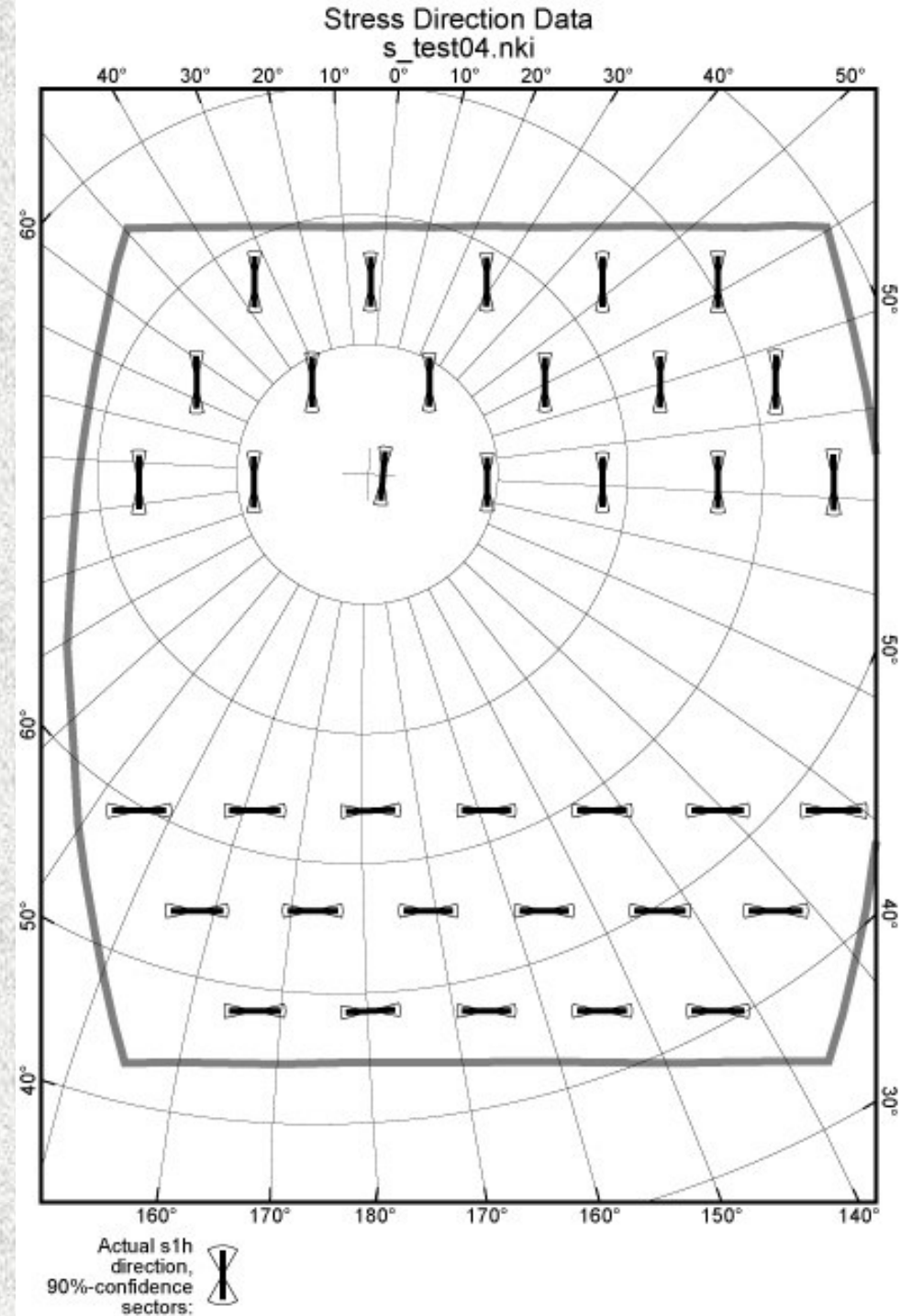
No input data,
uniform
extension driven
by boundary
conditions.



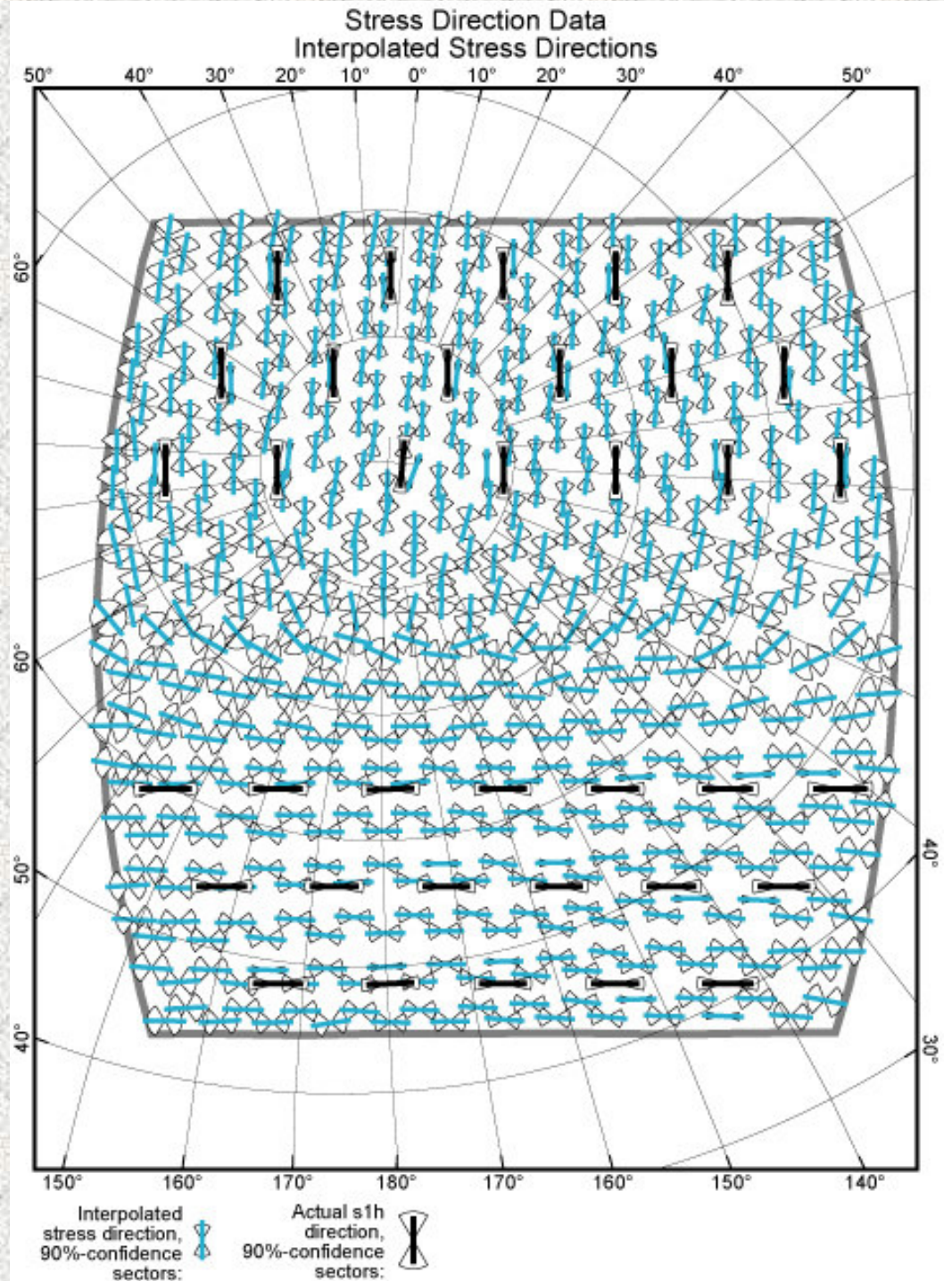
Note: In absence of data, lithosphere behaves as a uniform viscous sheet. Therefore, in uniform stress field far from BCs, it undergoes equal vertical and horizontal shortening.



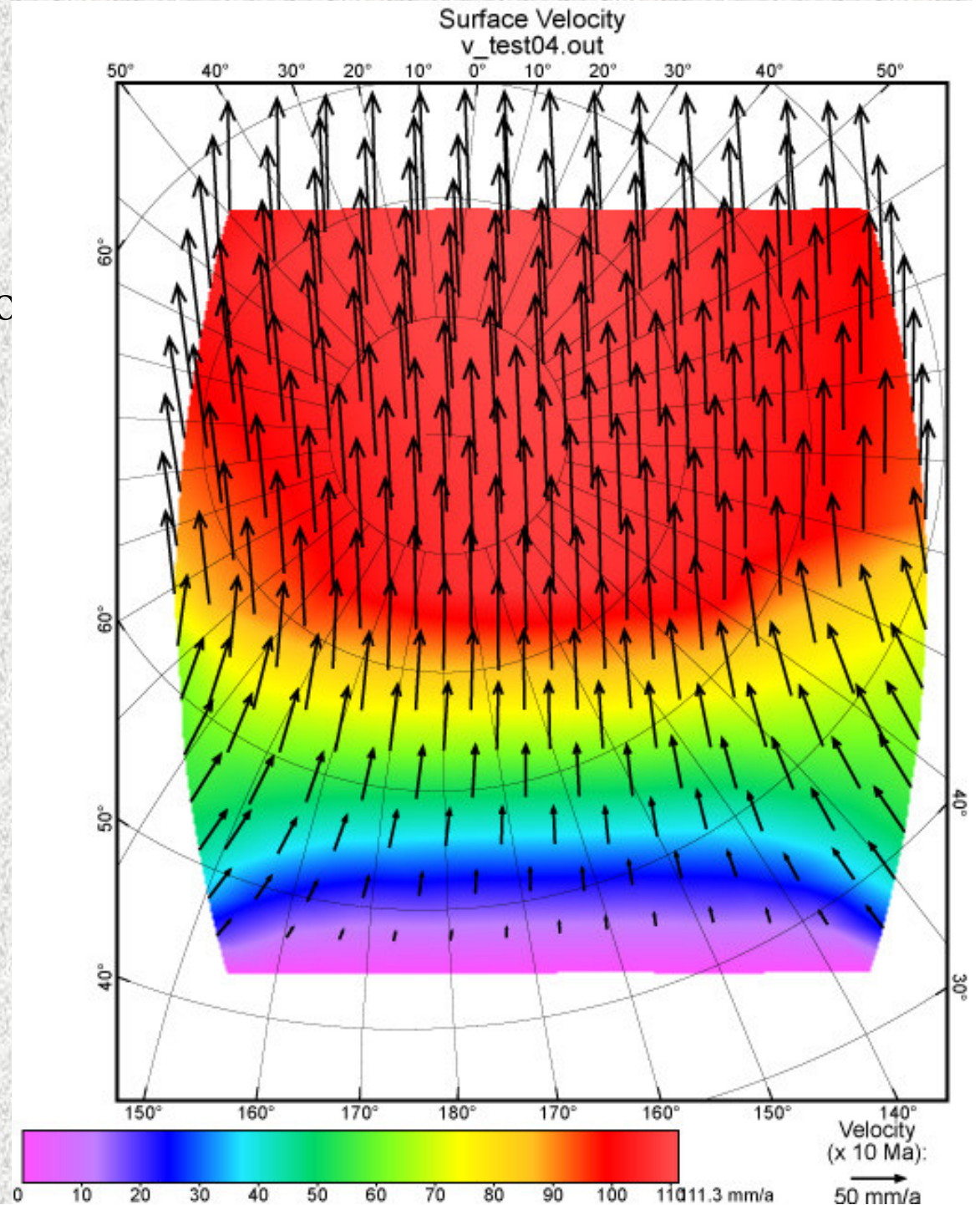
TEST04:
Data on the azimuth of the
most-compressive
horizontal principal stress
are given:



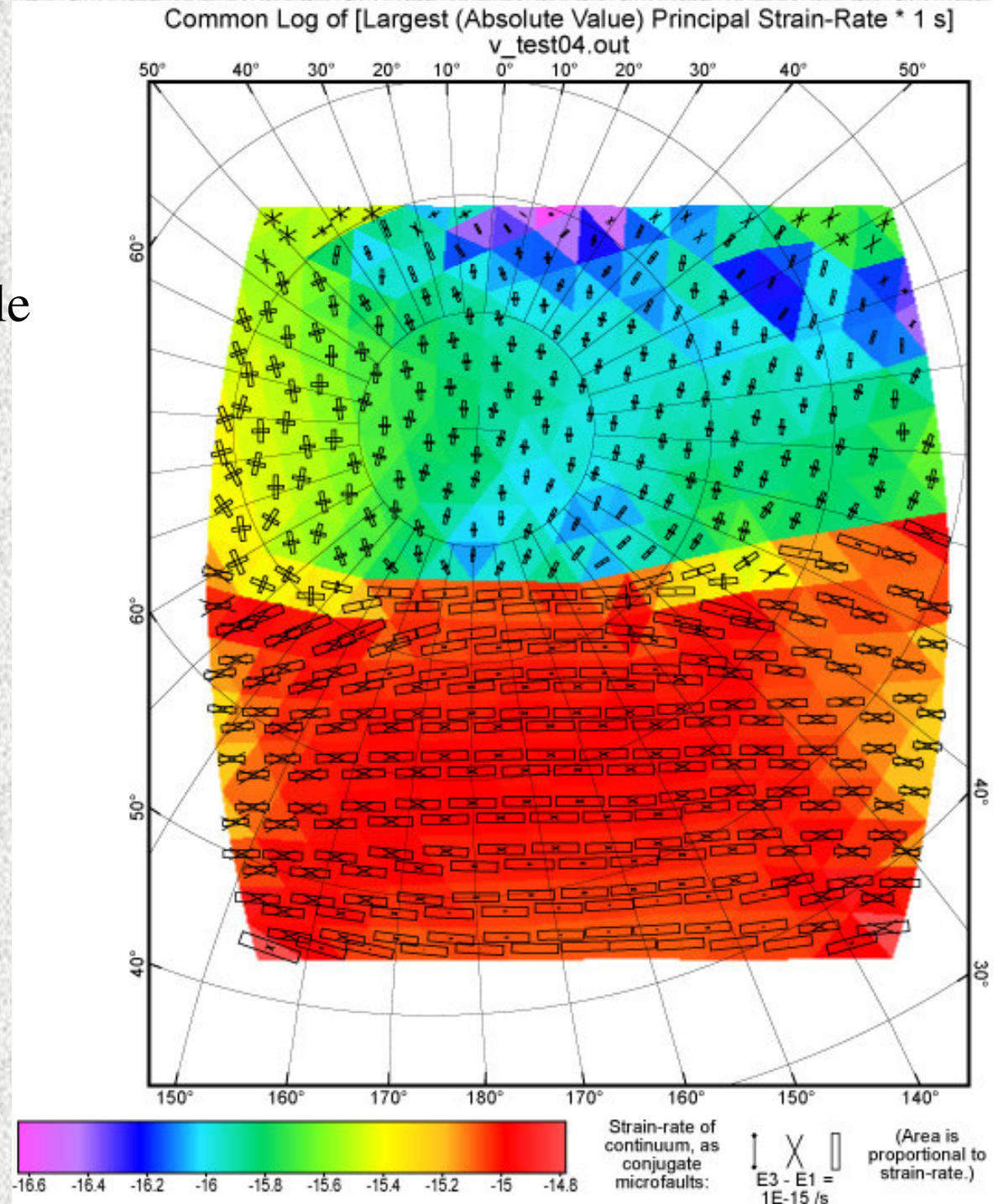
and **NeoKinema** interpolates these directions by the algorithm of *Bird & Li* [1996]:



When the same velocity boundary conditions are given (as in Test03), **NeoKinema** attempts to find a velocity solution that will honor these interpolated directions:

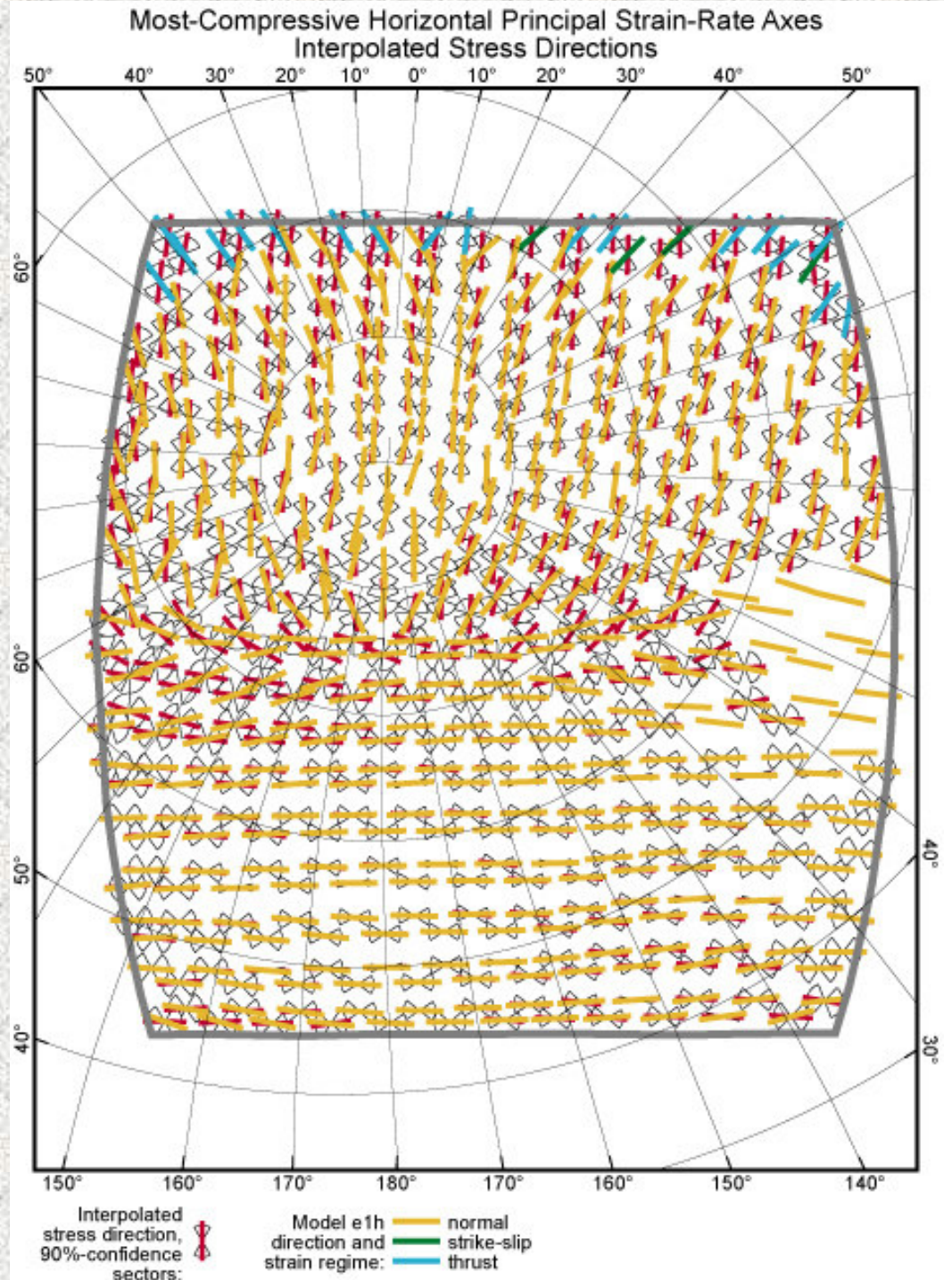


The new solution has nonuniform strain-rates (large where stress directions are compatible with the velocity BCs; small elsewhere):



and here is the (mis)match between the principal strain-rate azimuths of the solution and the target azimuths derived from the stress data:

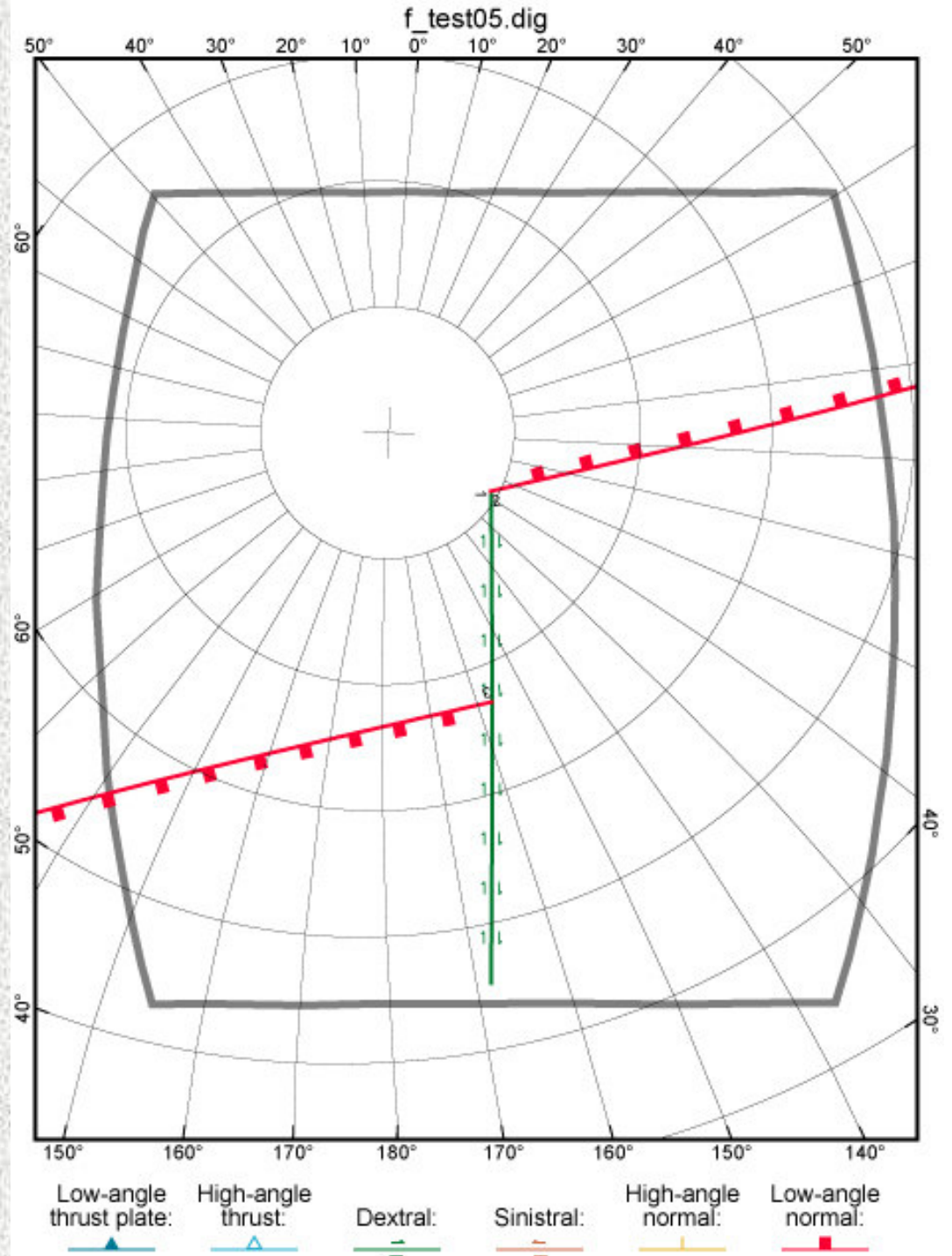
(Note that many of the red target azimuths are hidden by the yellow actual azimuths.)



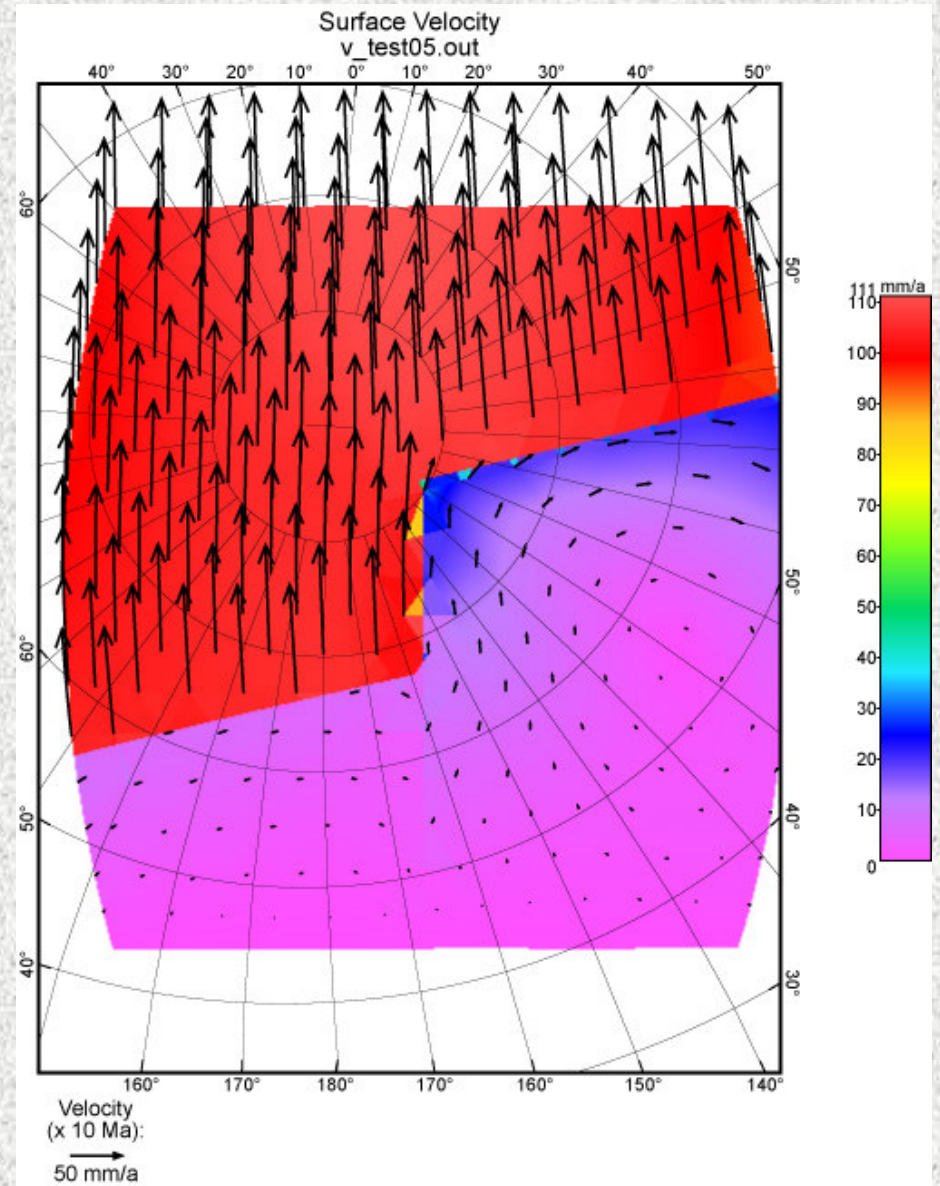
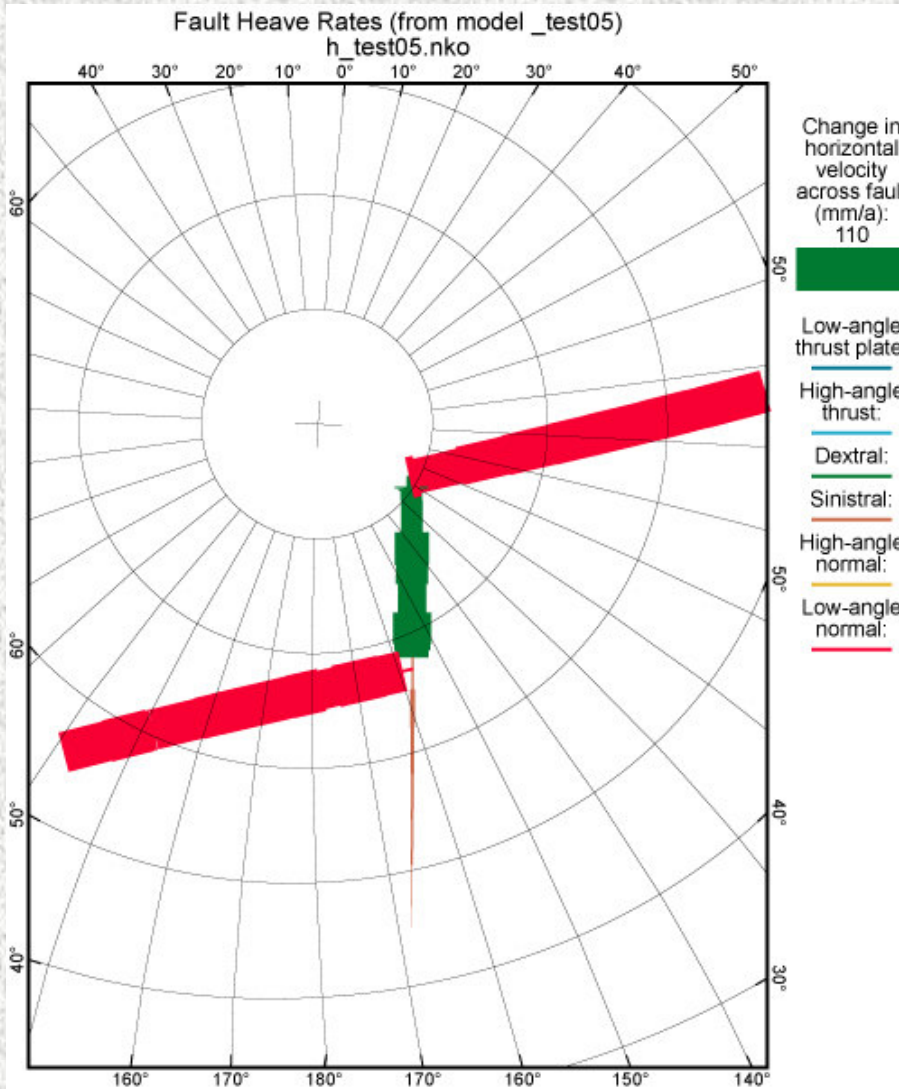
TEST05:

Three faults of unknown slip-rate make up a plate boundary system. Each dip-slip fault has assumed rake of -90° .

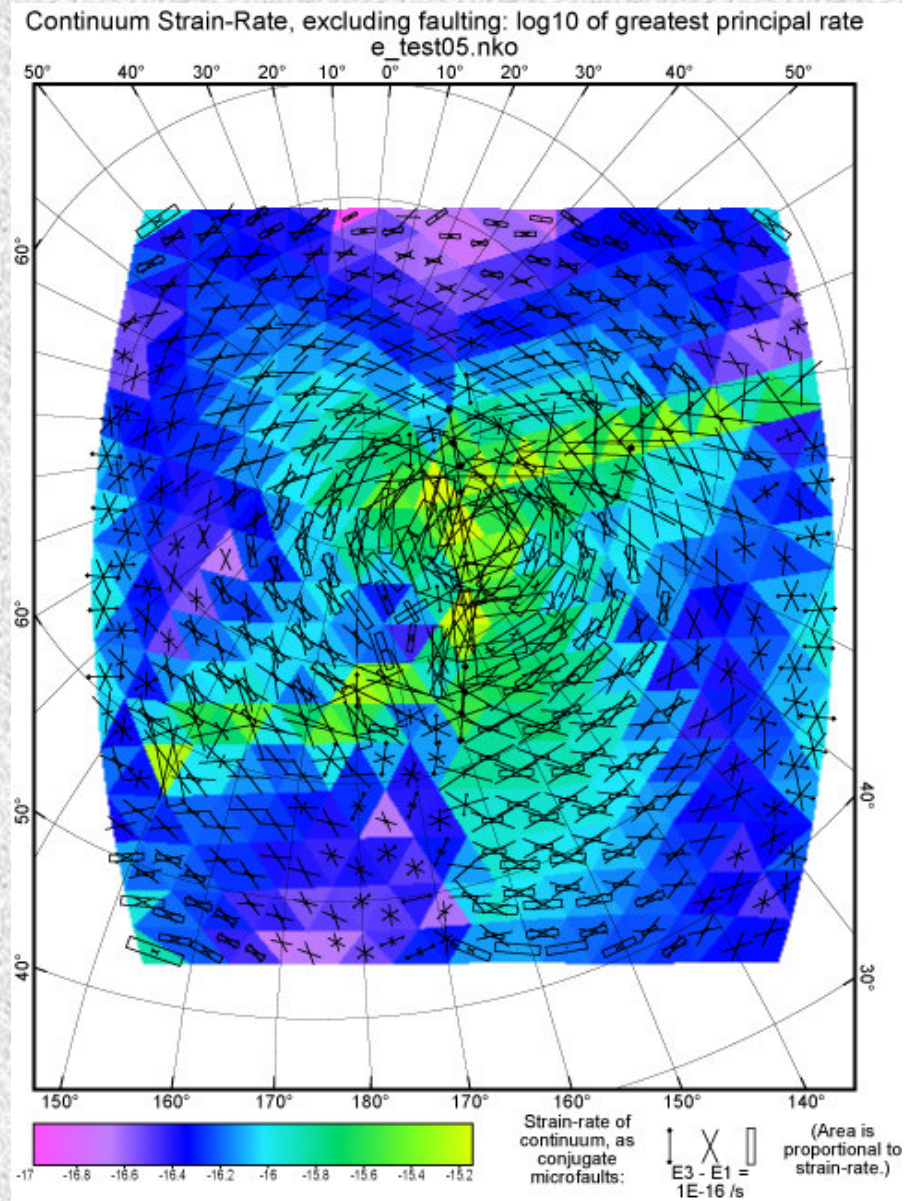
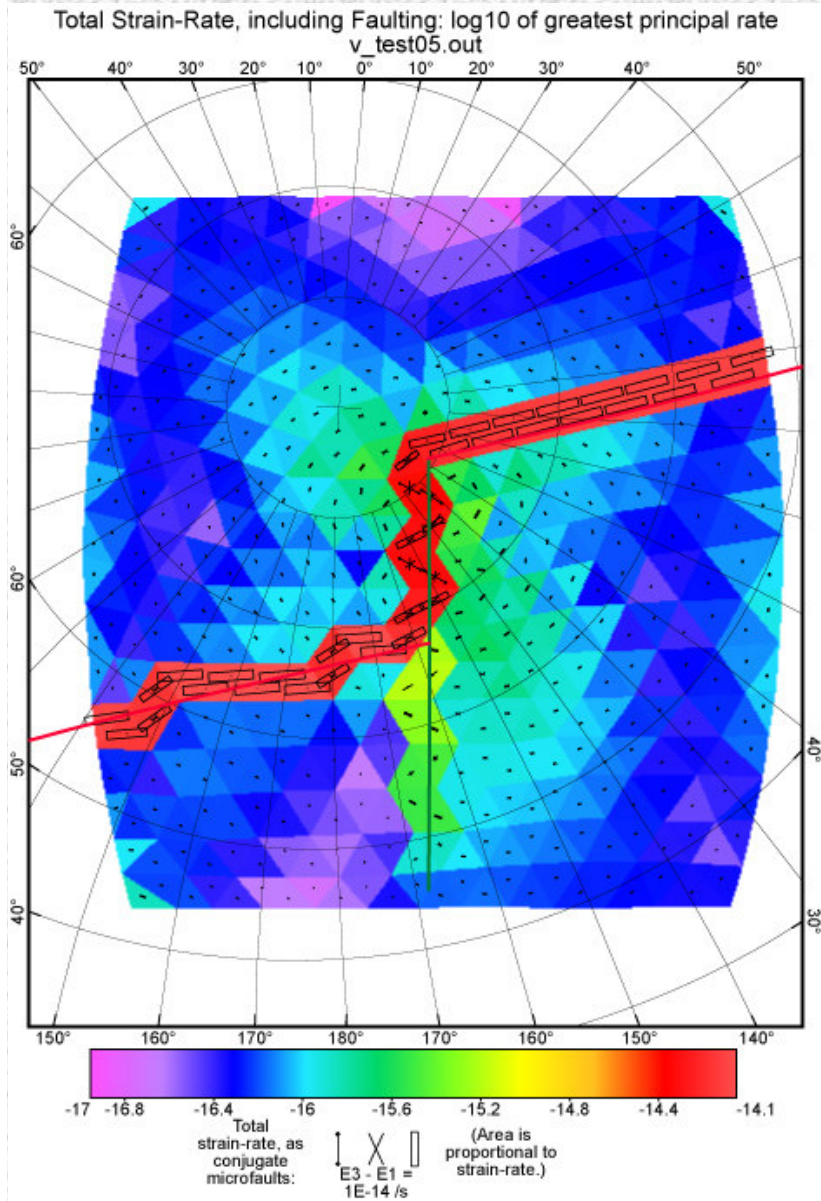
(Same velocity BCs as in Test03; however, no stress-direction data as in Test04.)



NeoKinema finds a solution with most of the deformation assigned to slip on the faults:

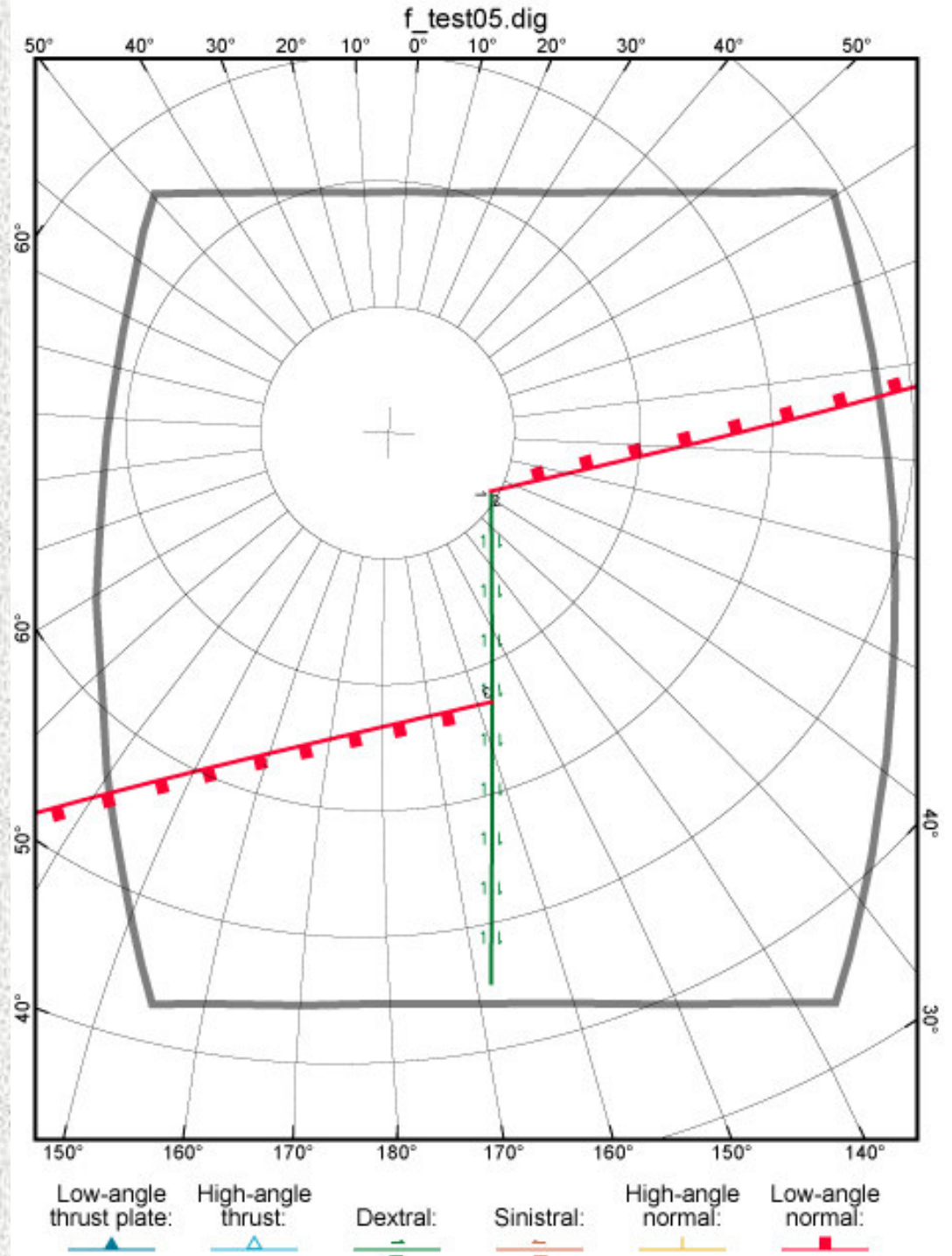


However, the requirement of purely dip-slip faulting on the two normal faults requires some significant continuum strain-rates:

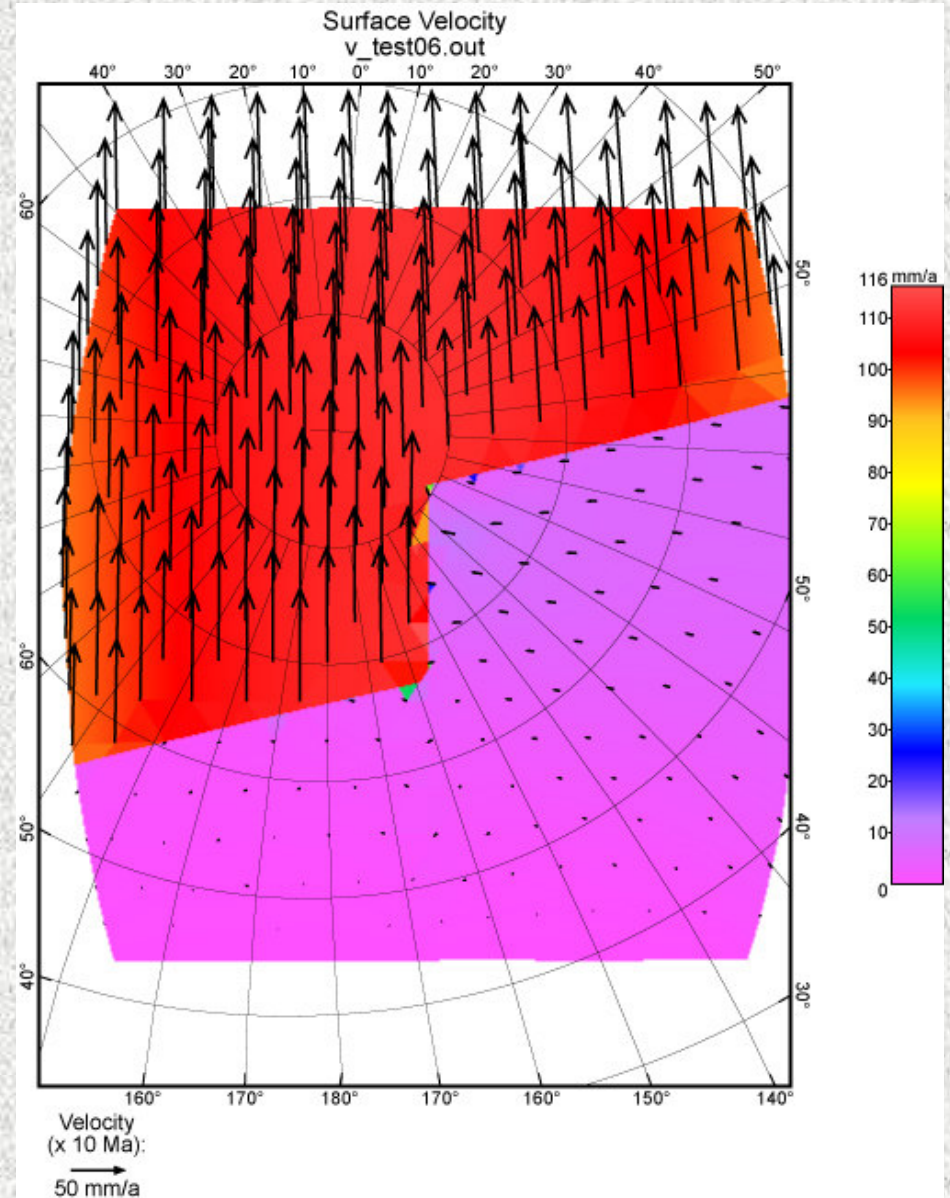
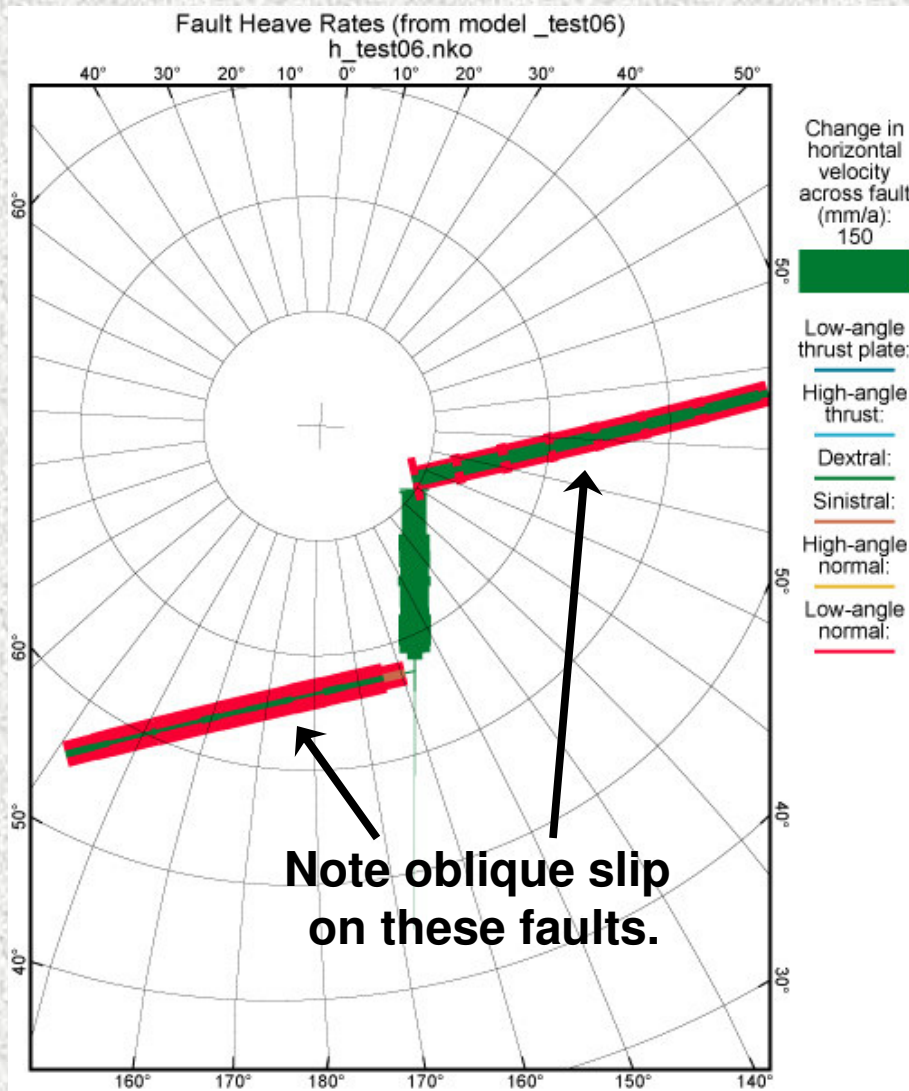


TEST06:

The same 3 faults of unknown slip-rate make up a plate boundary system. But now, each dip-slip fault has assumed rake of $-90^\circ \pm 20^\circ$ ($\pm\sigma$). (Same velocity BCs as in Tests03~05.)



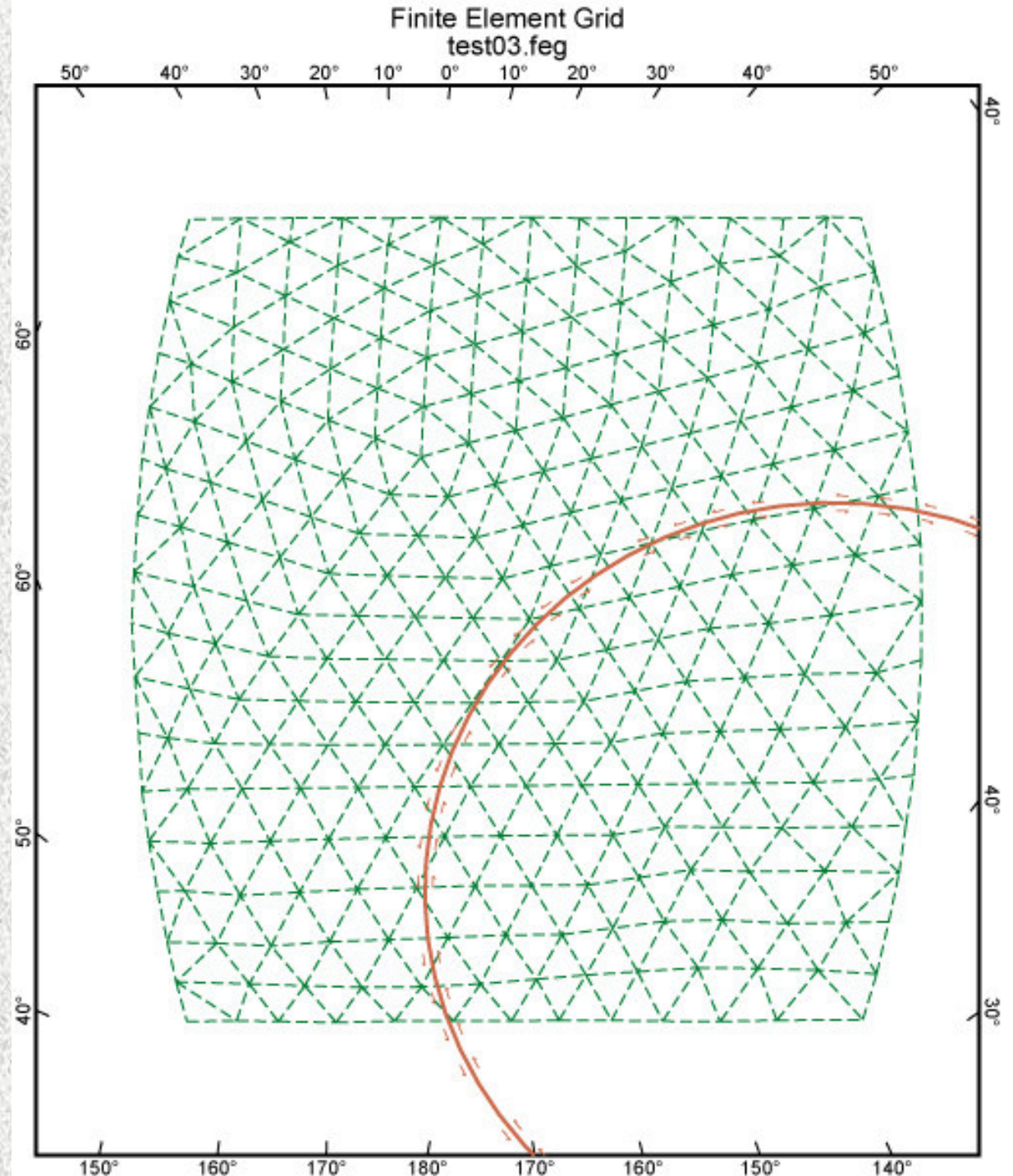
NeoKinema finds a solution with virtually all of the deformation assigned to slip on the faults, and continuum strain-rates are smaller:



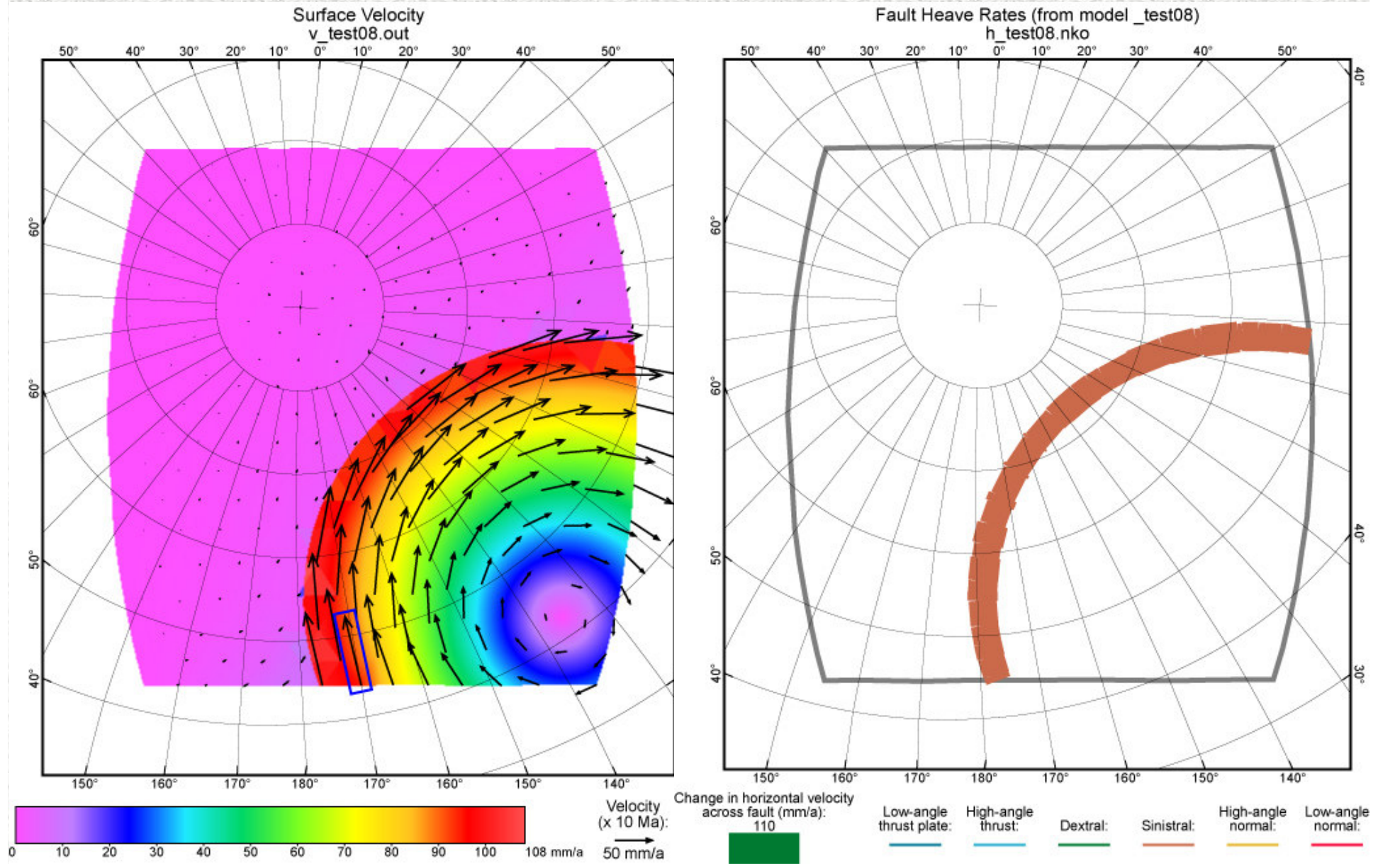
TEST08:

A strike-slip fault whose trace is a small circle is entered with unknown slip rate.

(Note that it is *not* necessary to outline fault zones with slender elements, although one may choose to do so.)



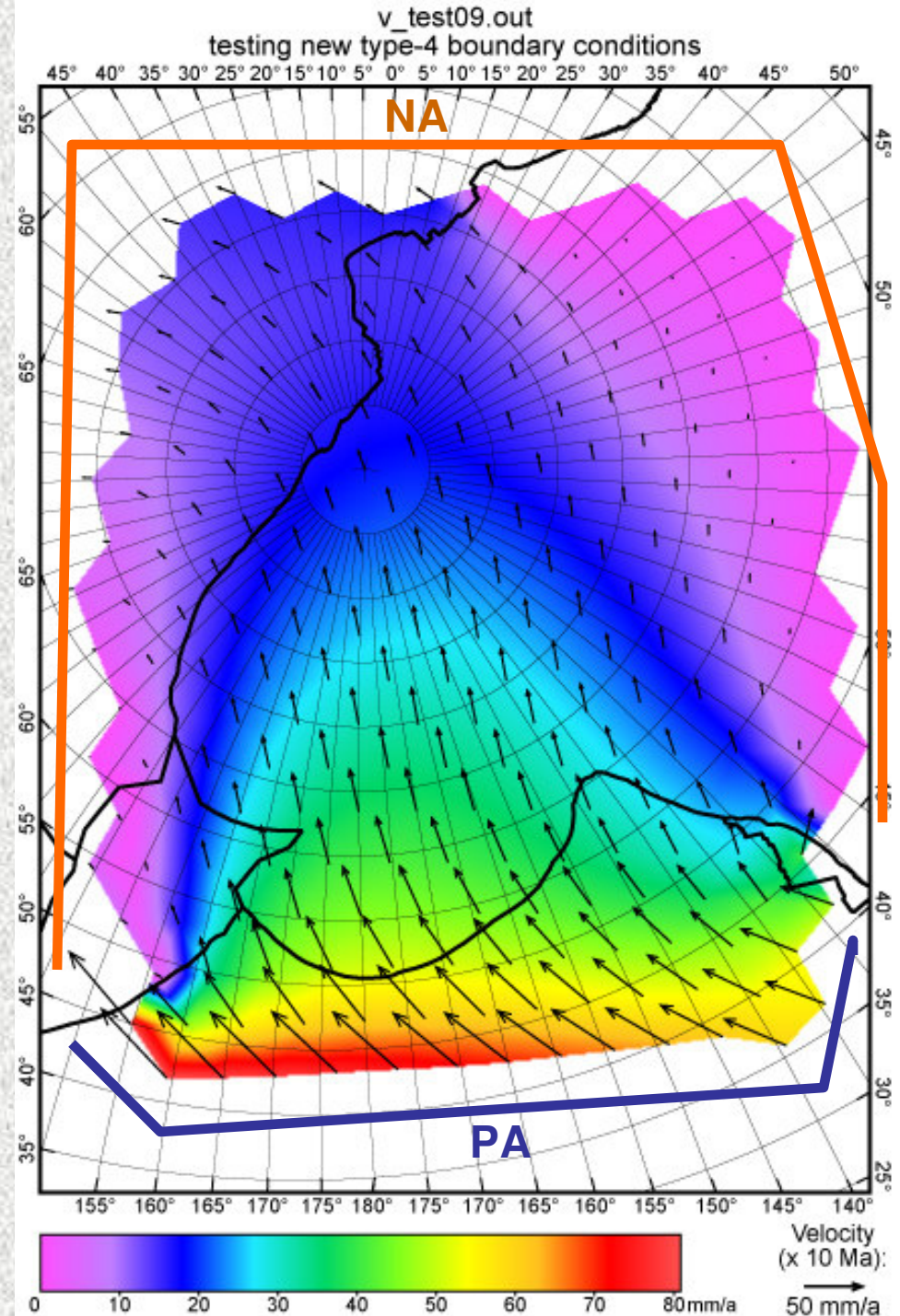
When the solution is driven indirectly by velocity at one node, the solution is Eulerian plate tectonics, with minimal strain-rates:



TEST09:

Example of a convenience feature, the type-4 boundary condition, which allows boundary nodes to be assigned to a major plate by simply giving its abbreviation (e.g., “NA”, “PA”); the necessary velocity is calculated within **NeoKinema** by the Euler formula.

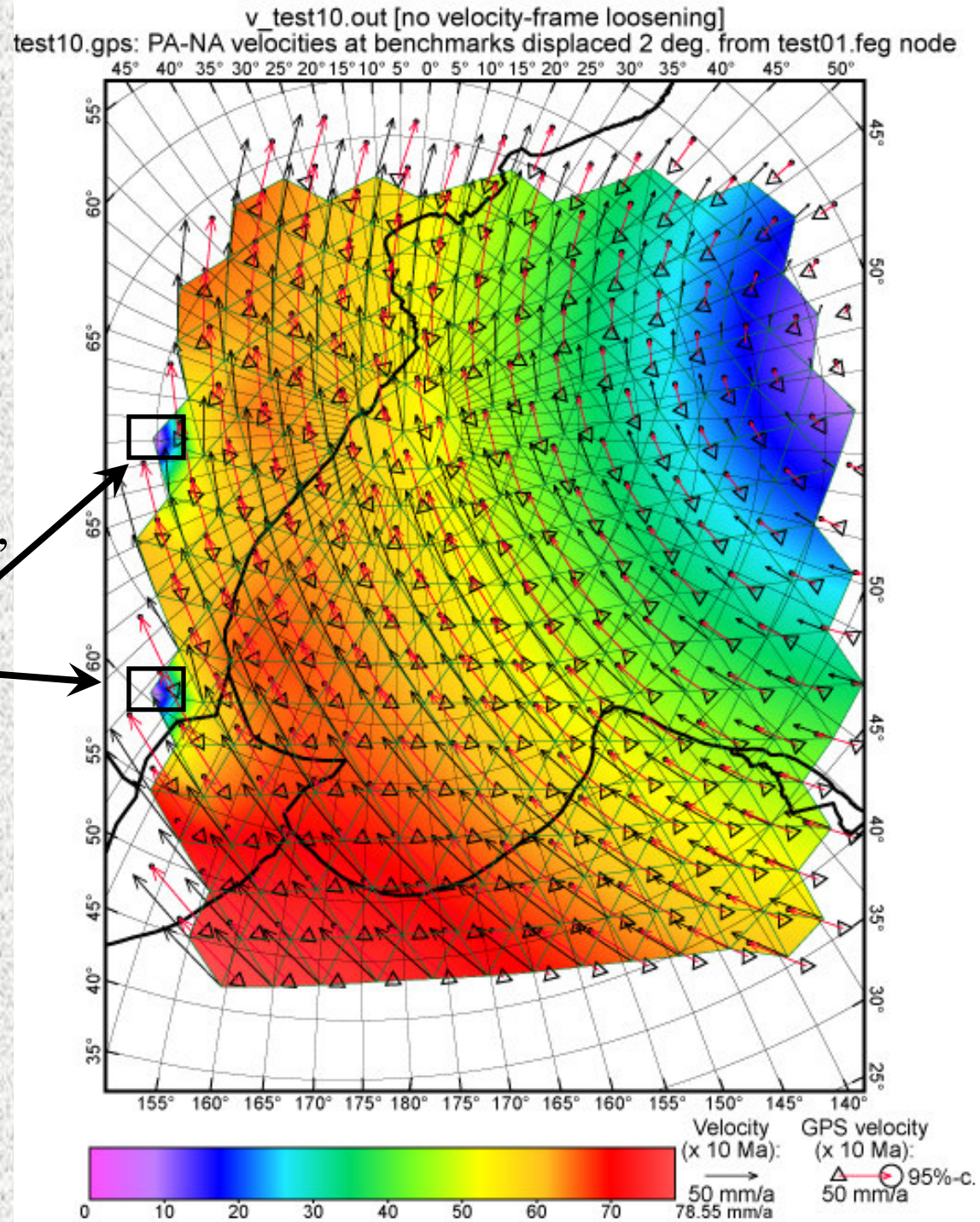
(Note: Lacking any data, the program finds a uniform-viscous-sheet solution to this problem.)



TEST10:

Synthetic GPS velocities, which are consistent with uniform plate rotation, are input at many internal points.

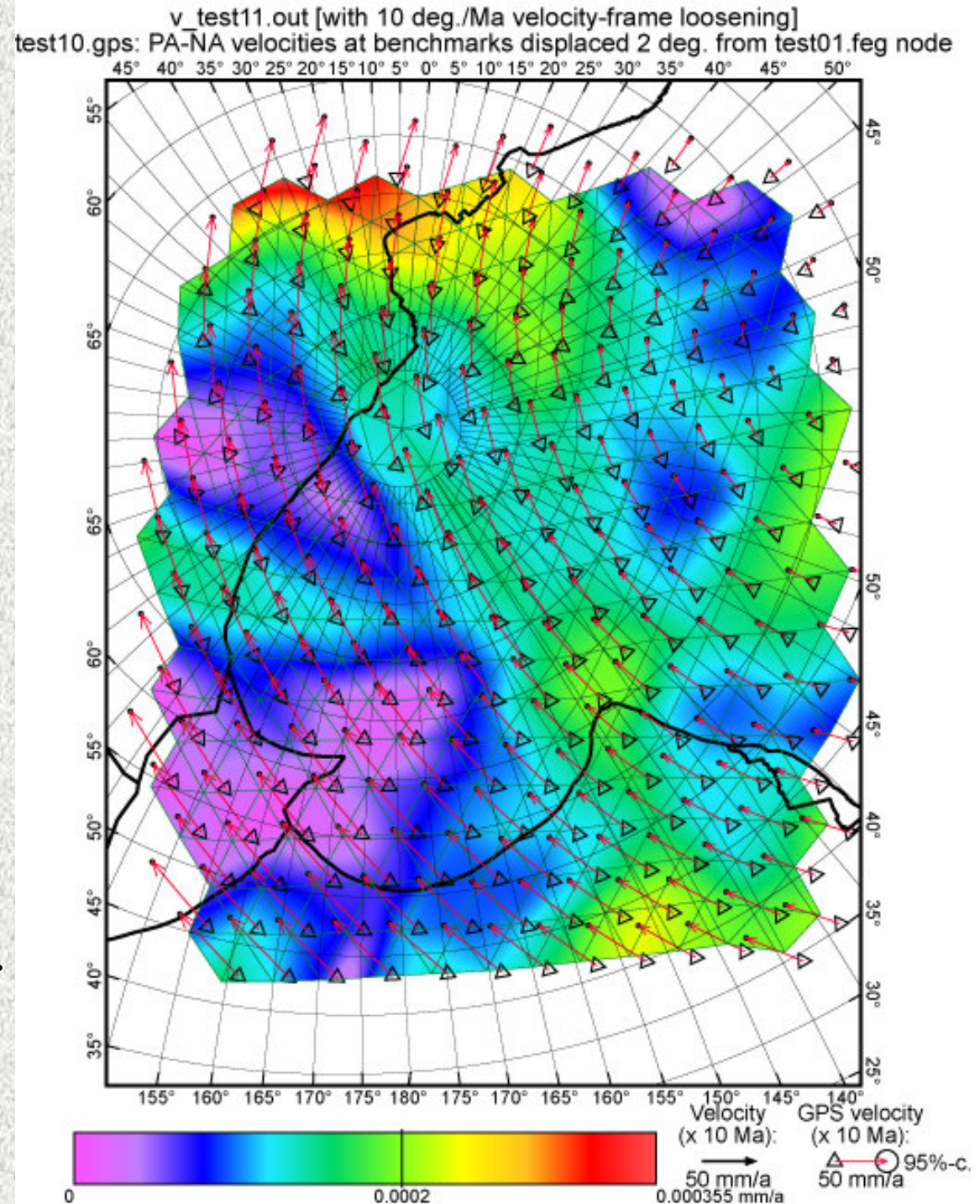
Model boundaries are free, except at 2 boundary nodes which are fixed:



TEST11:

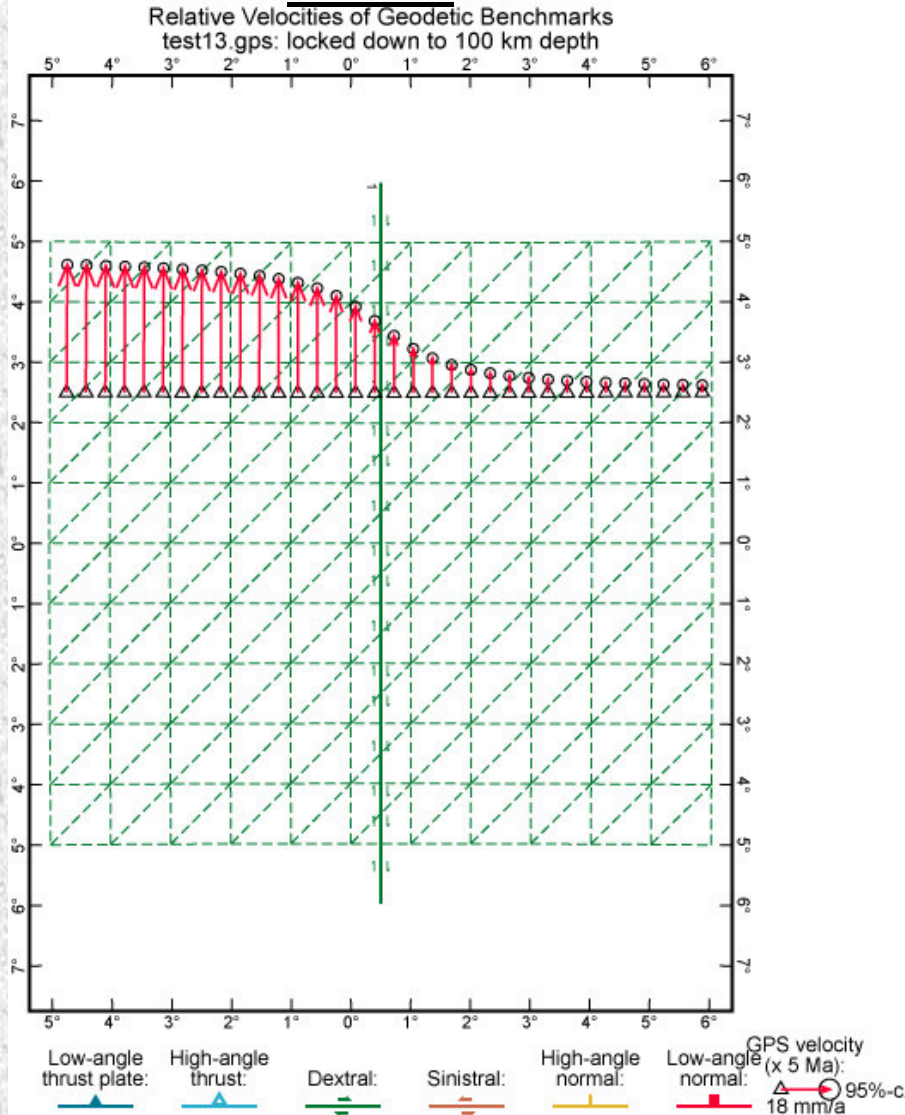
Same as Test10, except that now the velocity reference frame of the GPS data is treated as unknown, or free-floating.

The result is that the velocity reference frame is determined by the 2 fixed boundary nodes, and all motion is reduced to less than 0.0004 mm/a.

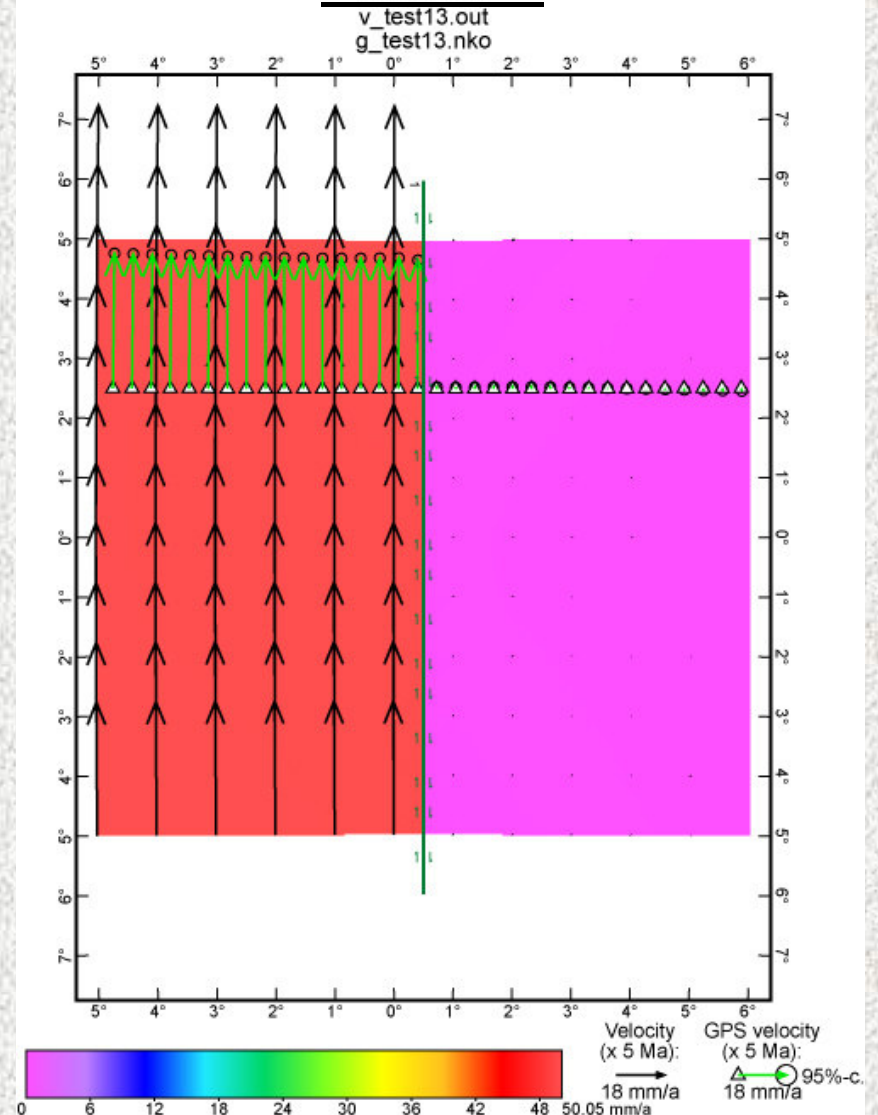


TEST13: Conversion of input short-term GPS velocities (left) to long-term corrected velocities (right), along a strike-slip fault which is temporarily locked down to 100 km depth. (In this test, velocity BCs “enforce” the right plate-motion solution.)

INPUT:



OUTPUT:

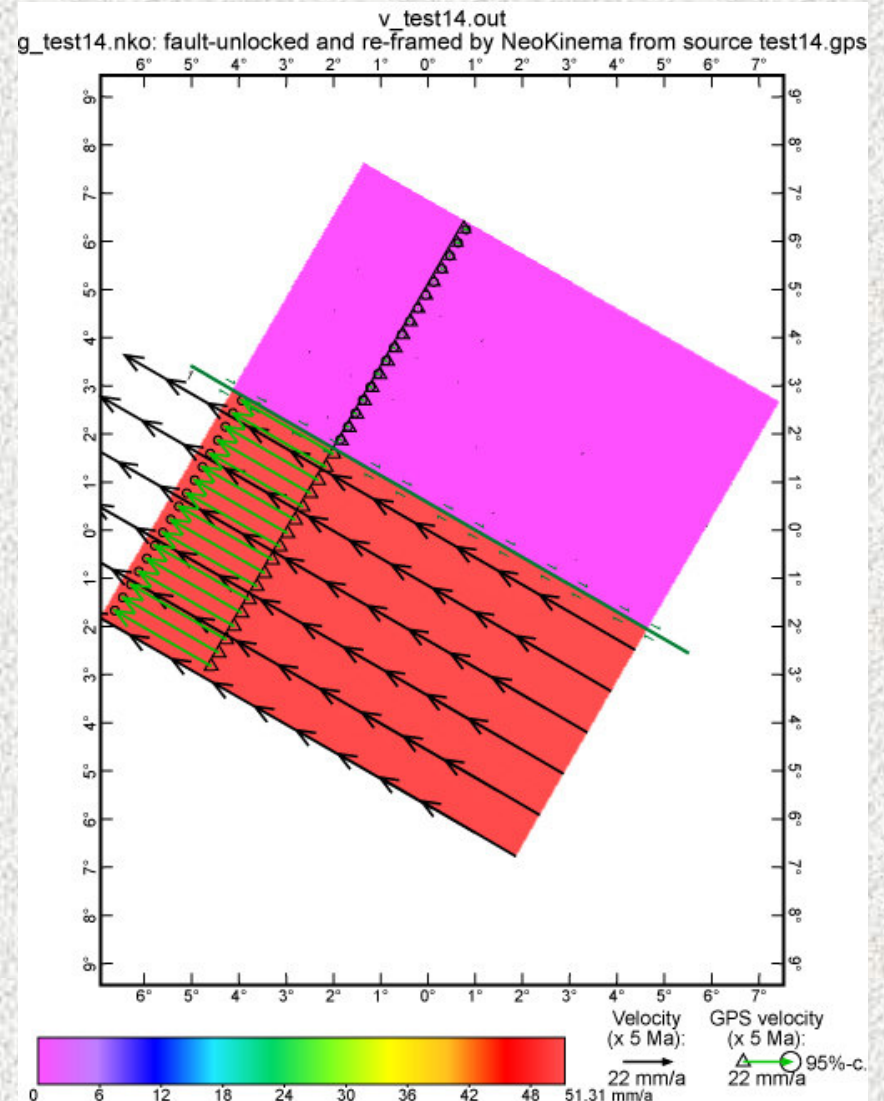
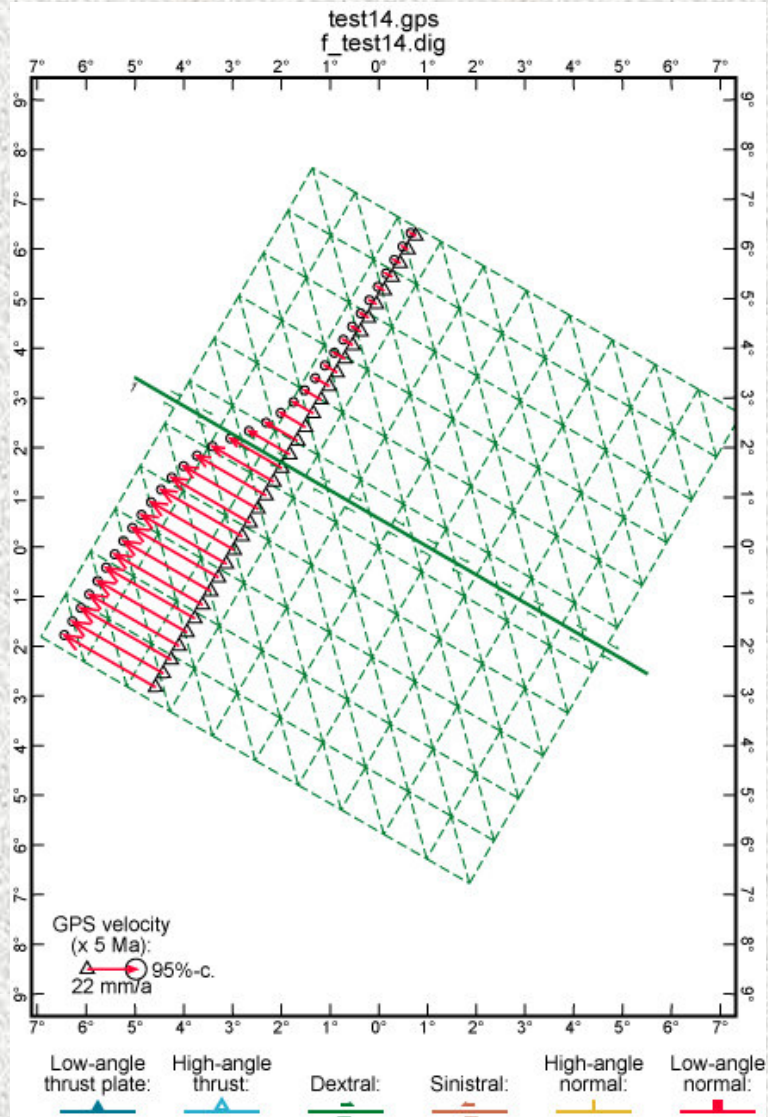


TEST14: Conversion of input short-term GPS velocities (left) to long-term corrected velocities (right), along a strike-slip fault which is temporarily locked down to 100 km depth.

(In this test, the southwestern plate is free, and GPS data determines its velocity.)

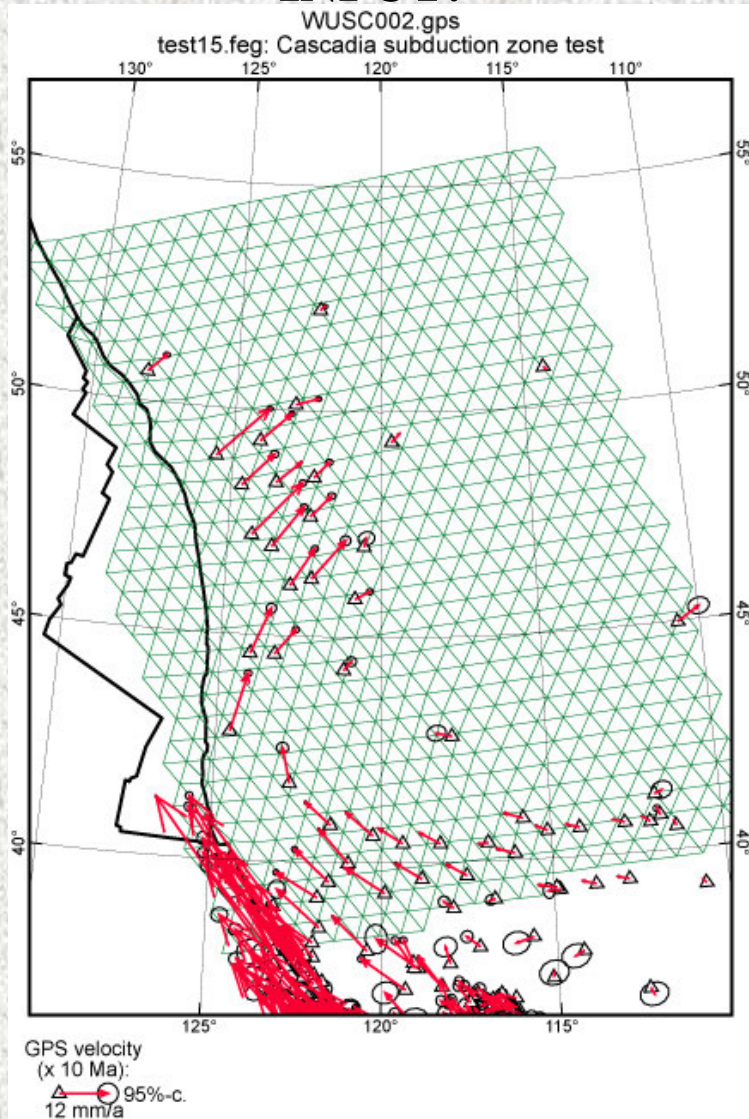
INPUT:

OUTPUT:

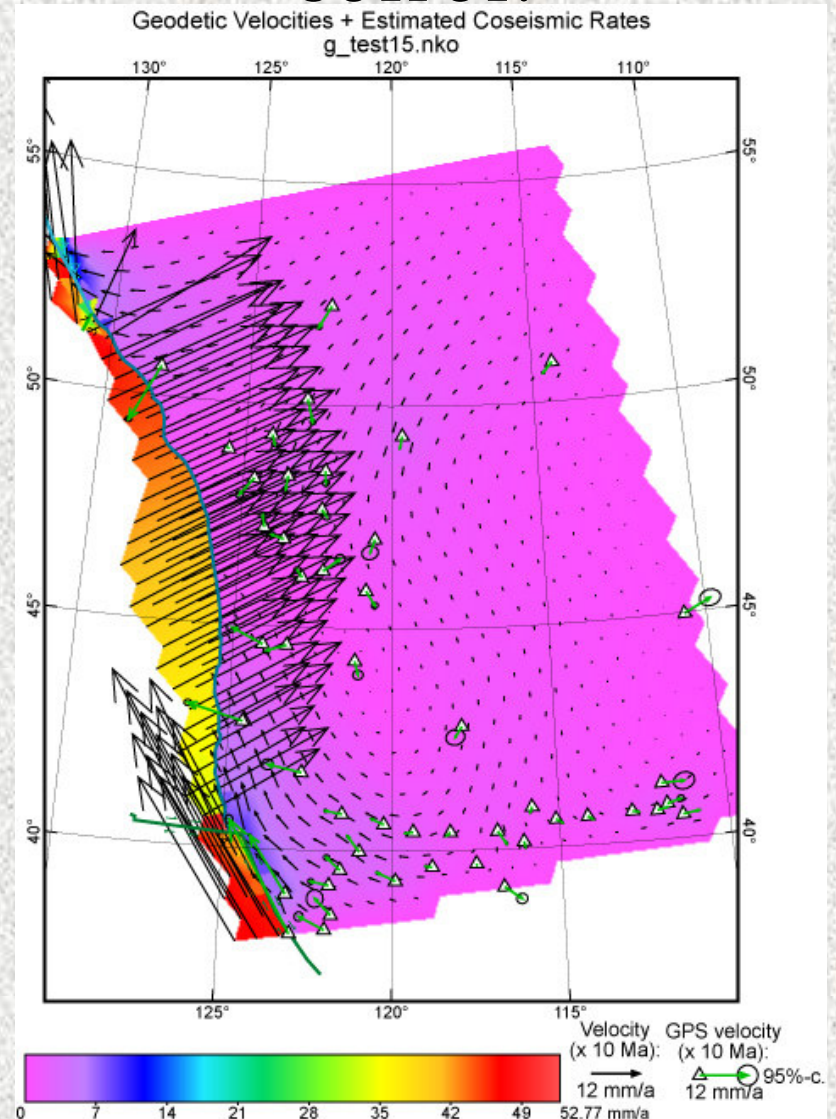


TEST15: Conversion of input short-term GPS velocities (left) to long-term corrected velocities (right), along the Cascadia subduction thrust, which is temporarily locked from 10 km to 40 km depths. (Note that long-term relative velocities within NA are less than short-term.)

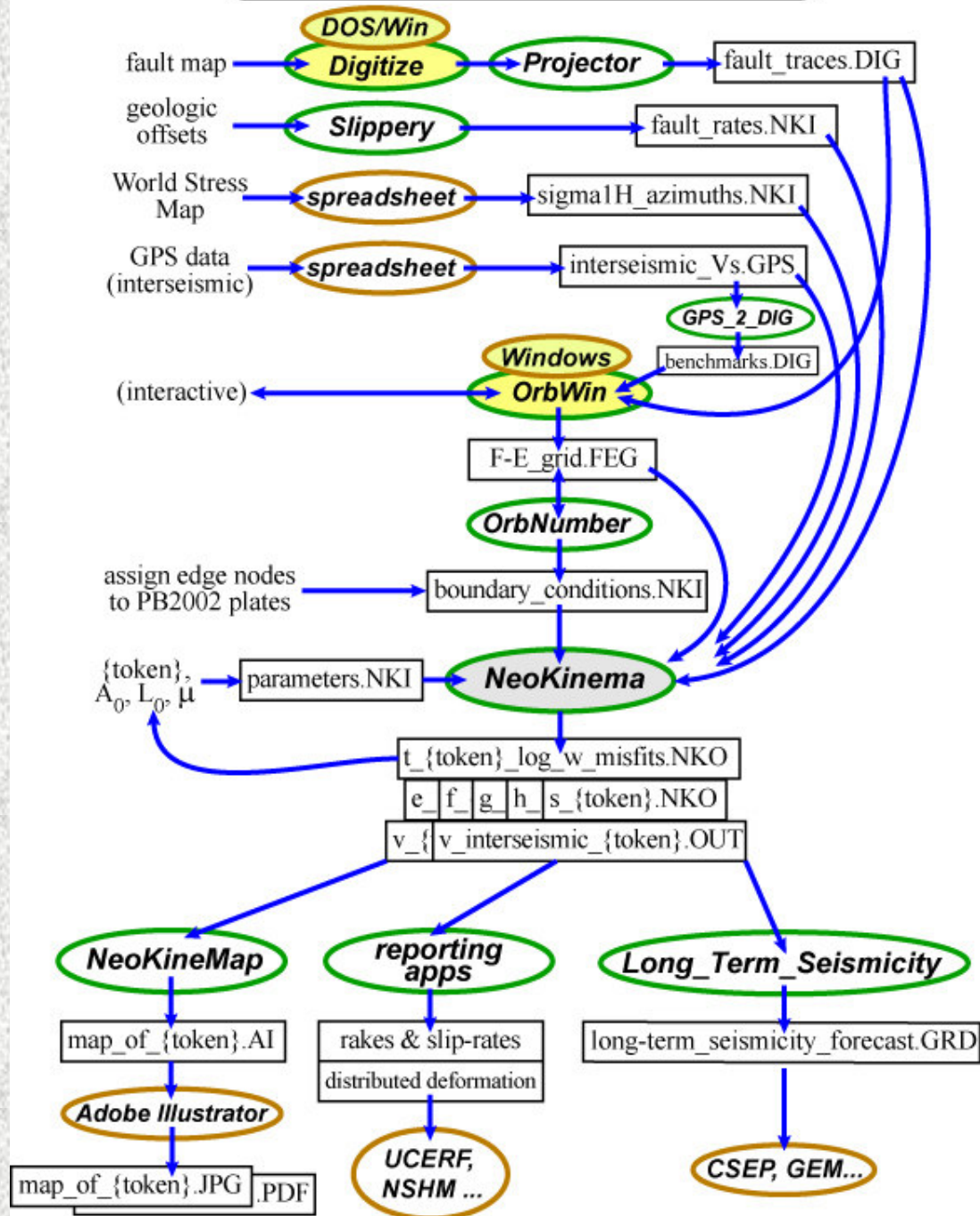
INPUT:



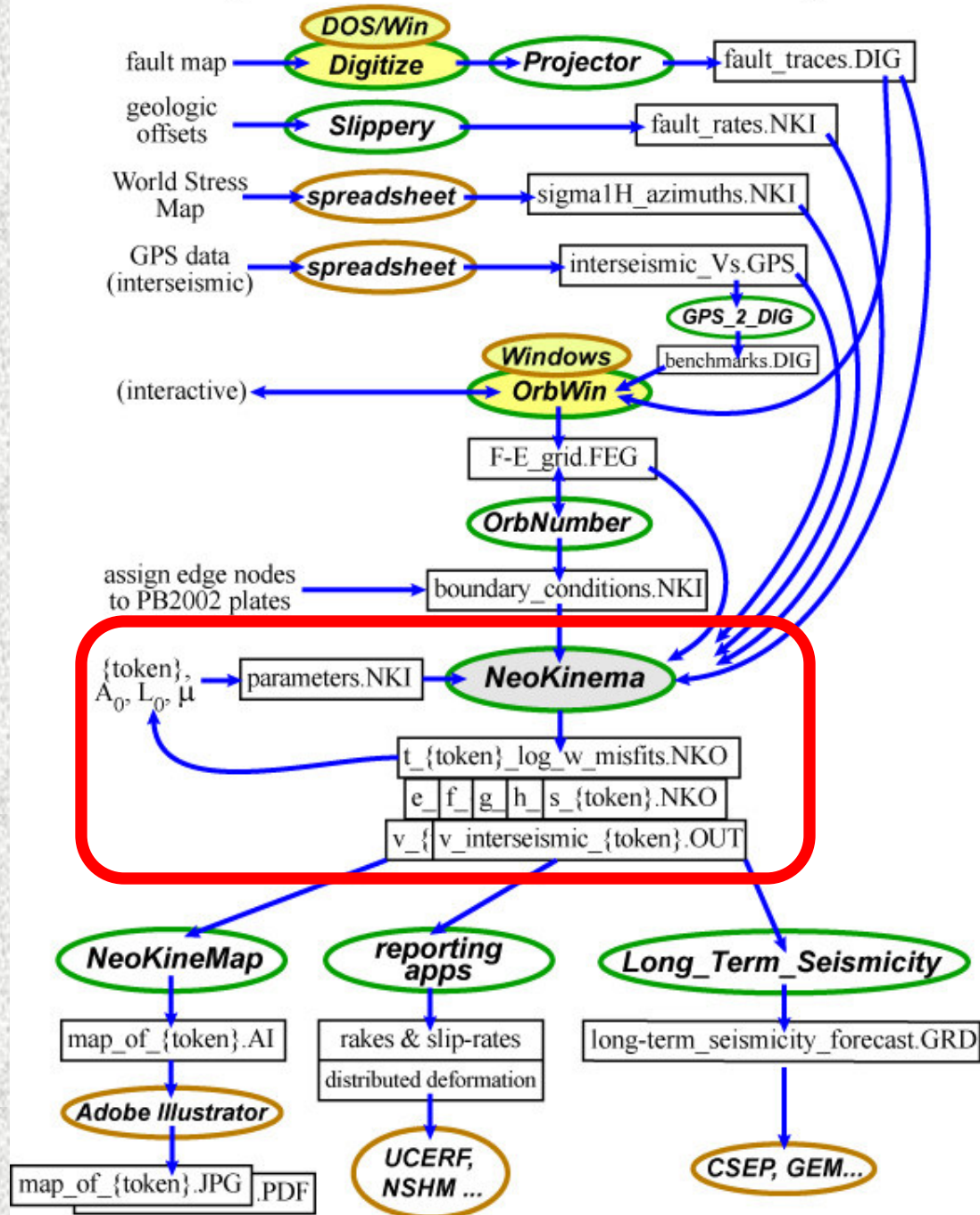
OUTPUT:



NeoKinema modeling process:



NeoKinema modeling process:



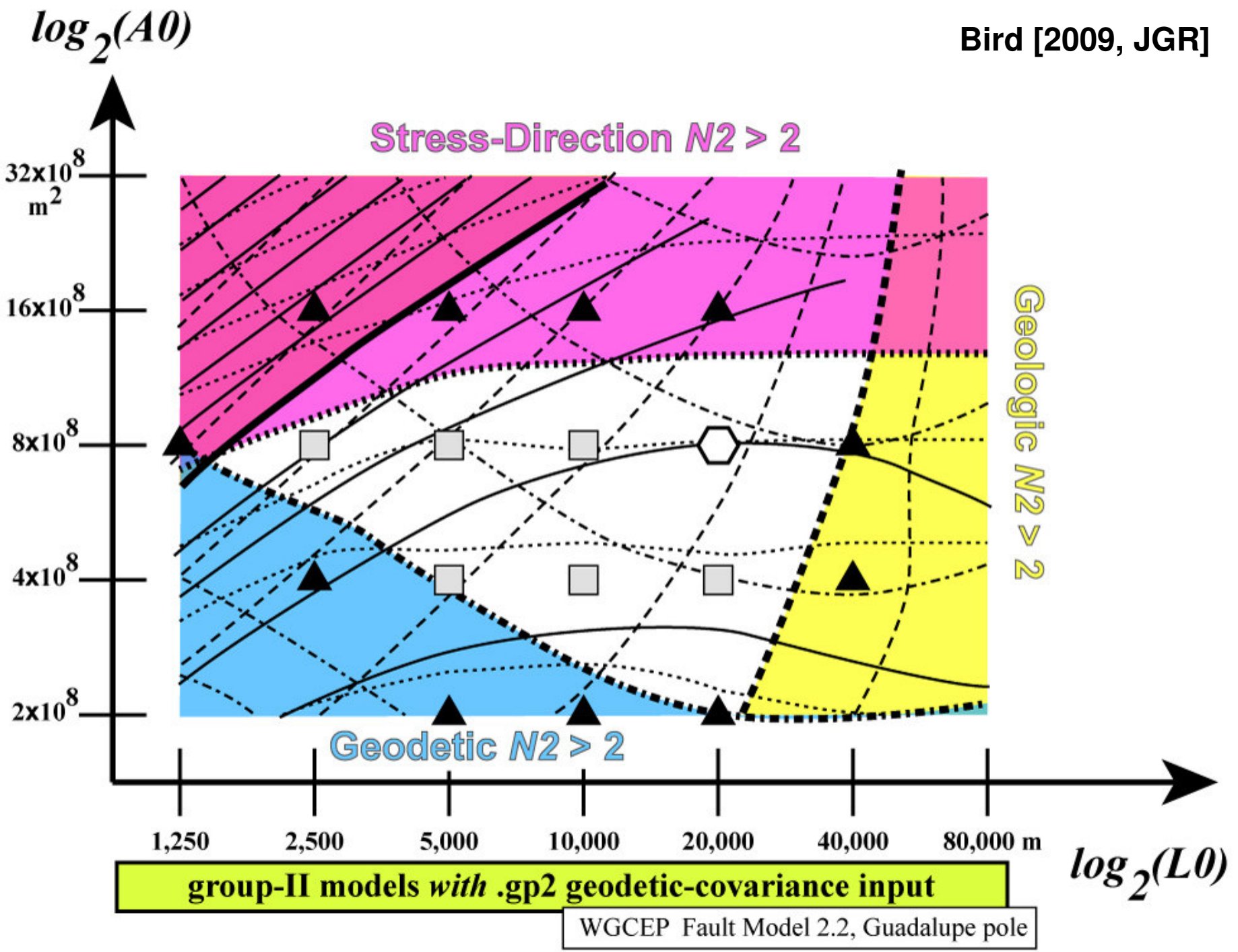


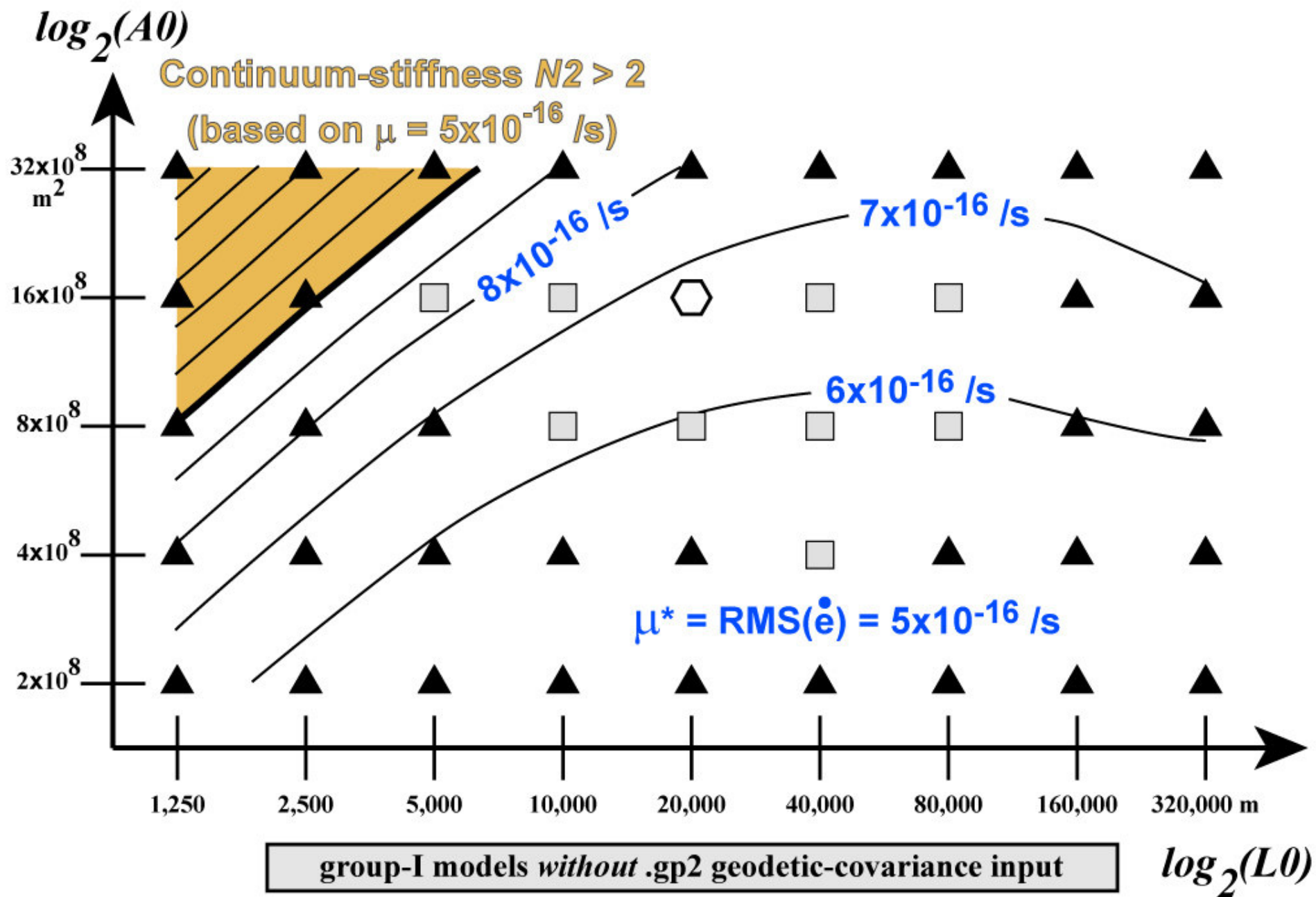
Non-dimensional measures of misfits to input data:

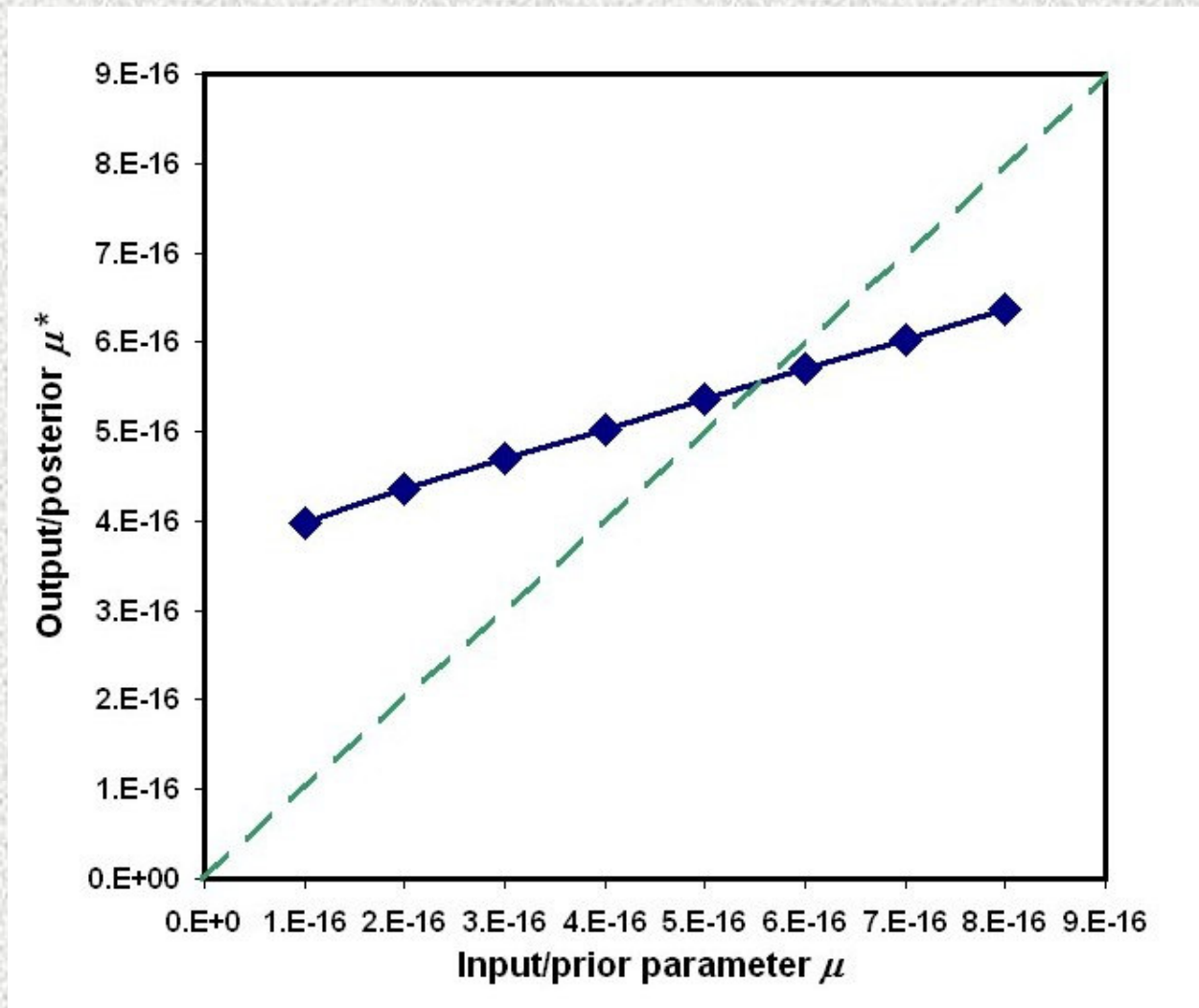
$$N_2^{\text{geodetic}} \equiv \sqrt{\frac{1}{2B} \sum_{b=1}^B (\vec{p}_b - \vec{r}_b)^T [\tilde{C}_b^{-1}] (\vec{p}_b - \vec{r}_b)}$$

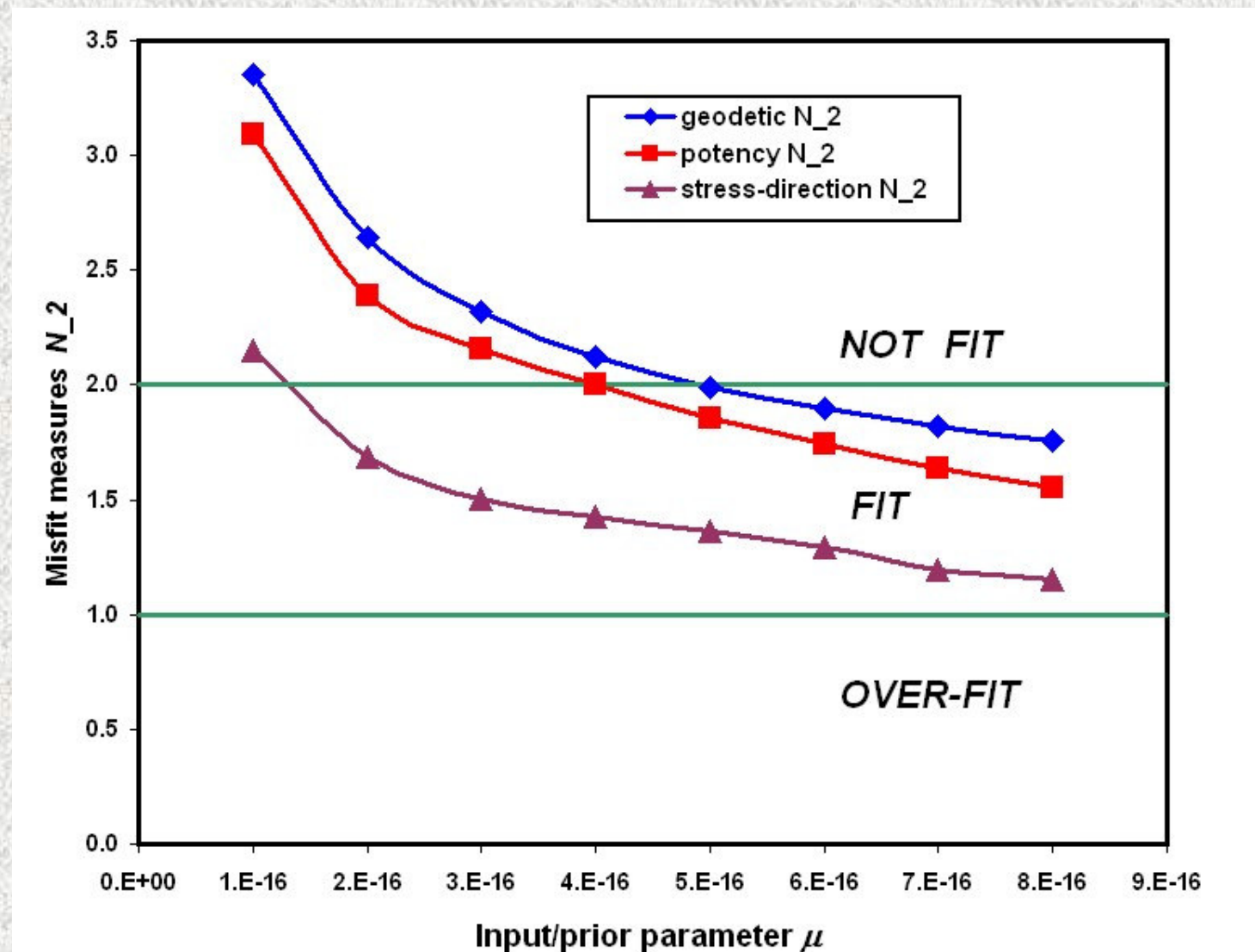
$$N_2^{\text{stress}} \equiv \sqrt{\frac{1}{\sum a_i} \sum_{i=1}^{\text{elements}} a_i \left(\frac{p_i - r_i}{\sigma_i} \right)^2}$$

$$N_2^{\text{potency}} \equiv \sqrt{\frac{1}{\sum \sum \ell_{im} w_m h_{im}^{\text{sup}}} \sum_{i=1}^{\text{elements}} \sum_{m=1}^M \ell_{im} w_m h_{im}^{\text{sup}} \left(\frac{p_{im} - r_m}{\sigma_m} \right)^2}$$









The *NeoKinema* fault-based deformation model in UCERF3

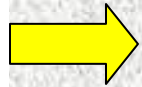
Very similar to models of Bird I 2009. JGR I, but using all-new input data.

Peter Bird
UCLA



2012.01.26, UCERF3 workshop, Menlo Park:
some models updated to 2012.06.01

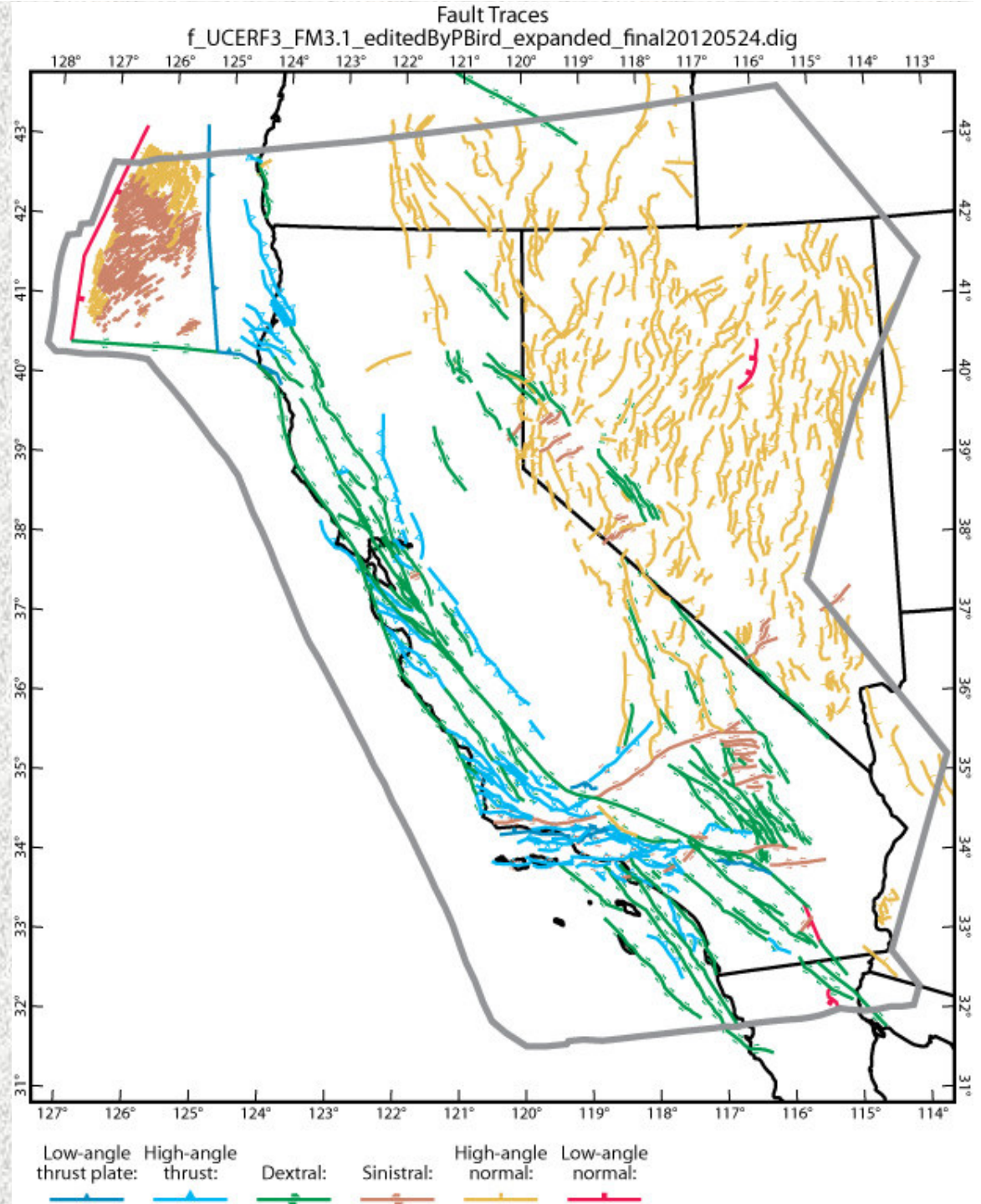
Input data:



- ✓ Traces of active faults
from Tim Dawson's UCERF3 compilation in CA, and *Bird* [2007] and *Chaytor et al.* [2004] outside;
- ✓ Long-term geologic offset rates
from Tim Dawson's UCERF3 compilation in CA, and *Bird* [2007] outside;
- ✓ Creeping fault patches in CA
from the UCERF2 table;
- ✓ Interseismic GPS velocities
from Tom Herring's UCERF3 compilation with Rob McCaffrey's edits;
- ✓ Most-compressive horizontal stress azimuths
from the World Stress Map website; and
- ✓ Relative-plate-rotation boundary conditions
from GPS of *Gonzalez-Garcia et al.* [2003].

UCERF3 Fault Models
3.1 & 3.2 covering CA
were provided by
Tim Dawson, CGS.

These fault models were
expanded (outside of CA)
using final block faults,
Chaytor et al. [2004]
faults in the
Gorda “plate,” and
my database of faults
in the Great Basin.



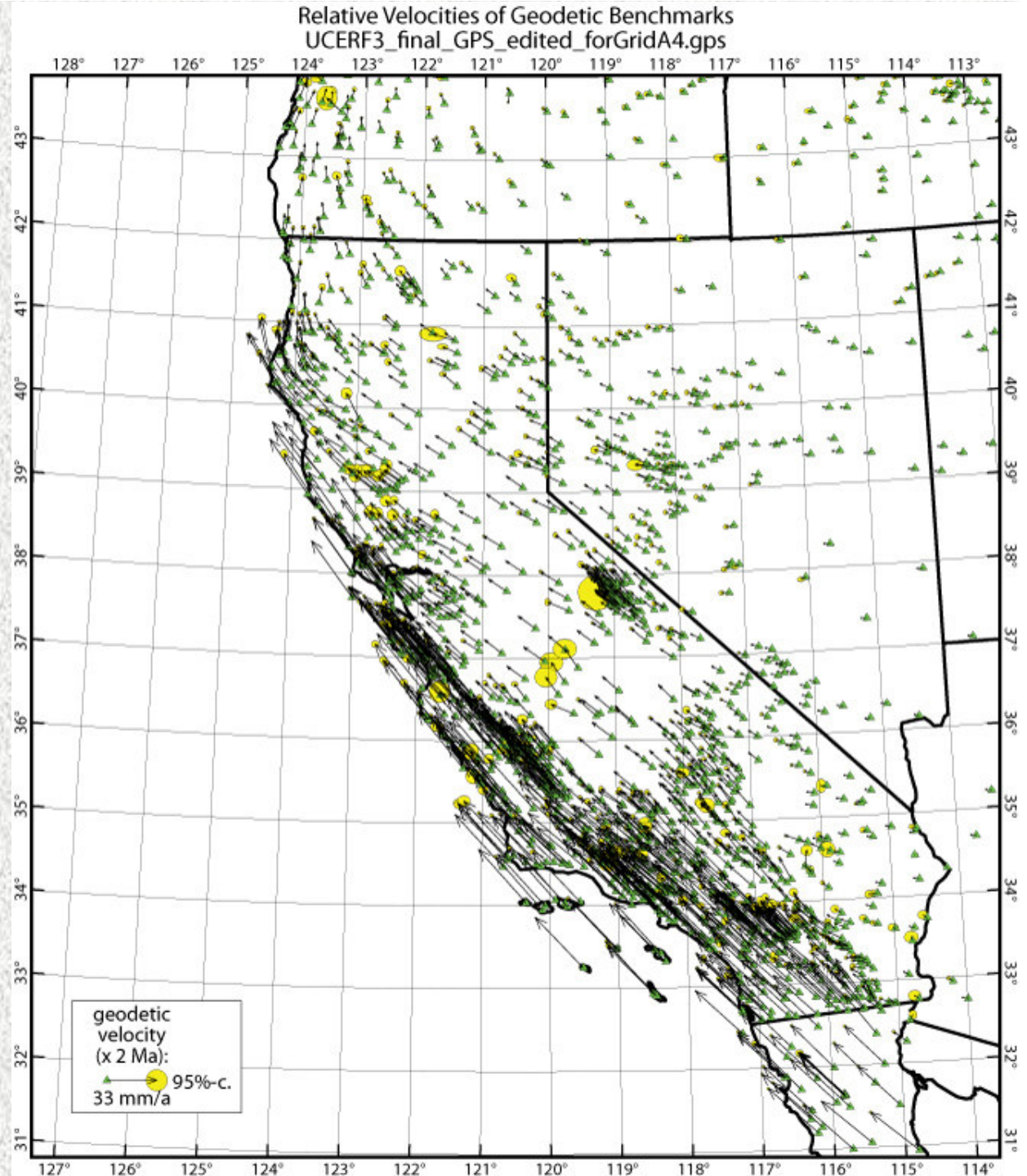
Input data:

- ✓ Traces of active faults
from Tim Dawson's UCERF3 compilation in CA, and *Bird* [2007] and *Chaytor et al.* [2004] outside;
- ✓ Long-term geologic offset rates
from Tim Dawson's UCERF3 compilation in CA, and *Bird* [2007] outside;
- ✓ Creeping fault patches in CA
from the UCERF2 table;
- ✓ Interseismic GPS velocities
from Tom Herring's UCERF3 compilation with Rob McCaffrey's edits;
- ✓ Most-compressive horizontal stress azimuths
from the World Stress Map website; and
- ✓ Relative-plate-rotation boundary conditions
from GPS of *Gonzalez-Garcia et al.* [2003].

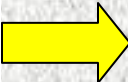
UCERF3 model
of GPS velocities
during interseismic
times.

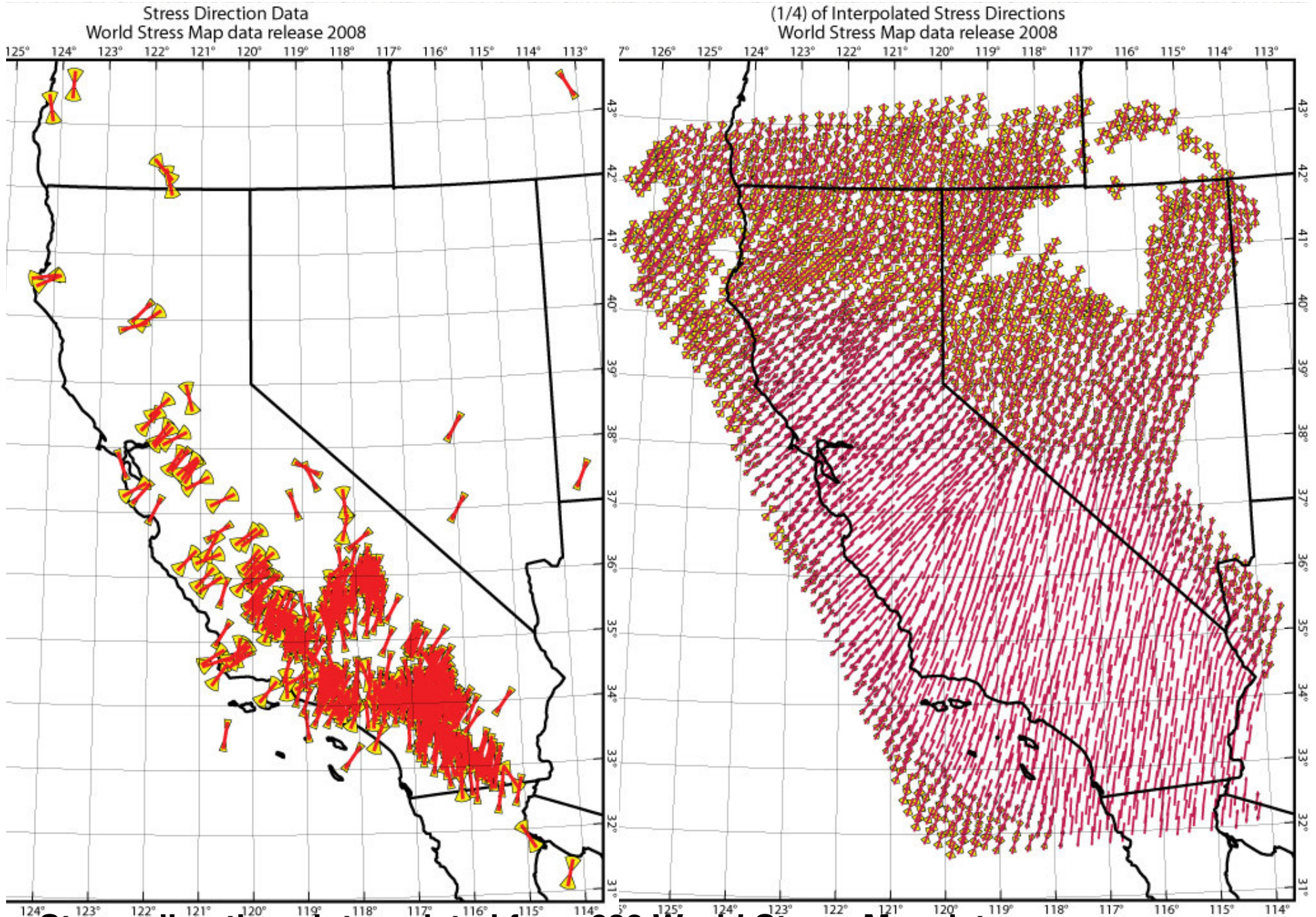
Relative to stable
eastern North
America plate.

Synthesized for
UCERF3 by
Tom Herring, MIT.



Input data:

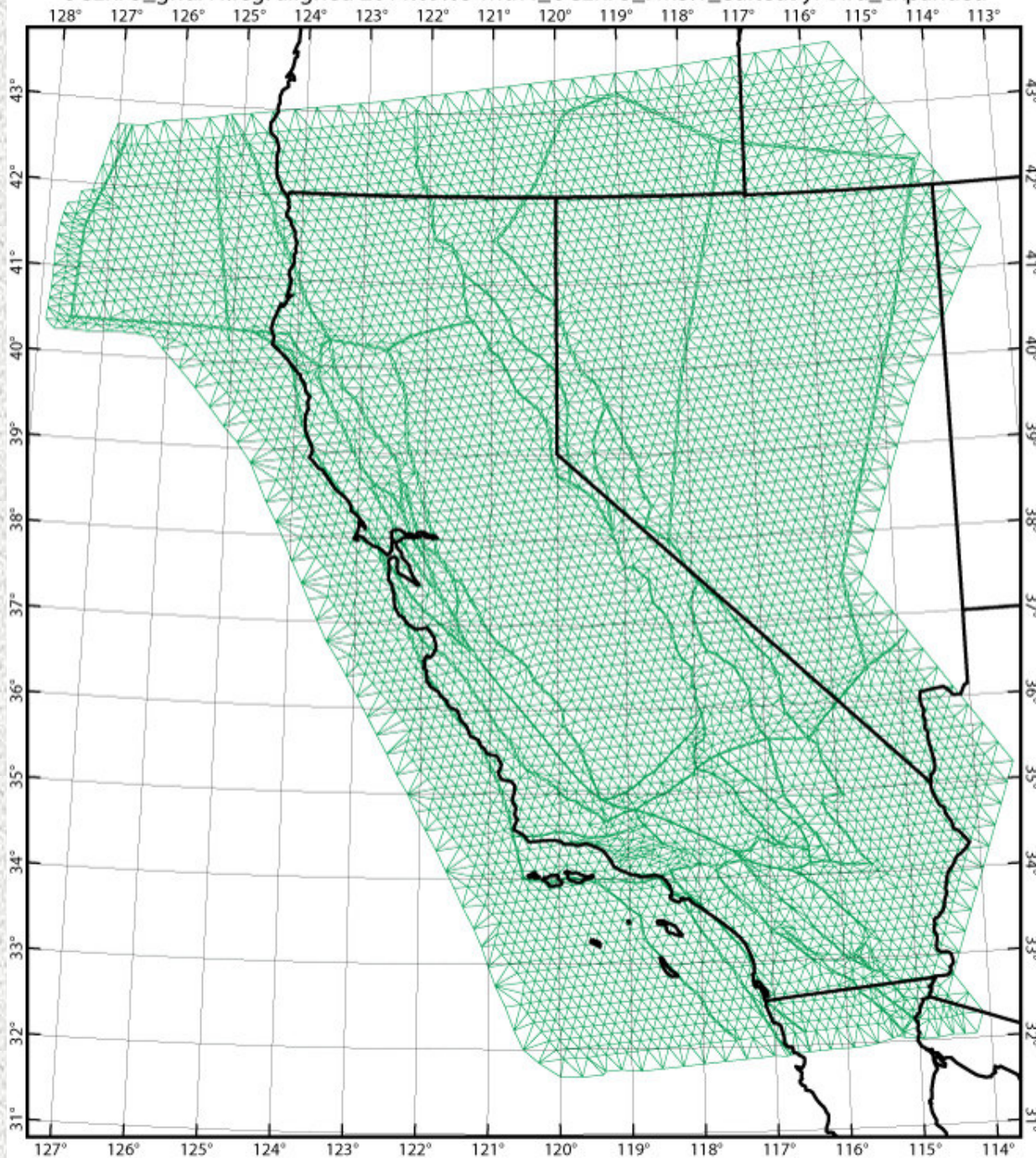
- ✓ Traces of active faults
from Tim Dawson's UCERF3 compilation in CA, and *Bird* [2007] and *Chaytor et al.* [2004] outside;
- ✓ Long-term geologic offset rates
from Tim Dawson's UCERF3 compilation in CA, and *Bird* [2007] outside;
- ✓ Creeping fault patches in CA
from the UCERF2 table;
- ✓ Interseismic GPS velocities
from Tom Herring's UCERF3 compilation with Rob McCaffrey's edits;
-  ✓ Most-compressive horizontal stress azimuths
from the World Stress Map website; and
- ✓ Relative-plate-rotation boundary conditions
from GPS of *Gonzalez-Garcia et al.* [2003].



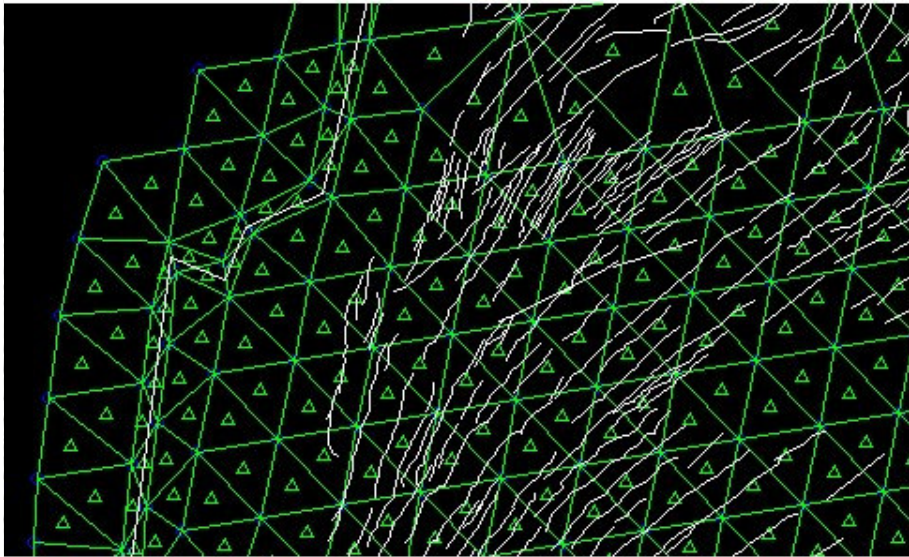
Stress directions interpolated from 638 World Stress Map data provide needed constraints on the orientation of strain-rates between faults.

Finite Element Grid

UCERF3_gridA4.feg: aligned 2011.09.03 with f_UCERF3_FM3.1_editedByPBird_expanded

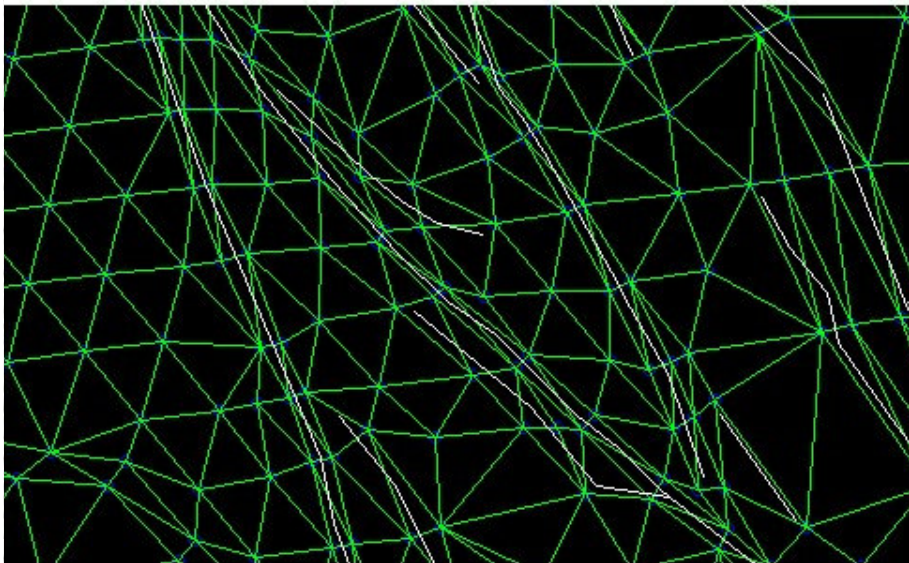


Alignment(?) of faults & F-E grid in *NeoKinema*



**Alignment is not required;
any number of faults can cut
through a single finite-element.**

(Example: Gorda "plate")



**However, GPS benchmarks are not allowed
in the same element with a fast-slipping
fault. So, aligning elements with a few
fast faults reduces the number of GPS
data that must be excluded.**

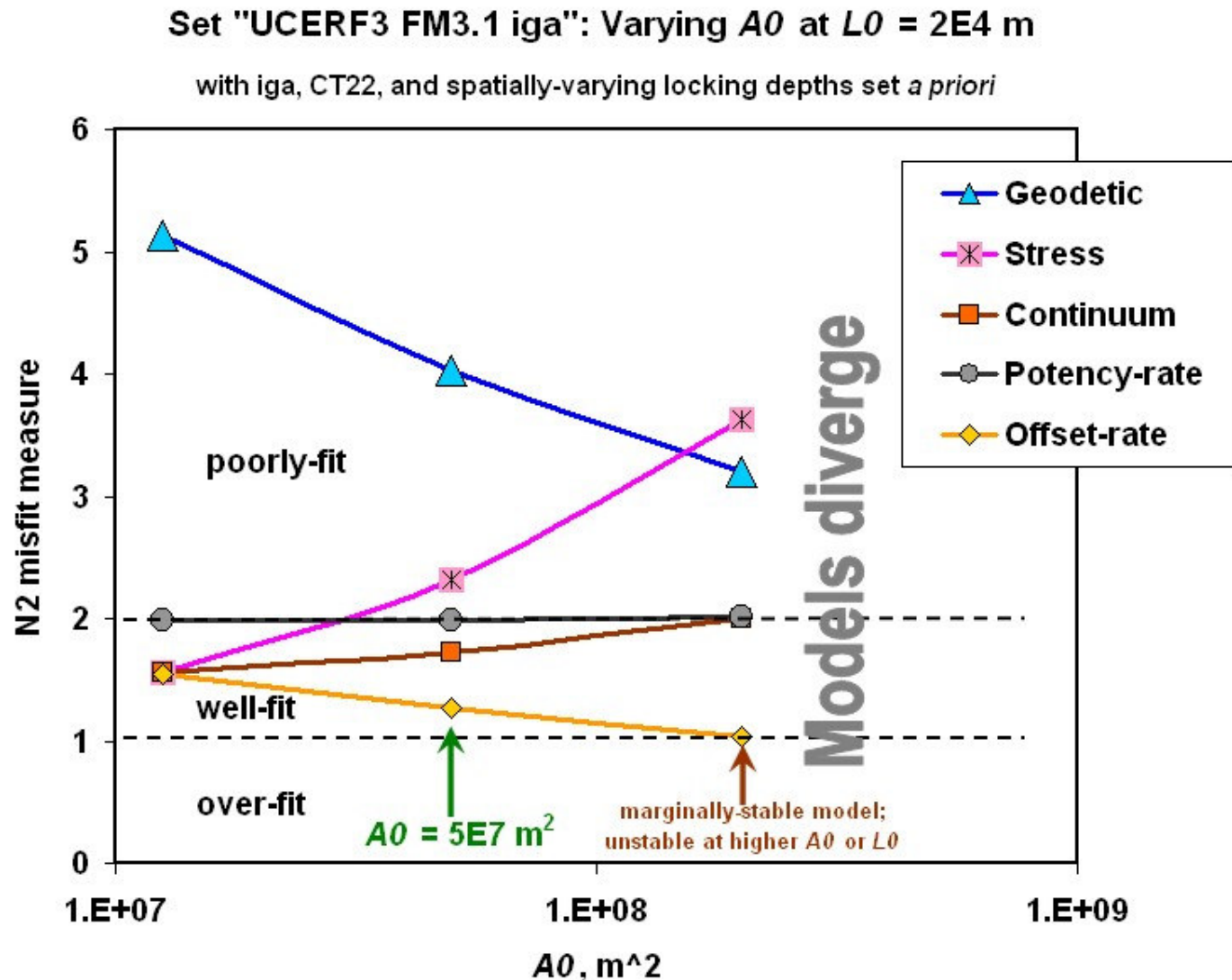
**It may also give a better representation
of the stiffness of the "microplate"
blocks between major faults.**

(Example: central California)

RMS values of residual misfits:

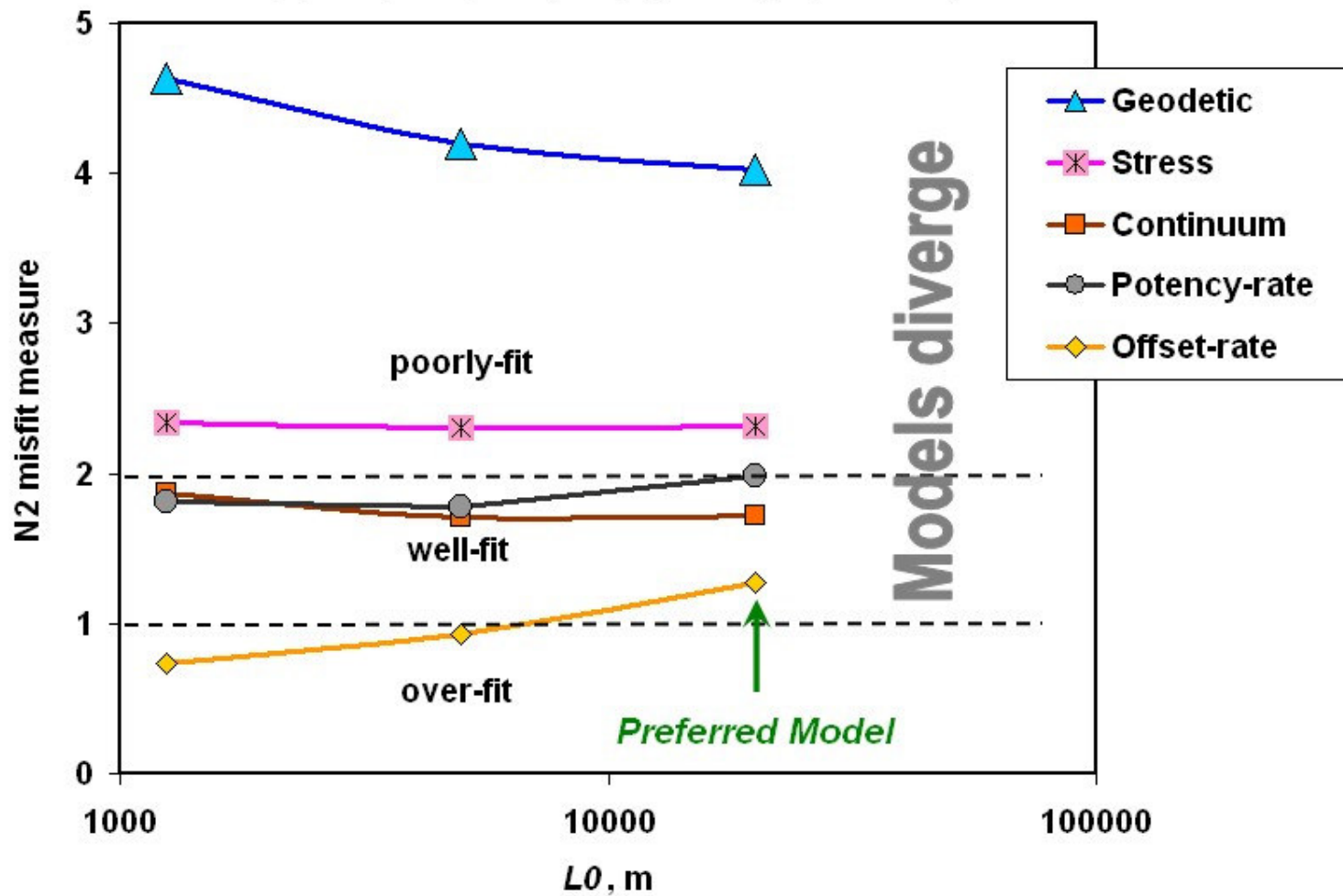
CLASS OF DATA	Residuals in sigma units (σ s)	Residuals in data units
GPS velocities [<i>N.B.</i> no error inflation]	4.01	2.29 mm/a (median 1.46 mm/a)
Geologic offset rates [unweighted; tends to emphasize low rates]	1.29	2.31 mm/a (median 0.18 mm/a)
Geologic offset rates [with weighting by model fault potency rate]	1.93	
Principal strain-rate azimuths [off-fault, where constrained by data]	2.18	13.7° (median 2.9°)

GPS misfit of $N_2 = 4$ could be somewhat reduced (to $N_2 = 3.2$) by increasing modeling parameter A_0 — but, then models are only marginally stable, distributed deformation rates rise, and stress-direction fitting degrades. I recommend **this** model.



Set "UCERF3 FM3.1 iga": Varying $L0$ at $A0 = 5E7 \text{ m}^2$

with iga, CT22, and spatially-varying locking depths set *a priori*



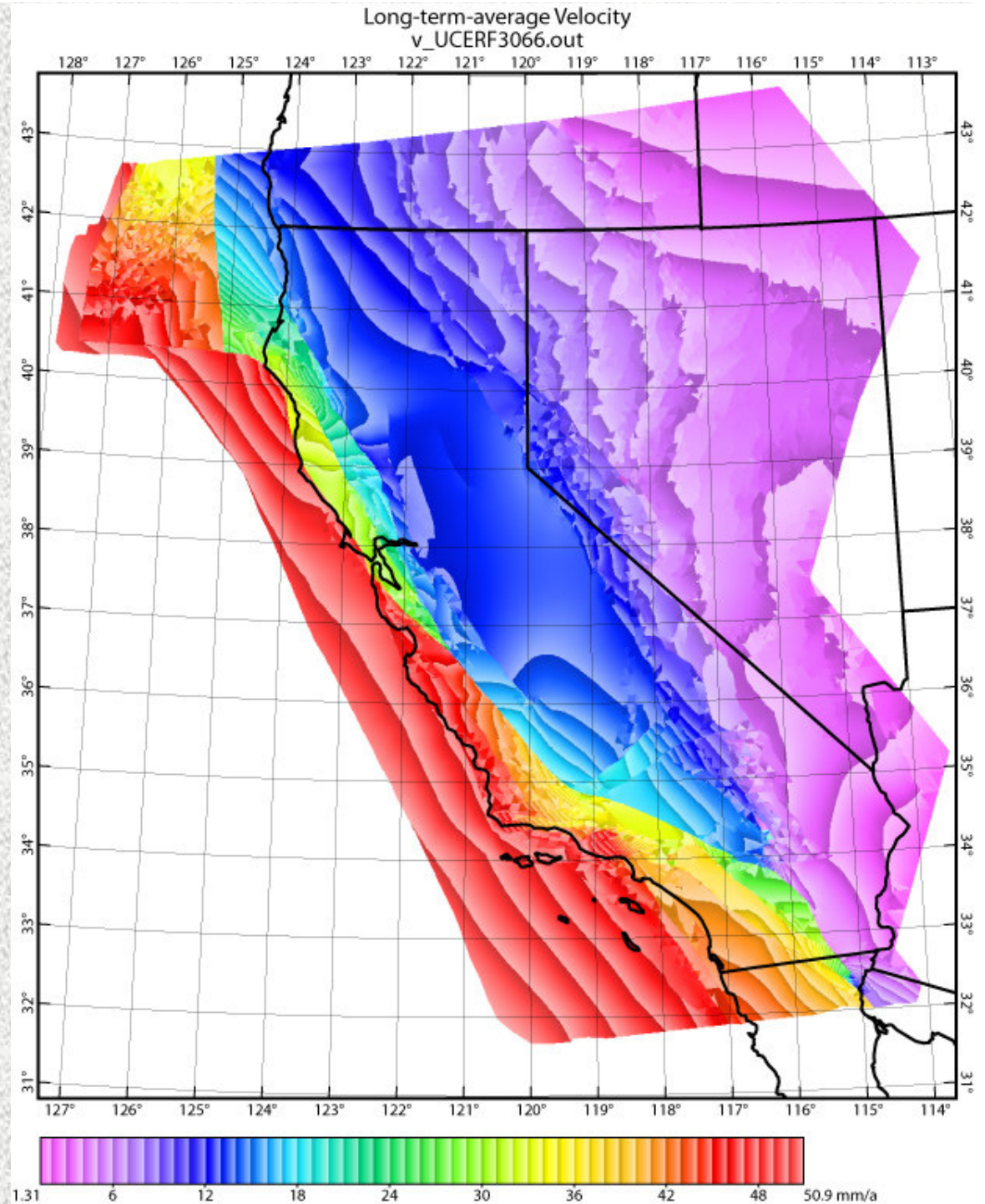
Q: How can you justify recommending a model in which the RMS GPS misfit is 4 (rather than 1 to 2) sigmas?

A: The sigmas attached to the GPS velocities are formal uncertainties in the *mean velocity during a particular time window*. What we would like to use (but don't know) are the uncertainties when time-specific GPS velocities are used as estimates of the *long-term-average of interseismic velocities*. These must clearly be larger.

Thus, formal GPS velocity uncertainties (input to NeoKinema) are only lower limits on the uncertainty in the long-term-average of the interseismic velocities. So, it would not be reasonable to expect to fit the velocities within 1~2 of *these* sigmas, in complex realistic cases.

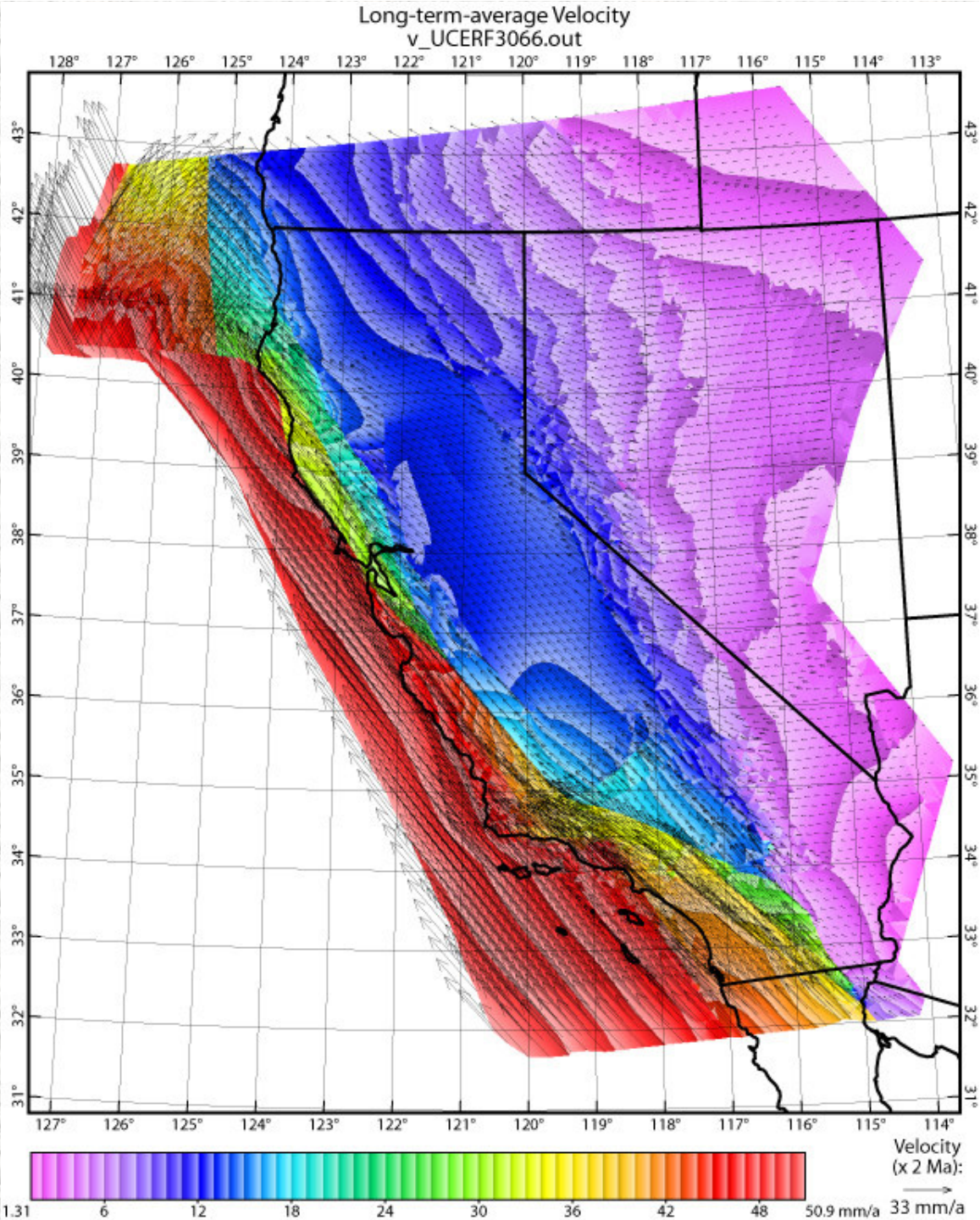
**Long-term-average
velocity field
of the
final model
UCERF3066**

**(shown without
vector overlay;
contour interval
is 1 mm/a)**



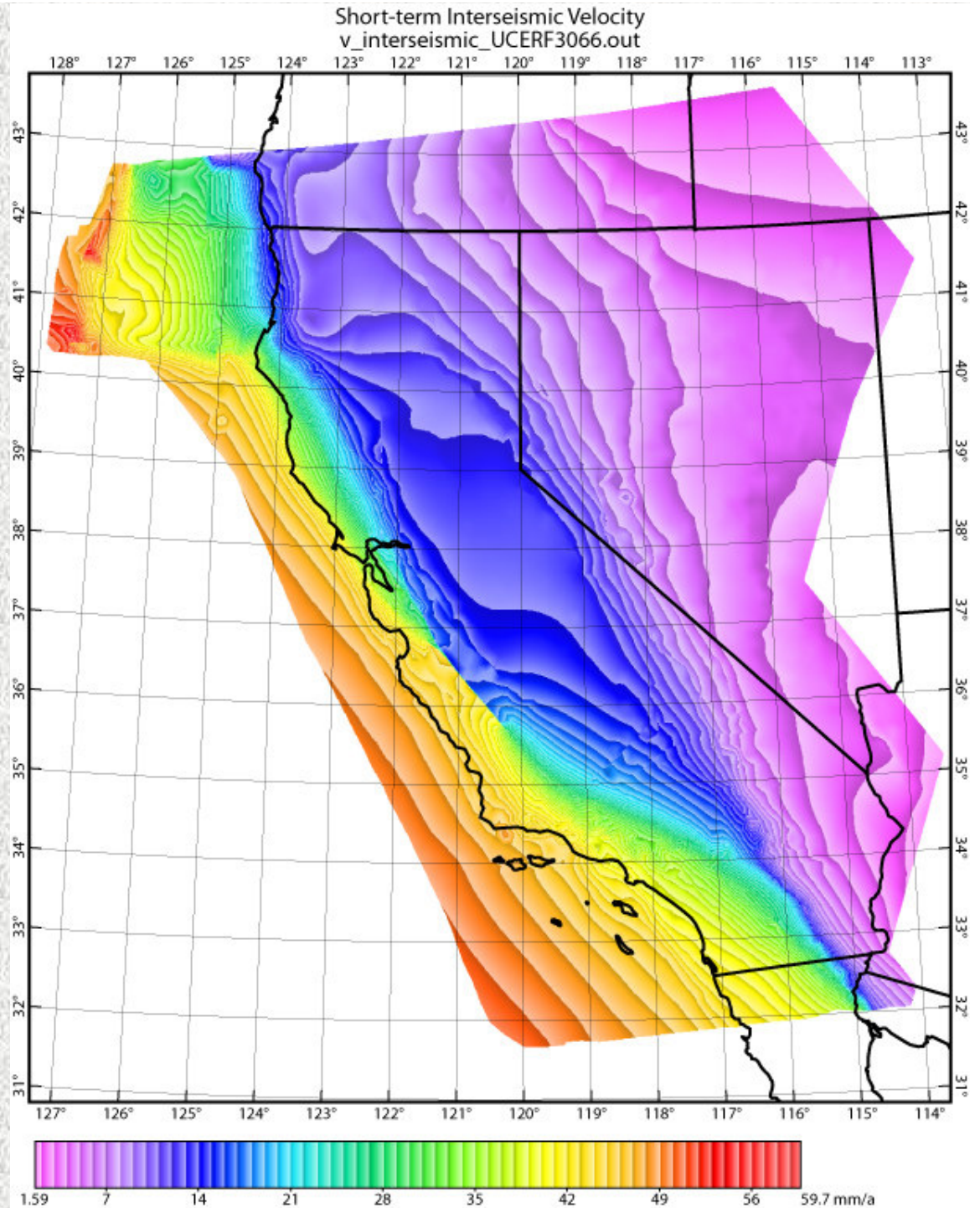
**Long-term-average
velocity field
of the
final model
UCERF3066**

**(shown with
vector overlay;
contour interval
is 1 mm/a)**

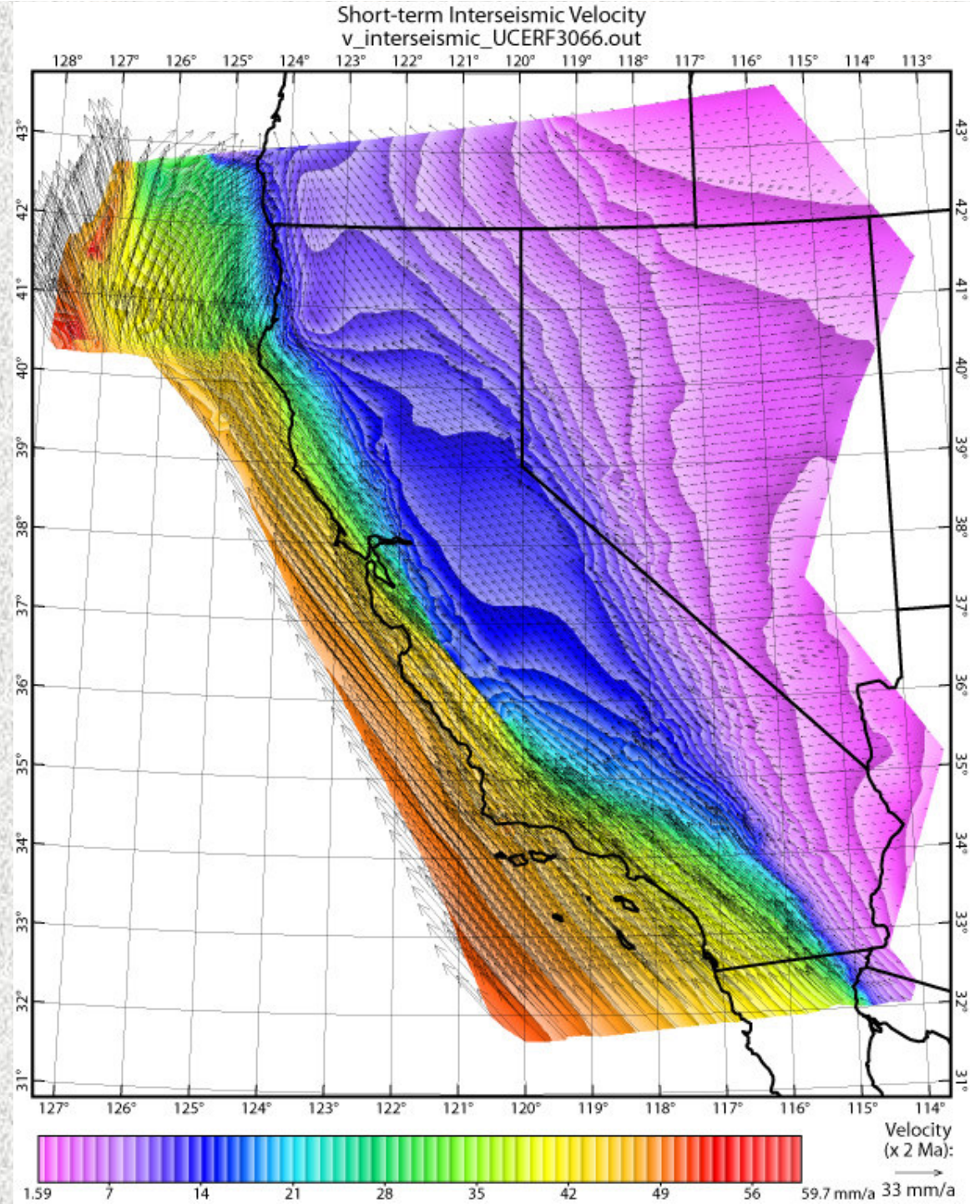


**Interseismic velocity field
of the
final model
UCERF3066**

**(shown without
vector overlay;
contour interval
is 1 mm/a)**

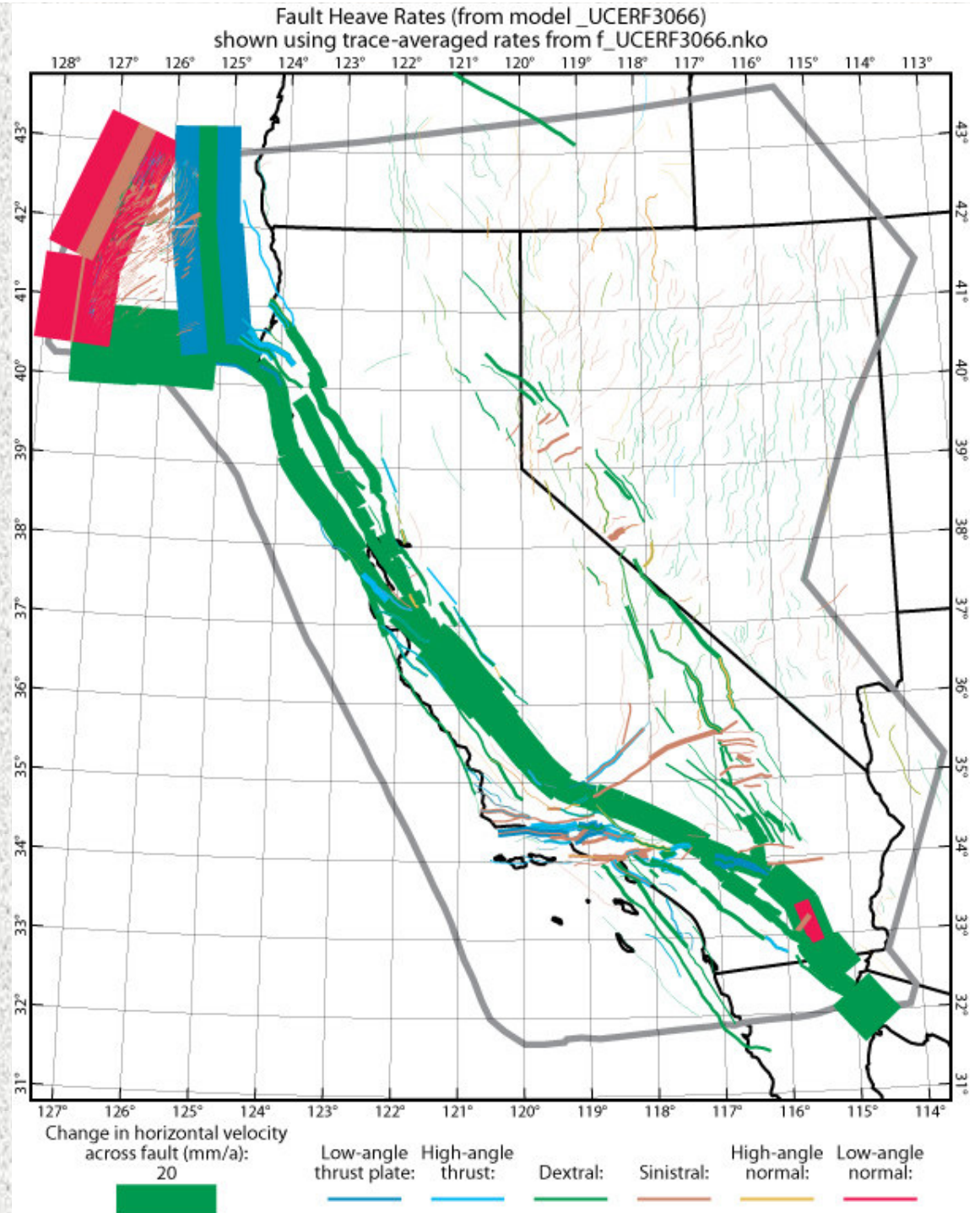


Interseismic velocity field of the final model UCERF3066
(shown with vector overlay; contour interval is 1 mm/a)



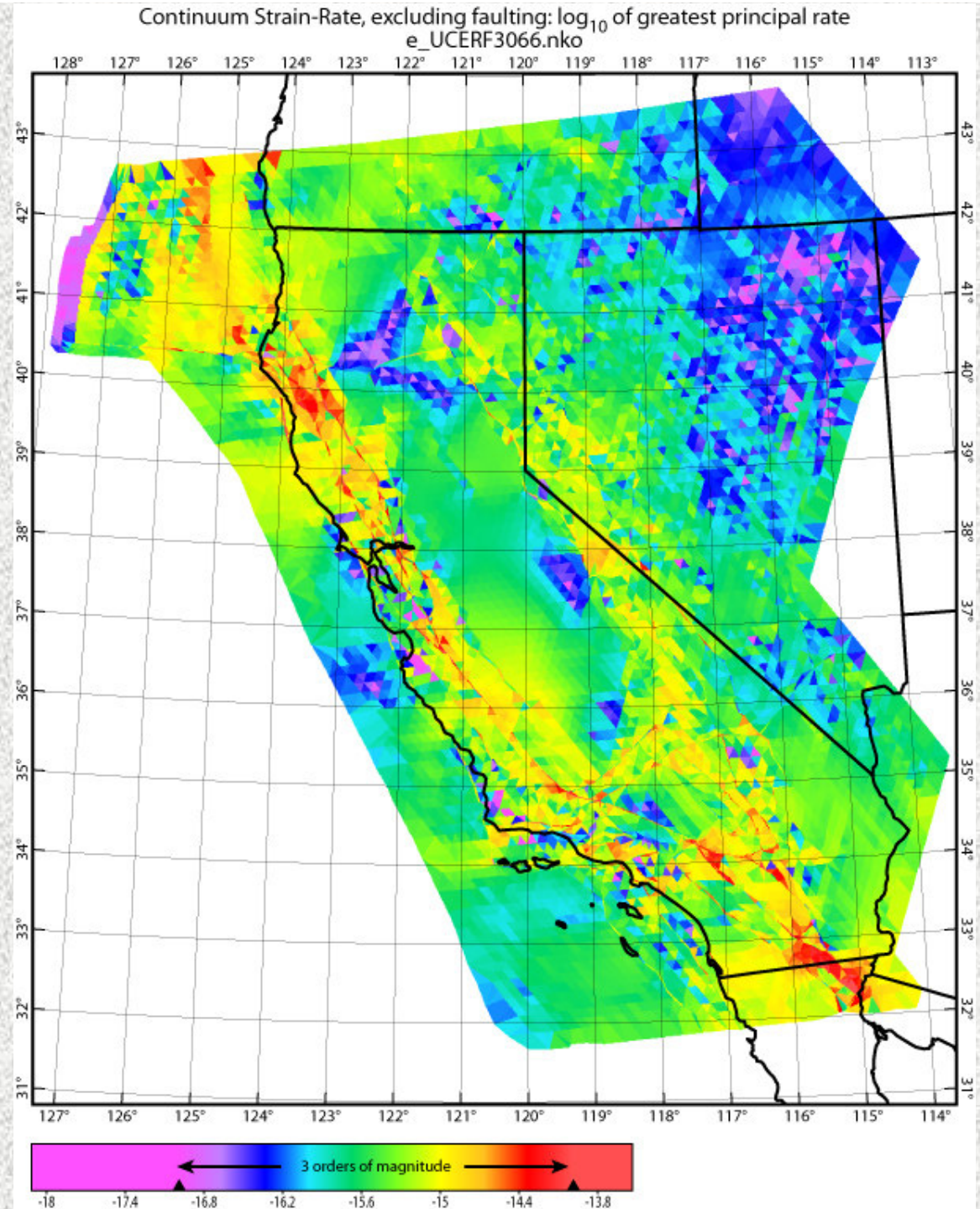
**Long-term-average
fault heave rates
of the
final model
UCERF3066**

**(oblique slip is
shown with two
superposed
ribbons)**



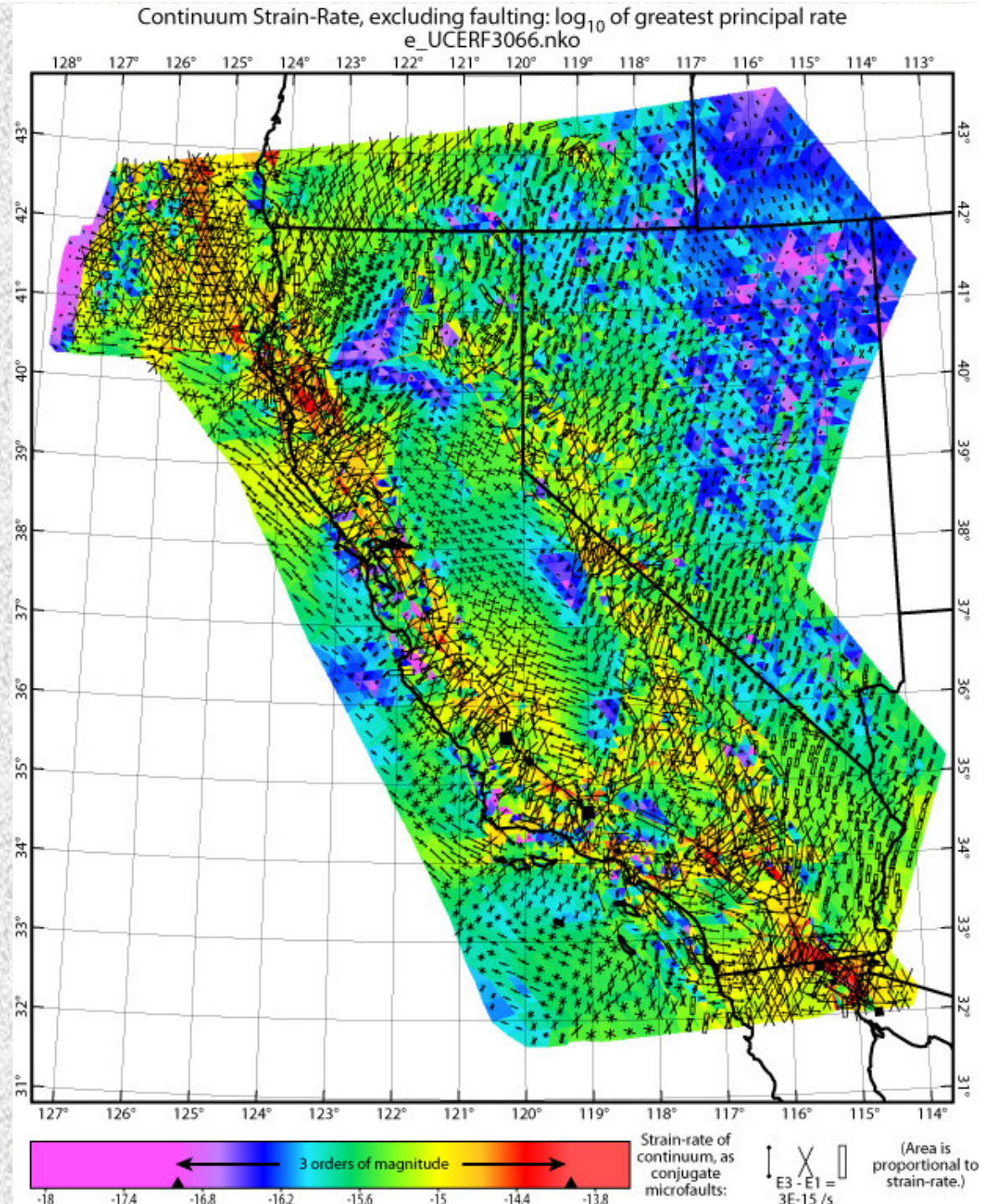
**Long-term-average
distributed
(off-fault)
strain-rates
of the
final model
UCERF3066**

**(Shown without
tensor overlays.
Note that
the color
scale is
logarithmic;
green is ~3% of red,
and
violet is ~3% of green.)**



**Long-term-average
distributed
(off-fault)
strain-rates
of the
final model
UCERF3066**

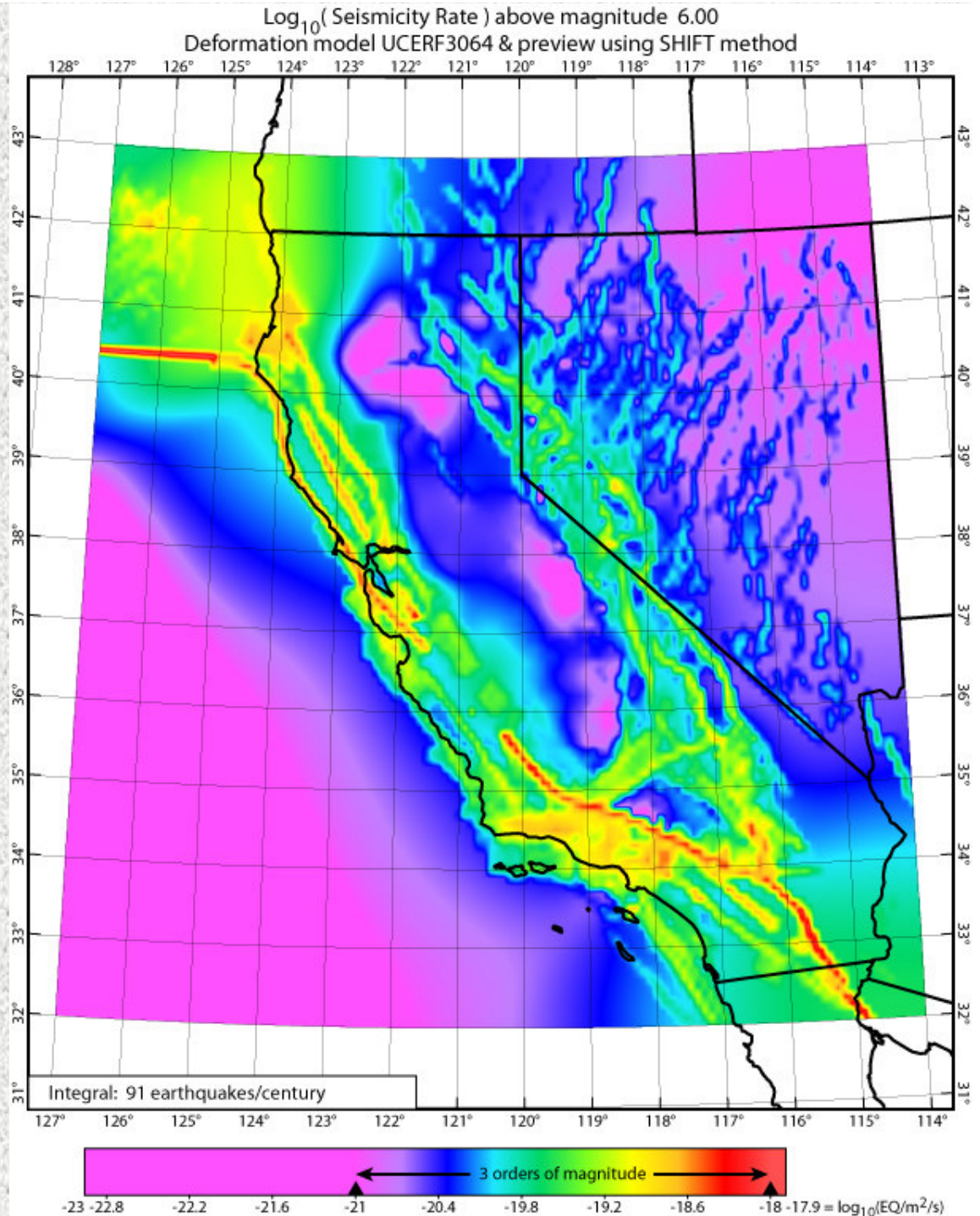
**(Shown with
tensor overlays.
Note that
the color
scale is
logarithmic;
green is ~3% of red,
and
violet is ~3% of green.)**



**A rough estimate
of long - term seismicity
implied by this model**

**(using the SHIFT method of
Bird & Liu [2007] and
Bird *et al.* [2009]
instead of the more
accurate UCERF3 method).**

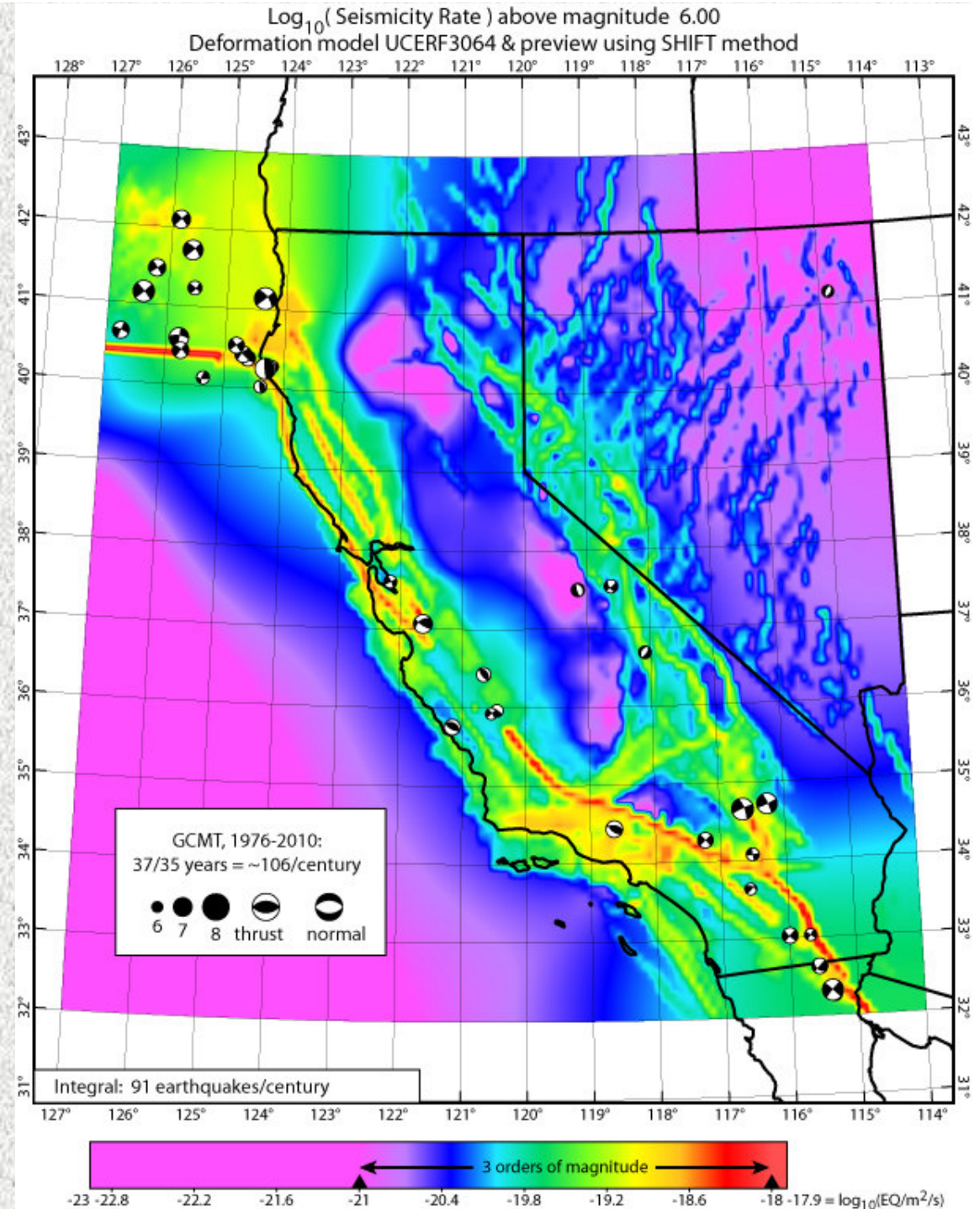
**Note that color scale
is logarithmic, so
green is ~40x less
intense than red.**



Comparison to the GCMT catalog for 1976-2010 shows generally good agreement, except:

*well-known seismic gaps on most sections of the San Andreas fault;

*2 embarrassing m6 events occurred in purple areas of low forecast rate.

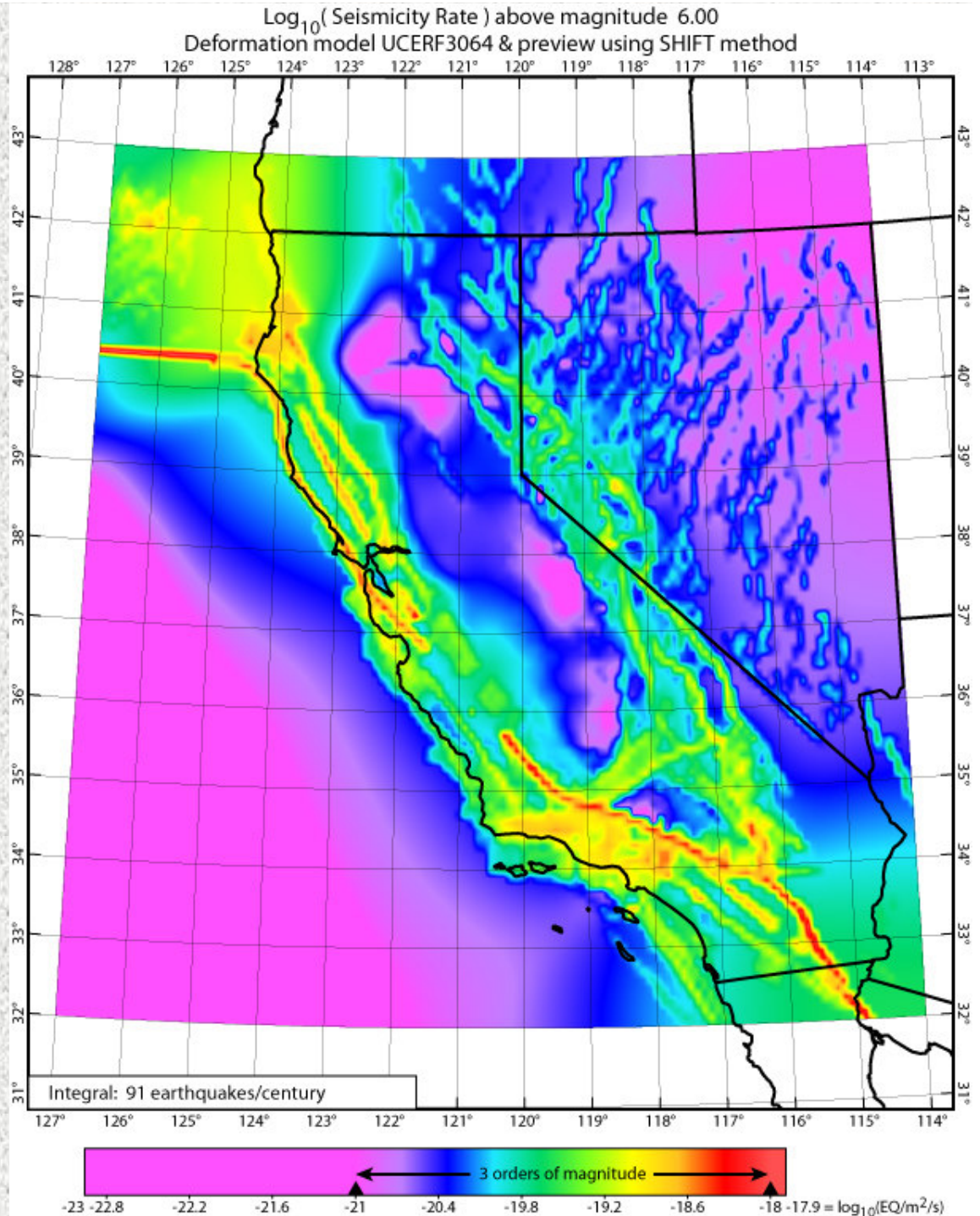


**A rough estimate
of long - term seismicity
implied by this model**

**(using the SHIFT method of
Bird & Liu [2007] and
Bird *et al.* [2009]
instead of the more
accurate UCERF3 method).**

**Note that color scale
is logarithmic, so
green is ~40x less
intense than red.**

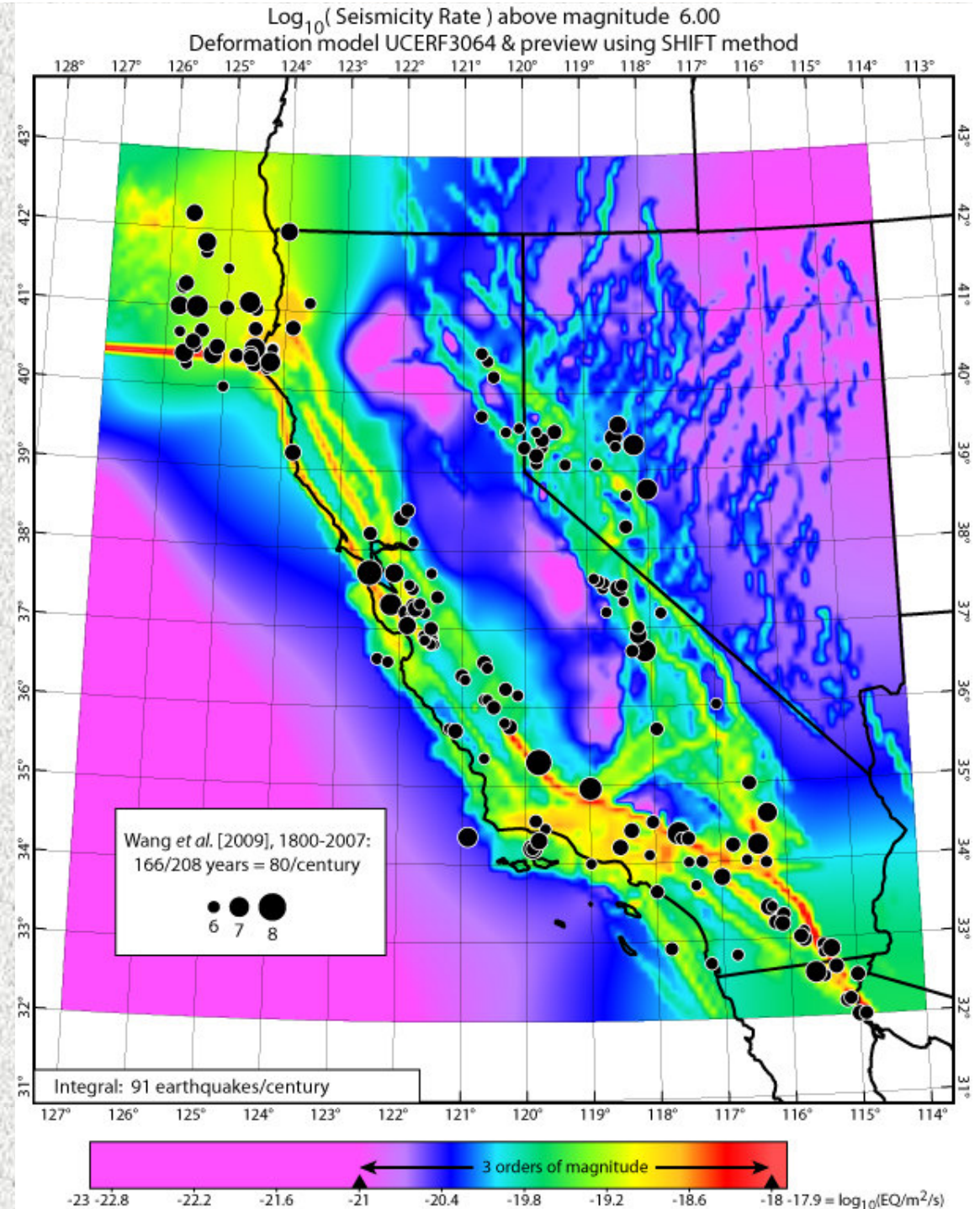
(repeated slide)



Comparison to the Wang *et al.* [2009] catalog for 1800-2007 shows generally good agreement, except:

*one has to allow for the along-fault extents of the 1857 & 1906 EQS, and perhaps some unreported aftershocks(?);

*long-lasting seismic gaps are identified on the -Maacama fault, the -Bartlett Springs fault, the -Garlock fault, and the -southern San Andreas.



CSEP-like* retrospective tests:

[*My code; no declustering included; threshold $m_t = 6.00$]

Test catalog:	GCMT, 1976-2010	<i>Wang et al.</i> [2009], 1800-2007
L-test:	0.056 Passed	0.103 Passed
N-test:	0.807 Passed	0.033 Passed
S-test:	0.164 Passed	0.042 Failed (below 0.05)
ASS-test: [relative to PI from <i>Wang et al.</i> , 2009]	0.856 Superior	<i>Not computed</i> <i>(no PI available).</i>

Access to codes:

- All source codes (mostly Fortran 90), manuals, and sample input/output datasets may be downloaded freely from:

<http://peterbird.name/oldFTP/>

- There are also executable images for 32-bit (and maybe 64-bit?) Windows.
- I suggest that you “register” by e-mailing me your contact info and intended application. (I may want to follow-up if bugs are found or improvements are added.)